Contractor Report 194433

Computational Simulation of Composite Structures With and Without Damage

Thomas F. Wilt
University of Akron
Akron, Ohio

March 1994

National Aeronautics and
Space Administration

ABSTRACT

A methodology is described which uses finite element analysis of various laminates to computationally simulate the effects of delamination damage initiation and growth on the structural behavior of laminated composite structures. The delamination area is expanded according to a set pattern. As the delamination area increases, how the structural response of the laminate changes with respect to buckling and strain energy release rate are investigated. Rules are presented for laminates of different configurations, materials and thickness. These results demonstrate that computational simulation methods can provide alternate methods to investigate the complex delamination damage mechanisms found in composite structures.

ACKNOWLEDGEMENTS

I would like to express my sincere thanks to Dr. C.C. Chamis for his guidance and technical expertise in helping me develop my research and thesis. His guidance has allowed me to derive the most benefit from my masters work in terms of experience and knowledge, which will be of great value in my career. Most of all, I want to thank Dr. Chamis for his time and patience, for this masters thesis has truly been a learning experience in many more ways than one.

Thanks also to Dr. P. L. N. Murthy who provided me with assistance in starting my initial research. His experience with MSC/NASTRAN has been of great value. Finally, I would like to thank Dr. D. G. Fertis for selecting me to participate in the NASA fellowship program. This study was performed under NASA Grant NAG 3-50.

TABLE OF CONTENTS

LIST OF TABLES

LIST OF FIGURES

CHAPTER 1

INTRODUCTION

The high strength-to-weight ratio and the ability to tailor the composite strengths and behavior according to design requirements gives composite materials a distinct advantage over some of the more conventional structural materials. But in order to use these composite materials to their full advantage, a complete understanding of the damage mechanisms encountered must be achieved. Also, as composite materials are used for the more critical components, such as turbine blades, primary airfoils, etc., a more accurate prediction of the structural behavior and fracture of these components is required.

Unlike conventional materials, the failure modes encountered in composite materials are far more complex. This is due to the presence of both fiber and matrix constituents which possess markedly different material properties and which result in complex fiber-matrix interactions not found in other materials. Some of the damage mechanisms found are fiber-matrix debonding, fiber breakage, transply cracking and interply delamination. These failure modes can occur either individually or in combination. Also, they are found to be micromechanical as well as macromechanical in nature and as a result can be present long before any visible evidence of damage can be observed. Because of this,

it needs to be determined to what degree the various damage mechanisms affect composite behavior. This type of knowledge would be important in all phases in the life of the structure; design, fabrication and in-service life.

Of the failure modes mentioned, two of those, transply cracking and interply delamination, are considered matrix dominated failure modes. That is, these forms of damage occur in the lower strength, brittle matrix material. The damage mechanism of interply delamination is what will be the focus of the study undertaken here.

Interply delamination may form due to a variety of factors. In the actual fabrication of the laminate, problems such as the possible introduction of a foreign particle between the plies, or voids during the curing process, could produce delaminations. Also, during the in-service life, the structure could be subjected to an impact by an object and thereby cause a near-surface delamination to form.

The most prevalant delamination problem to receive attention is that of the free-edge delamination. This form of delamination has been attributed to the presence of high interlaminar stresses along the free-edge. Some of the past work has been in trying to analytically determine the high interlaminar stresses present along the free-edge region [1,2]. What was found is that the stresses actually become singular at that point and thus cannot be expressed analytically. Because of this and the basic complexity of the three-dimensional elasticity approach that is required, rigorous analytical solutions are difficult to produce and those that are available are limited to specific problems, such as,

symmetric, uniform laminates. As soon as more realistic structural problems are attempted, simplifications must be introduced in order to make the problem mathematically tractable. For example, in studying laminate buckling problems where complex behavior, such as, warping of the laminate may be present, it is not easy to account for such effects in the analytical approach and as a result are usually neglected. Therefore, an alternate approach must be used in order to be able to fully predict composite structural response.

The use of finite element techniques in studying interply delamination on a local level is quite common. For example, three-dimensional finite element analysis has been used to investigate the previously discussed interlaminar stresses [3,4]. Also, previous work has focused on using finite elements to investigate the delamination crack using a classic fracture mechanics approach. In these studies, the focus is primarily on the determination of critical strain energy release rates. These quantities are used to predict the onset and growth of delamination in laminates of varying configurations, thicknesses, etc. [5-8].

But an area that needs attention is the analysis of delamination on a global or structural level. Some work has been done to investigate these changes in structural response. For example, the effects on edge delamination on the laminate tensile stiffness and strength have been investigated. Simple expressions of laminate stiffness have been developed to take into account the presence of delamination [6,9]. Another study was performed to see how prescribed delaminations would affect buckling loads and vibrational frequencies of laminated composite

panels [10]. Not only were experimental tests done, but also finite element models of the test specimens were used to see if the test results could be duplicated accurately.

Similarly, the objective of the study presented here is to use finite element models of various laminates to computationally simulate the effects of damage initiation and growth on the structural behavior of laminated composite structures. This methodology has previously been used to evaluate the strain energy release rate as a means of determining composite structural fracture toughness for composite beams due to static load [11]. Also, the post-buckling analysis of a delaminated laminate due to an impact load has been investigated [12]. The approach adopted in this study is that used in reference [12]. But unlike previous studies, the delamination area is expanded according to a set pattern, as is discussed in Chapter 2. And as this increase in delamination area occurs, how does the structural response of the laminate change? Also, the strain energy release rate is evaluated as the delamination increases as a means of determining the structural fracture toughness of the laminate.

By using computational simulation, laminates of different configurations, materials and thicknesses can all be analyzed. The need to consider a wide range of cases is necessary in order to thoroughly investigate composite behavior in the presence of delaminations and to demonstrate that computational methods can provide an alternate means of investigating the complex damage mechanisms found in composite structures.

CHAPTER 2

THEORY

2.1 Approach

One of the objectives of this study is to characterize and quantify the effects of delamination damage on the structural response of laminated composite structures. This is done by choosing structural parameters which are considered to be fundamental in the analysis and design of a structure or component. These parameters are stiffness, vibration frequency, and structural stability in the form of the critical buckling load. An additional parameter of strain energy release rate is also chosen and used as a means of evaluating the structural fracture toughness of the laminate.

Since these parameters have normally been measured experimentally, the study is conducted in a similar manner. Thus, a series of computationally simulated experiments on various composite laminates is performed. Using this approach allows a number of different cases to be analyzed which is necessary to fully investigate the effects of delamination on structural response and damage tolerance.

2.2 Finite Element Models

2.2.1 Laminates Modeled

Accordingly, the finite element models are given overall dimensions similar to those of a test specimen. The model specimen's aspect ratio of length to width is 14 to 1, with the thickness varying according to the number of plies in the laminate, figure 1.

In the first model, the laminate is divided into two equal layers so the delamination can be modeled in the center. This model is used for the $[\pm 30/90]_s$ 6-ply center and the $[\pm 30/90/\pm 30/90_2]_s$ 14-ply center cases.

A second model is constructed which simply included more of the sublaminate layers. By including these additional layers, the laminate can be modeled with multiple delaminations through the thickness. This model is used for the $[\pm 30/90/\pm 30/90_2]_s$ 14-ply offset case.

By constructing the models in this manner, the models are quite adaptable in that by varying the thicknesses of the two layers and the corresponding number of plies in each, the delamination can be placed at any location through the thickness of the laminate. For example, in the first model, figure 1c, instead of having the delamination located at the center of the laminate, it could be placed at some distance offset from the center, figure 1e. This type of capability is used for studying the buckling behavior of a near surface delamination, Sec. 2.6.

Laminate Specimens Modeled

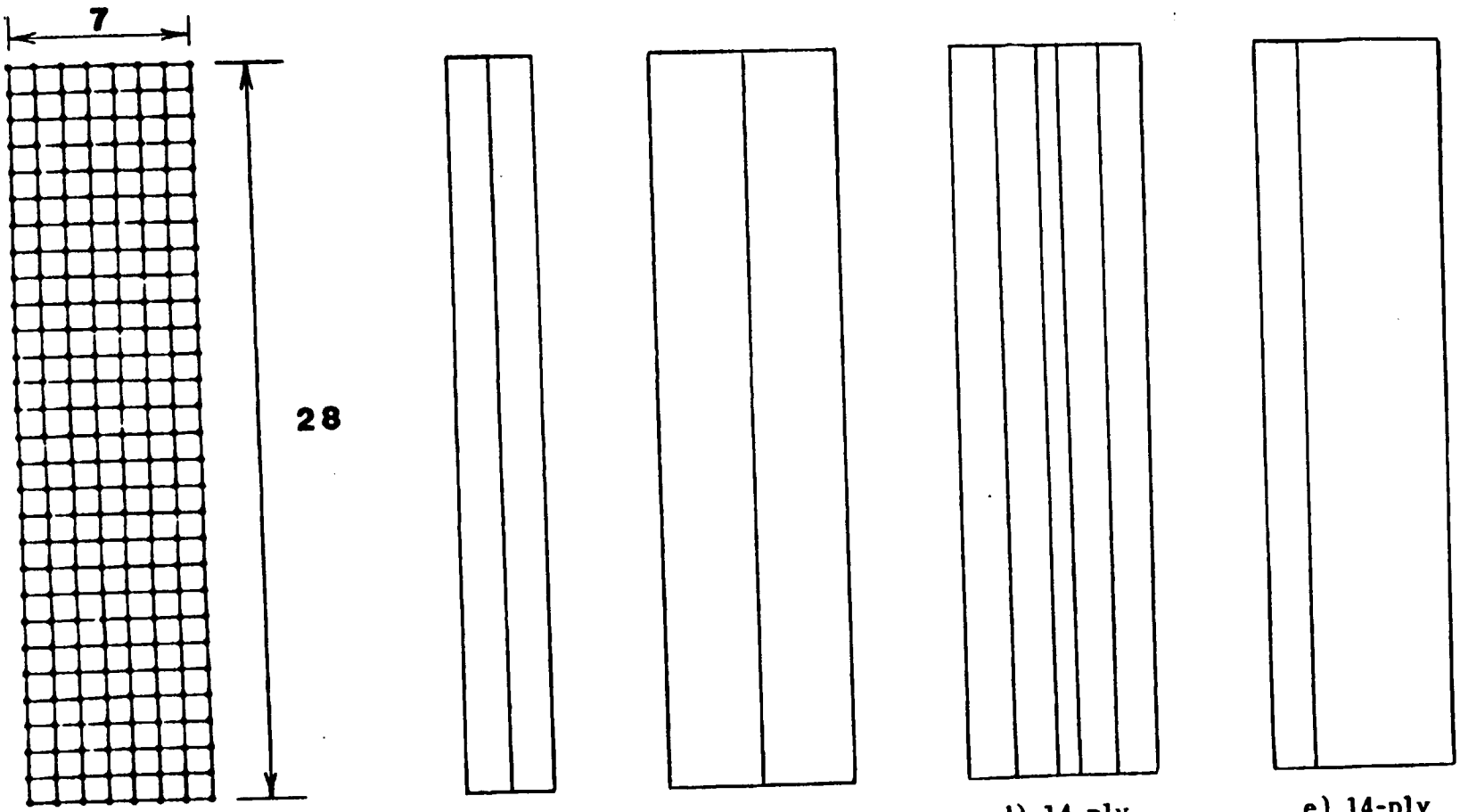

a) planform of model

b) 6-ply center

c) 14-ply center

d) 14-ply multiple

e) 14-ply offset

Figure 1

2.2.2 Sublaminates

In forming the models, it is necessary to construct them so that it will be possible to simulate delamination occurring between plies in the laminate. In order to do this, the laminate is divided into a group of layers with each layer representing a sublaminate. Each of these sublaminates consists of a layer of 4-noded isoparametric quadrilateral plate elements, CQUAD4 in MSC/NASTRAN, which are located at the midplane of the sublaminate, figure 2. The CQUAD4 elements are used in conjunction with PSHELL cards that define the thickness of the sublaminate and the associated material properties of the CQUAD4 elements. The PSHELL card allows the input of material properties such as the membrane, bending, and coupling stiffnesses that correspond to the properties of the group of plies that the sublaminate is representing.

The values for the material properties are obtained by using the Integrated Composite Analyzer (ICAN) computer program [13]. This computer program utilizes composite micromechanics, along with laminate theory, to calculate the associated composite properties for a given laminate configuration. Also, the program allows for different temperature and moisture conditions to be used, thus allowing these effects to be included in the analysis if desired. For these studies, ICAN is run with the group of plies in the sublaminate as input, and the required MSC/NASTRAN MAT2 card values for the membrane, bending and coupling stiffnesses are output.

Laminate Finite Element Model

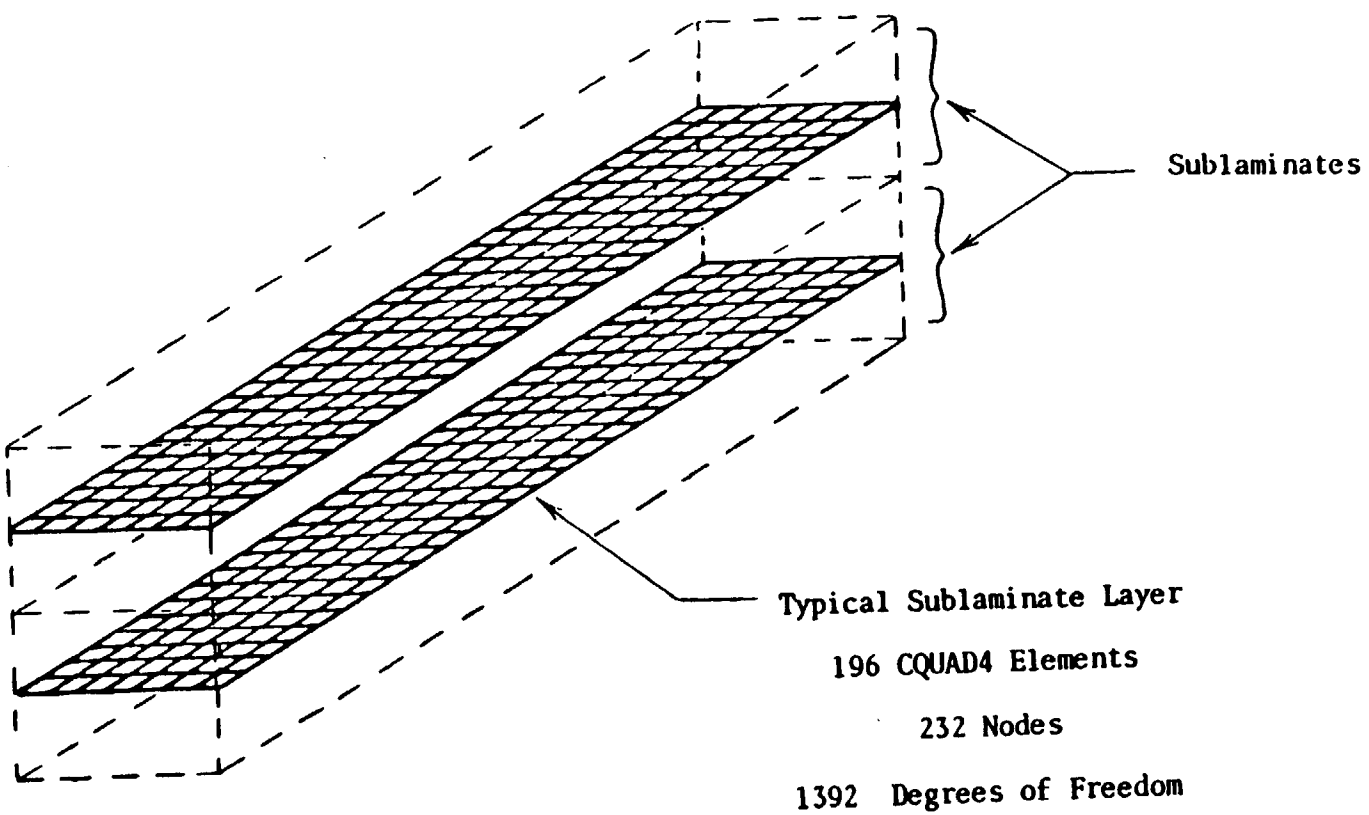

Figure 2

2.2.3 Boundary Conditions

The boundary conditions on the models are chosen so that realistic end conditions are represented. In the cases of strain energy release rate, buckling load, and axial stiffness, one end of the specimen is clamped with all six degrees of freedom restrained while the remaining end is only restrained to prevent any out-of-plane (z direction) translation. In the frequency analysis, one end remains clamped and the other end is pinned with both x and z translations restrained so that no axial displacements are allowed.

2.3 Multi-Point Constraints

2.3.1 Purpose

Since the laminated structure has been divided into a series of individual layers, it is necessary to tie these layers together. The method used to initially connect the adjacent nodes is through the use of multi-point constraints. These equations are implemented into the finite element model through a series of MPC (multi-point constraint) cards located in the bulk data deck. The constraint equations used form a linear relationship between a series of nodes. When all of the constraint equations are in effect for each and every node, all of the individual layers will combine and act as one intact laminate with no delaminations present. By releasing the constraints between the nodes, the requirements set forth are no longer in effect for those nodes, and the nodes are now free to move independent of one another. It is through the use of multi-point constraints and bending-extensional

coupling of the plate elements that progressive delamination damage is simulated in the composite structure.

2.3.2 Formulation

In the multi-point constraint equation formulation, one node is chosen to contain the independent degrees of freedom and all remaining nodes degrees of freedom are considered dependent on the first node. When developing the multi-point constraint equations for these models, the requirements of elementary beam theory are satisfied, i.e. plane sections remain plane. Also, the equations are written so as to allow bending in both the x and y directions, enabling plate behavior to be modeled. A group of five equations are written for each node; three translations and two rotations. The third rotation, that in the z-direction, is fixed for the entire model to eliminate any stiffness singularities of the CQUAD4 plate elements used here. Thus, referring to figure 3, the following constraint equations are formed. The first group of equations for the x and y translations enforce that the displacements are linearly continuous between plies, i.e. no slippage of the plies. The through-the-thickness translations between each ply are assumed to be equal, i.e. no separation of plies, and the rotations through the thickness are constant.

Multi-Point Constraints

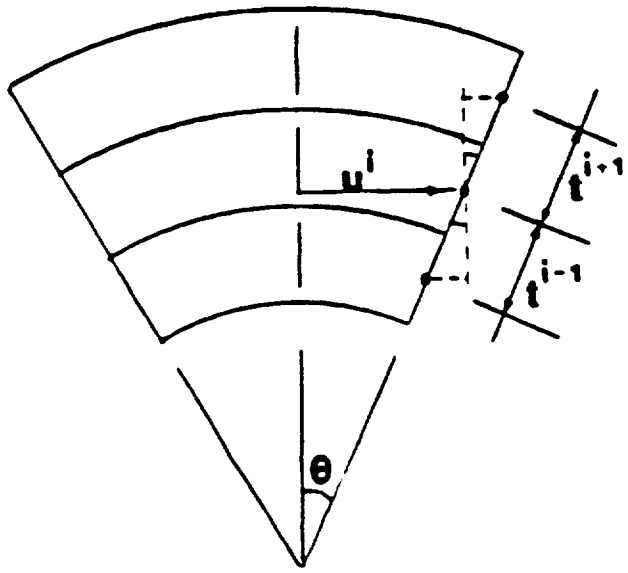

In-plane Displacements

$$u^{i+1} = u^i + \theta_y t^{i-1} \qquad u^{i-1} = u^i - \theta_y t^{i-1}$$

$$v^{i+1} = v^i + \theta_x t^{i-1} \qquad v^{i-1} = v^i - \theta_x t^{i-1}$$

Transverse Displacements

$$w^{i+1} = w^i = w^{i-1}$$

Rotations

$$\theta^{i+1} = \theta^i = \theta^{i-1}$$

Figure 3

2.4 Delamination Patterns

2.4.1 Uniform Free-Edge Delamination

In particular, the delamination patterns observed in uniaxially loaded tensile experiments are used for the free-edge delamination. In the free-edge studies, two patterns of release sequences are used. The first is shown in figure 4. This particular pattern will be referred to as uniform delamination. As can be seen in figure 4, the delamination begins in the center of each side edge for the composite specimen. The nodes are then released, according to the prescribed pattern, in a sequential manner proceeding from the center, down along the edge, and then inward towards the center of the specimen. As shown in the figure, the delamination spreads slowly along the edge in the form of an element by element advance. Once the delamination begins to spread inward, it does so in a uniform manner whereby entire rows of elements are released simultaneously. This delamination pattern is similar to that observed in experiments. The patterns observed assume a slightly parabolic shape as the delamination initially spreads inward. But, as the delamination proceeds further inward, the parabola flattens out and proceeds as a uniform shape. Thus, the pattern used here is consistent with experimental observations.

2.4.2 Pocket Free-edge Delamination

Upon closer study of the delamination patterns observed, small pockets of delamination are what initially appear along the free-edge. These pockets would be the result of the formation of transply cracks. These transply cracks are also a matrix dominated failure mode, as is

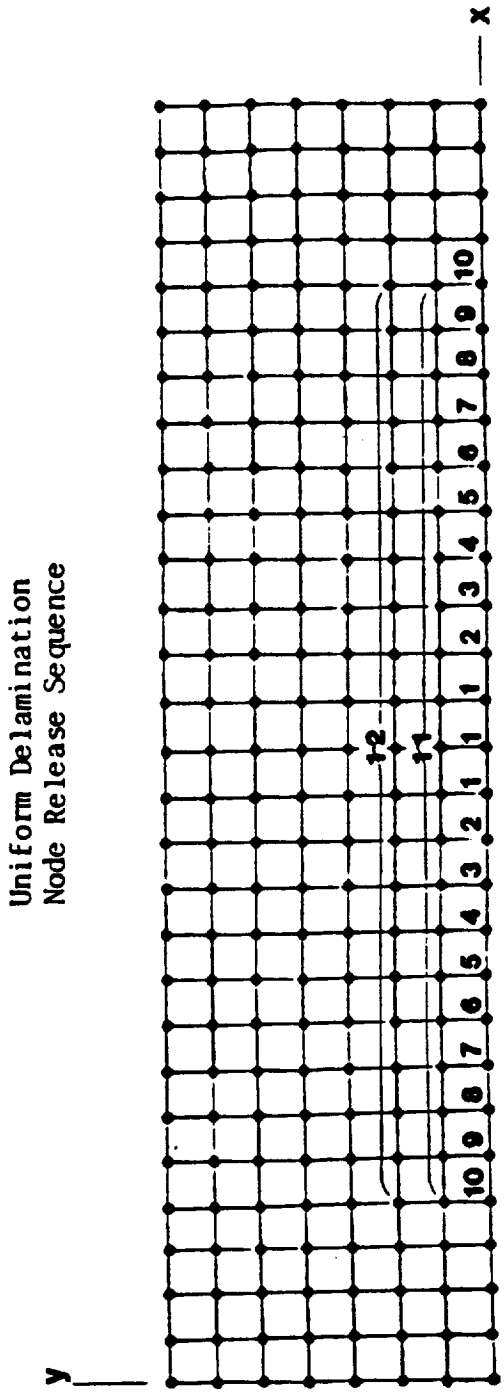
Uniform Delamination
Node Release Sequence
y
x
1 2 3 4 5 6 7 8 9 10
1 2 3 4 5 6 7 8 9 10
1 1
1 2
1 1

Figure 4

interply delamination, and occur in those plies whose strength in the load direction is also matrix dominated. The crack forms completely through the thickness of the ply and usually terminates at the interface with the adjacent ply. At this point, the crack spreads along the ply interface in the form of interply delamination. Thus, the transply cracks result in the initial formation of small pockets of delamination at the crack location. It should be noted that transply cracks are not included in the analysis. Since small pockets seem to be the pattern in which delamination initially develops, it is desirable to also simulate this pattern in the study to see if it would lead to any significant changes in the observed delamination effects. This will be referred to as the pocket delamination pattern, figure 5. The pattern is somewhat idealized, in that, the pockets initially are introduced at the center of each free-edge and then are uniformly spread along the edge. The remaining nodes are then released between the pockets to simulate the individual pockets coalescing into one large delamination along the free-edge. From this point on, the delamination proceeds as before.

2.4.3 Interior Delamination

One additional delamination pattern is used to investigate the effects of a delamination that occurs in some part of the interior of the composite. The motivation for including this type of delamination is that it could develop due to the impact of some object on the surface of the laminate. As shown in figure 6, the delamination is initially taken as a small square region in the center of the laminate. This delamination is then spread down the length and then outward towards the free-edges of the laminate.

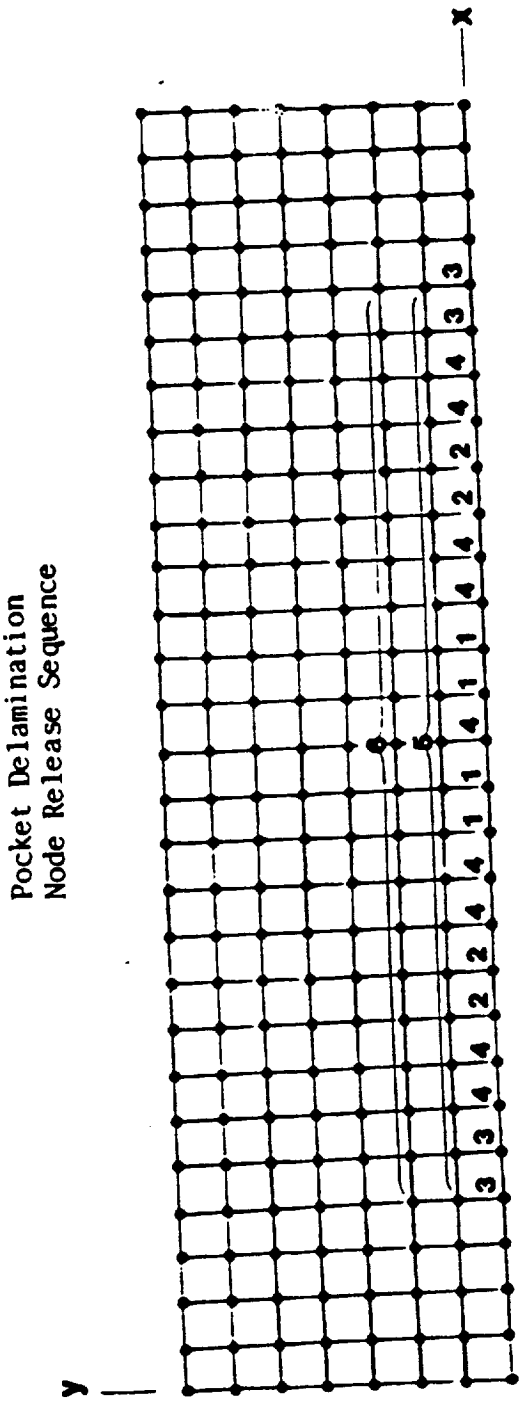

Figure 5

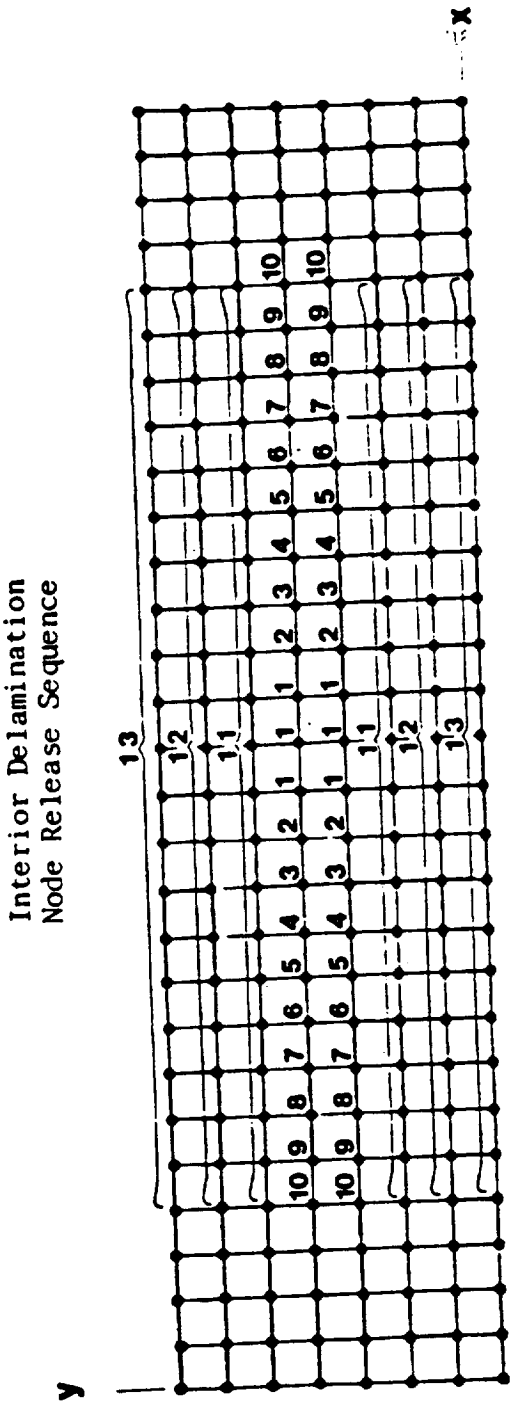
Interior Delamination
Node Release Sequence
y
x
13
12
11
10
9
8
7
6
5
4
3
2
1

Figure 6

2.5 Strain Energy Release Rate

The use of strain energy release rate (SERR) is one of the commonly used indicators of how susceptible a particular laminate is to delamination. In effect, the strain energy release rate gives a measure of the amount of energy that is required to propagate a defect in the laminate. The strain energy release rate has also been used to measure the fracture toughness of the laminate. At the point of interply delamination or transply cracking, the greater the amount of energy released, the more likely the particular damage state will occur for that laminate configuration. The strain energy release rate allows a direct comparison of the damage tolerance between different laminate materials, configurations and geometries. This provides the capability to see particular delamination influences, such as, thickness effects, material property dependence, etc.

The methods used to calculate the strain energy release rate are many. One of those commonly used is the crack closure method. In this method, nodal displacements and nodal forces, at the crack tip location, are used to determine the amount of work required to close the crack which has been extended by an incremental amount. This in turn will provide a measure of the amount of energy available to propagate the crack further. This approach can be considered as a local level approach.

Since the objective of this study is to characterize the effects of delamination using the overall structural response of the laminate, a global approach is used to calculate the strain energy release rate.

In this global approach, the work produced is calculated by considering the nodal displacements and nodal forces located at the end of the simulated specimen. The nodal forces are the applied loads used in the tensile loading case, and the nodal displacements are those at the same end nodes at which the load is applied. The equation given below is that used to calculate the strain energy release rate G,

$$G = \frac{dW}{dA} = \frac{1}{2} \frac{(F_2) - (F_1)}{A}$$

F = Loads applied at end nodes

U = Displacements at end nodes

A = Change in delaminated area

which simply stated, is the incremental change in work divided by the incremental change in the delaminated area. The applied tensile load F remains constant and the delaminated area is the amount of additional surface area that is "opened" for that particular node release step. The nodes are released according to the patterns discussed previously.

2.6 Laminate Post-Buckling Analysis

2.6.1 Modeling Considerations

An additional area of interest investigated in this study is the localized buckling behavior of a group of delaminated plies. Here, the delamination is modeled as a group of plies which have "popped-out", i.e. separated, from the remaining part of the laminate. It is the objective of this case to determine how this delaminated region of the laminate behaves as the laminate is subjected to an increasing compressive axial load. In effect, a post-buckling analysis is performed on the laminate.

As is consistent with the other models in this study, the laminate is divided into two sublaminates at the point where the delamination is desired to occur. A single delamination is modeled in a position offset from the center using the 14-ply laminate (refer to figure 1E). One sublaminate layer represents the [$\pm$30/90] plies and the other sublaminate layer represents the remaining [$\pm$30/90_4/$\pm$30/90/$\pm$30] plies. Since the laminate is to be modeled with an initial "pop-out", the initial coordinates of the nodes in the "pop-out" area are given a sinusoidal shape to simulate this "pop-out", figure 7. Note that in the delaminated area a finer mesh is used to allow a smooth sinusoidal curve to be used to represent the initial shape of the "pop-out". The initial separation distance between the "pop-out" sublaminate and the remaining laminate is set equal to the thickness of the delaminated plies (0.015 in.). No multi-point constraints are used in the "pop-out" area since the two sublaminates have separated and are independent of one another. The remaining adjacent nodes of the two sublaminates are connected using multi-point constraints of the same formulation discussed in section 2.3.

In order to see if boundary conditions have any influence on the buckling behavior, two sets of boundary conditions are used. One laminate is analyzed as a simply supported column and another is analyzed as a clamped-clamped column.

Laminate "Pop-Out" Model

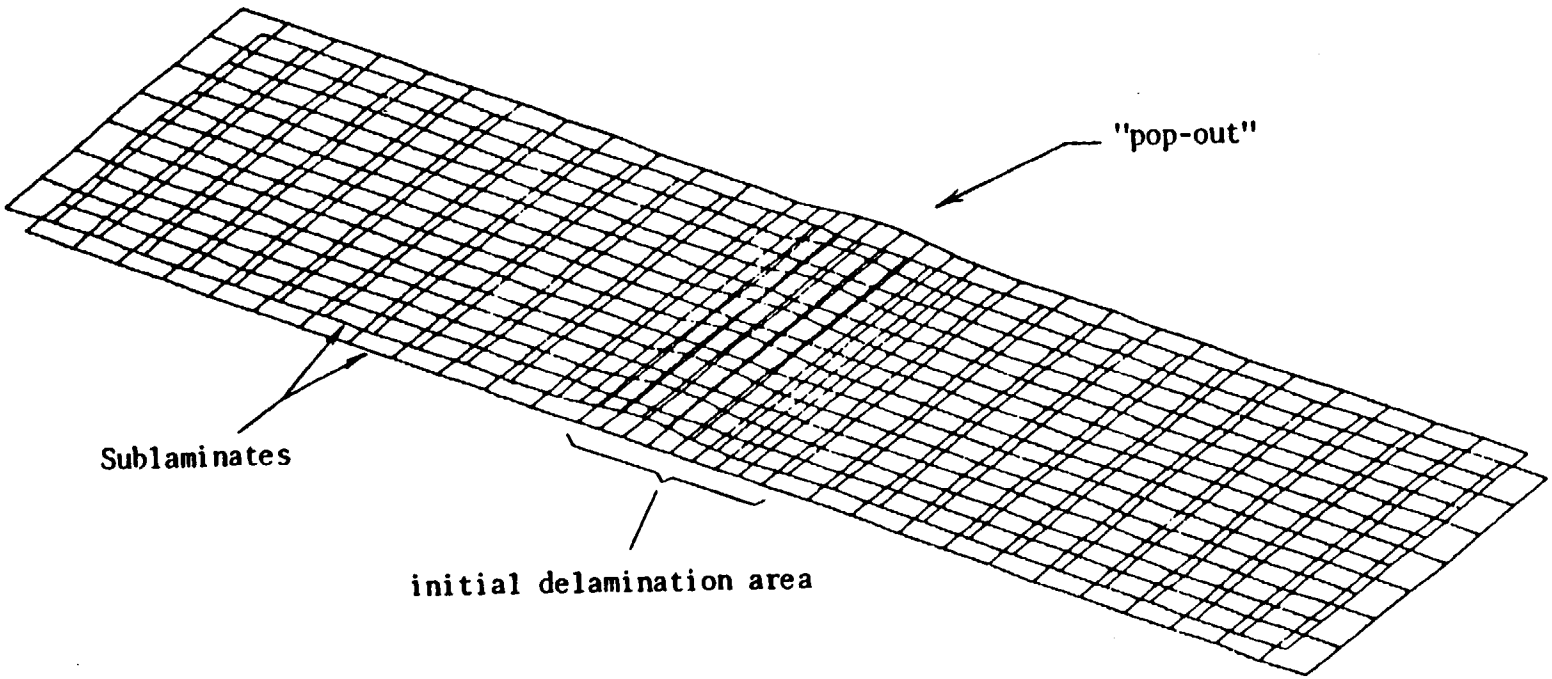

Figure 7

2.6.2 Geometry Updating

The objective of this particular case is to observe the behavior of a laminate with an initial through-the-width delamination. Specifically, since the sublaminate in the area of delamination has buckled locally, it remains to be seen how the laminate behaves as the laminate continues to deform. Thus, the post-buckling behavior of the laminate needs to be simulated, which is a nonlinear problem. As the compressive axial load is increased, the laminate bends further and changes shape. Therefore, it is necessary in the analysis to account for the changes in the geometric stiffness due to the excessive bending of the laminate. In order to do this, the shape of the laminate used in the finite element analysis must be updated as the load is increased.

Instead of using the nonlinear capabilities of MSC/NASTRAN, a small computer program is used to update the geometry so that a linear static solution sequence can be used. The computer program simply takes the output displacements from a run with a given load and adds these displacements to the original nodal coordinates. This produces a new, updated laminate shape. The load is then increased and the analysis rerun. Since the geometry is updated, the geometric stiffness now reflects the effects of the previous load increase. It is hoped that this approach will demonstrate that the large-displacement, geometric nonlinear problem can be approximated using a linear finite element analysis.

2.6.3 Analysis

The analysis for this particular case is conducted in two phases. In the first phase, each laminate, the simply supported and clamped-clamped, is subjected to an increasing compressive axial load. The object of this phase is to observe how the laminate behaves in the post-buckled state. The sequence of steps used in the analysis of this phase are as follows. The laminate is given an initial shape as shown in figure 7. A load is applied and the analysis is run using MSC/NASTRAN. The results from this run is then processed by the computer program discussed previously. The program produces an updated laminate geometry in the form of new grid point data. The user then substitutes the new grid data into the bulk data deck, increments the load, and re-runs the analysis. This sequences of steps are repeated until the lateral displacement of the column rapidly increases, indicating a total buckling of the laminate.

In the next phase, for specific post-buckled laminate shapes, the delamination area is increased according to the pattern shown in figure 8. In this phase, as the delamination area is increased, the load is held constant and a corresponding strain energy release rate is calculated as described in Sec. 2.5.

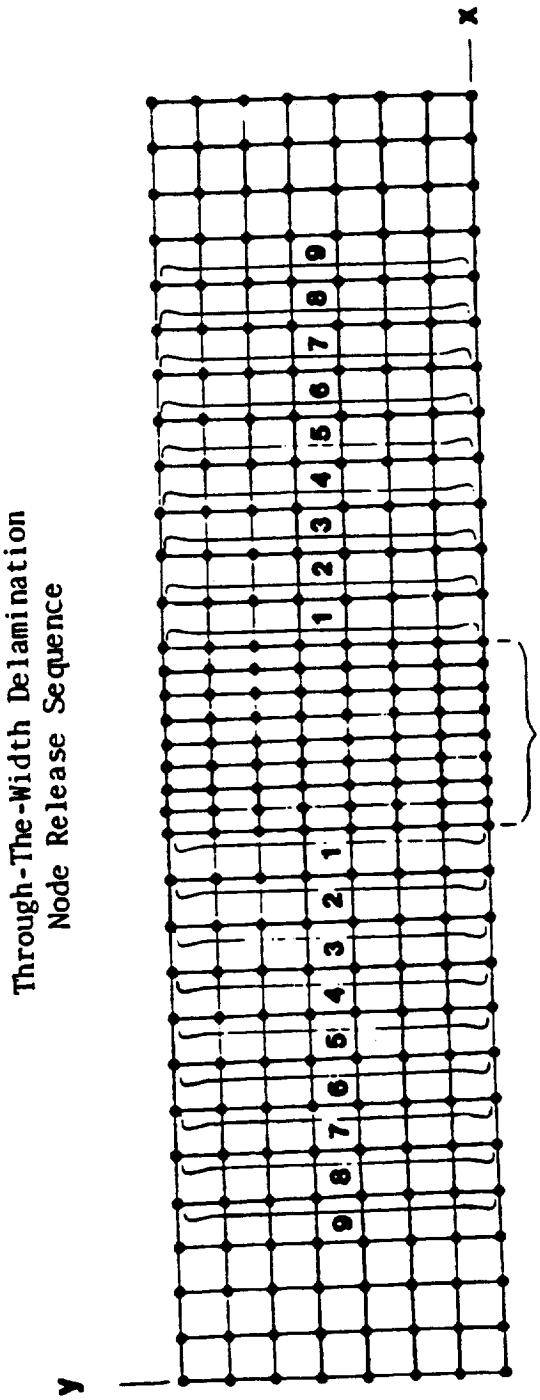
Through-The-Width Delamination
Node Release Sequence
x
y
1
2
3
4
5
6
7
8
9
initial delamination area

Figure 8

CHAPTER 3

RESULTS

3.1 Cases Studied

Since the damage mechanism of delamination is a complex process, a sufficient number of cases needs to be studied in order to investigate delamination effects on composite structural behavior, Table 1. The study is conducted using a variation in material properties, laminate configurations and thicknesses. Also, an area of interest is thickness effects on delamination, therefore, single and multiple delaminations through the thickness are studied. Three different material systems, AS-Graphite/Intermediate Modulus High Strength (AS/IMHS), AS-Graphite/ High Modulus High Strength (AS/HMHS), S-Glass/Intermediate Modulus High Strength (S-G/IMHS), are used to allow for fiber and matrix influences. In the first two systems, intermediate and high modulus matrix materials are used with a graphite fiber to see the influence of matrix stiffness variation. The last system, S-G/IMHS, has a lower stiffness fiber giving a much lower overall stiffness as compared to the graphite fiber systems. Table 2 gives both the fiber and matrix properties used in this study.

Table 1

Summary of Cases Studied

CASES	STATIC LOAD TENSILE		BUCKLING LOAD	VIBRATION FREQUENCY
	Axial Stiffness	Strain Energy Release Rate		
FREE-EDGE DELAMINATION:				
6-PLY CENTER				
$[+30/90]_S$				
AS/IMHS	*	*	*	*
AS/HMHS	*	*	*	*
S-G/IMHS	*	*	*	*
14-PLY CENTER				
$[+30/90/+30/90_2]_S$				
AS/IMHS	*	*	*	*
AS/HMHS	*	*	*	*
S-G/IMHS	*	*	*	*
14-PLY OFFSET				
$[+30/90/+30/90_2]_S$				
AS/IMHS	*	*	*	*
AS/HMHS	*	*	*	*
S-G/IMHS	*	*	*	*
INTERIOR DELAMINATION:				
6-PLY CENTER				
$[+30/90]_S$				
AS/IMHS		*		
AS/HMHS		*		
S-G/IMHS		*		

Table 2

FIBER PROPERTIES

Property			Fiber	
QUANTITIES	SYMBOLS	UNITS	AS	S-G
Density	ρ_m	lb/in^3	0.063	0.090
Long. modulus	E_{f11}	10^6 psi	31.0	12.4
Transv. modulus	E_{f22}	10^6 psi	2.0	12.4
Long. shear modulus	G_{f12}	10^6 psi	2.0	5.17
Transv. shear modulus	G_{f23}	-------	1.0	5.17
Long. Poisson's ratio	ν_{f12}	-------	0.20	0.20
Transv. Poisson's ratio	ν_{f23}		0.25	0.20

MATRIX PROPERTIES

Property			Matrix	
QUANTITIES	SYMBOLS	UNITS	IMHS	HMHS
Density	ρ_m	lb/in^3	0.044	0.045
Elastic modulus	E_m	10^6 psi	0.50	0.75
Shear modulus	G_m	10^6 psi	-----	-----
Poisson's ratio	ν_m	-------	0.35	0.35

Note: shear property is an estimate only, $G_m = E_m/(2*(1+\nu_m))$.

Two laminate configurations, $[\pm 30/90]_s$ and $[\pm 30/90/\pm 30/90_2]_s$, are chosen to observe any thickness effects. The configuration $[\pm 30/90]_s$ has a delamination located between the 90/90 plies. This will be referred to as 6-ply center delamination. The configuration $[\pm 30/90/30/90_2]_s$ is analyzed in two cases, a single delamination at the plane of symmetry and a second case where a delamination is offset from the center at the $90/\pm 30$ interface. These cases will be referred to as 14-ply center and 14-ply offset, respectively. Figure 9 gives an explanation of the delamination nomenclature that is used throughout the discussion of results.

Finally, two cases concerning localized buckling behavior of a near surface through-the-width delamination are investigated. The first case deals with how the "popped-out" plies behave as a gradually increasing compressive load is applied to the post-buckled laminate. Here, the amount of delaminated area is held constant at 14%. A second case is also considered where the initial delaminated area is allowed to increase and the corresponding strain energy release rate is calculated. Both of these cases use the 14-ply laminate.

3.2 Delamination Simulation

The two laminates in figure 10 show the results of the method presented here in effectively simulating the delamination process under investigation. Both of the laminates shown in the figure are under a uniaxial tensile load. In the areas where the multi-point constraints have been released, the individual layers of elements have separated and a delamination area has opened up. In the approach used here, the

Delamination Nomenclature

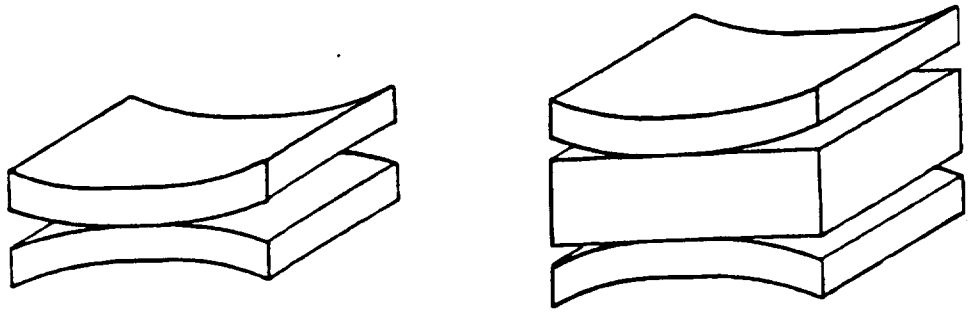

Center

Offset

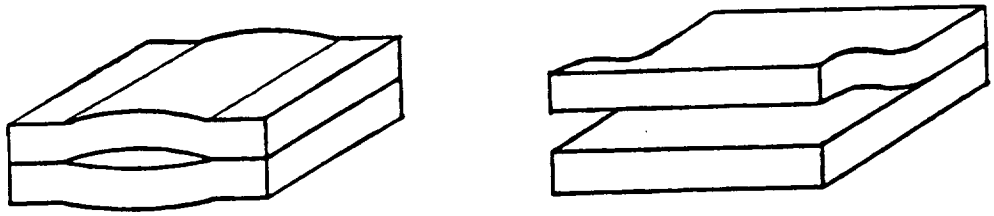

Interior

Through-The-Width

Figure 9

Delamination Simulation Results

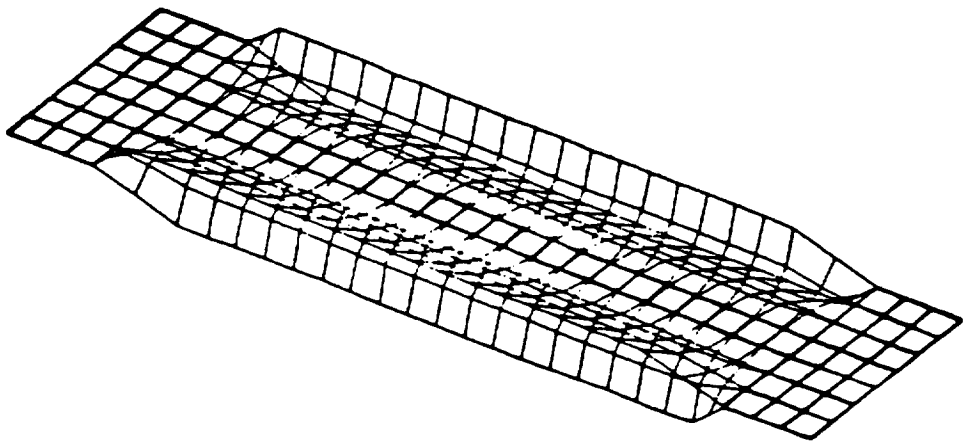

uniform

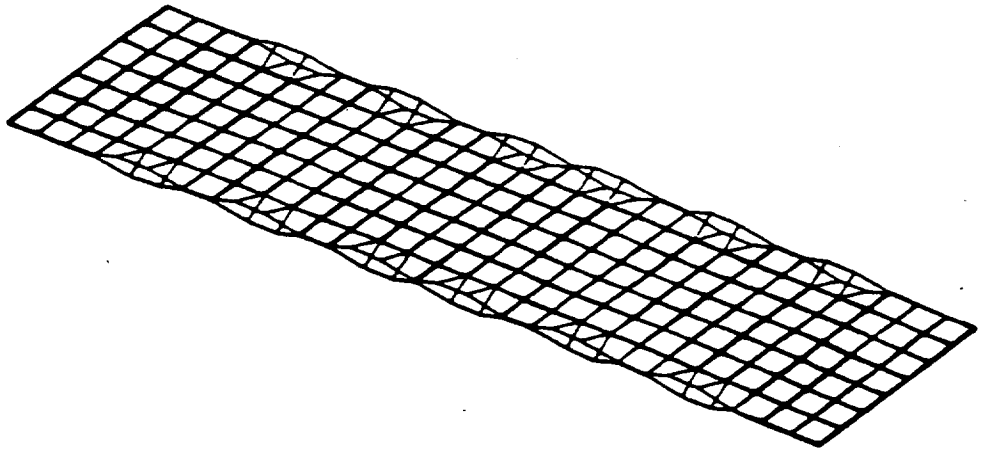

pocket

Figure 10

delamination area opens due to the curling of the adjacent layers of plate elements.

Figure 11 shows a typical cross-section of both the center and multiple delamination models and the curling of the sublaminate plate elements can be clearly seen. The bending-extensional coupling, which is characteristic of nonsymmetric angle-ply laminates, is what causes the sublaminates to curl and separate from one another. Recall that these elements contain the material properties of the corresponding sublaminate that they represent and, although the overall laminate is symmetric, the group of individual layers are nonsymmetric, thus accounting for the bending-extensional coupling effects. Therefore, with this methodology, the simulation of delamination damage in laminated composite structures can be studied on a three-dimensional level, yet utilize rather simple plate-bending finite element models.

3.3 Fracture Toughness

To evaluate the structural fracture toughness, a uniaxial tensile load of 28,000 lbs. is applied to the laminate. The magnitude of the load is that which produces the high interlaminar stresses required for delamination, as determined by a previous three-dimensional finite element analysis [4].

The first series of results for the fracture toughness, in terms of strain energy release rate (SERR), of the various laminates are described below. A comparison between the 6-ply center and 14-ply center, using AS/IMHS, shows a decrease in SERR as the overall laminate thickness increases, figure 12. This means that as the laminate thickness

Laminate Cross-Sections

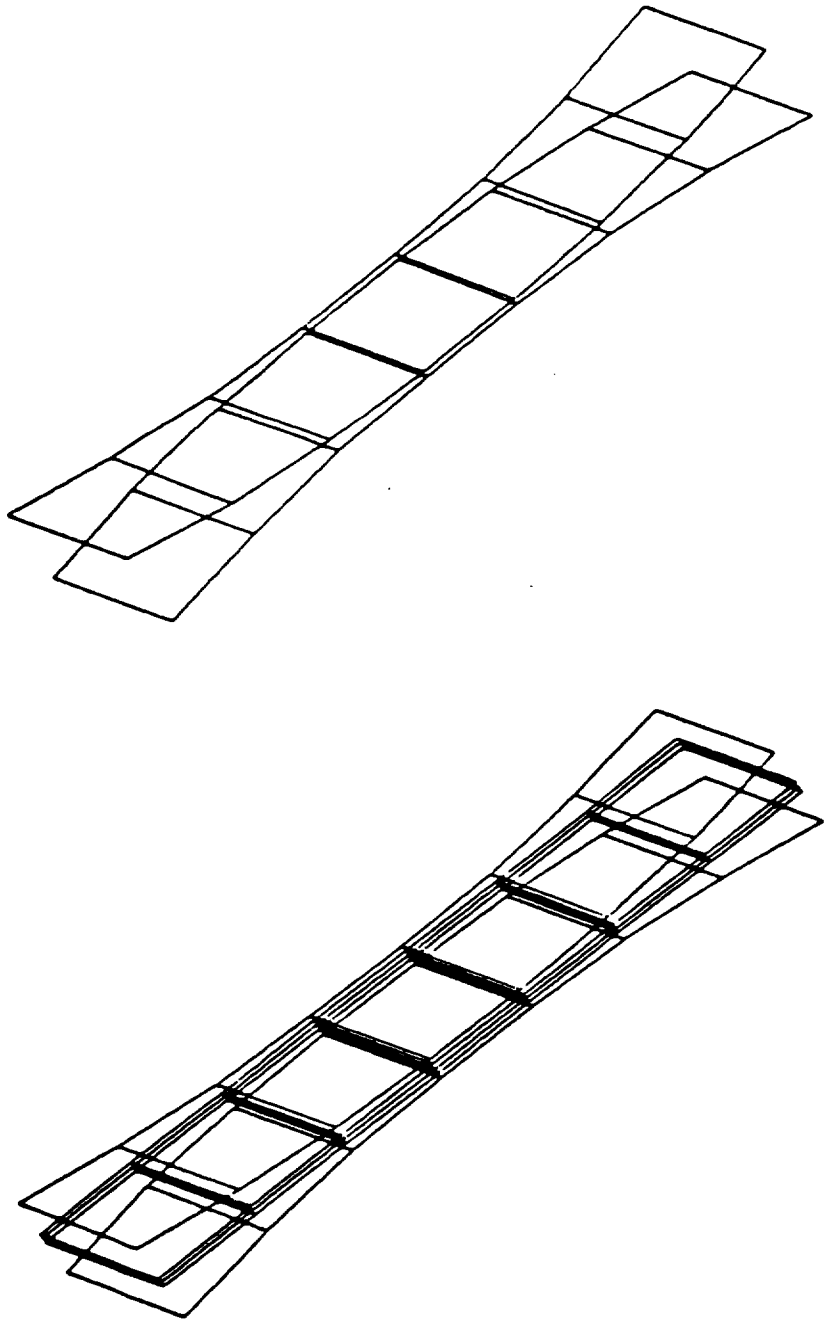

Figure 11

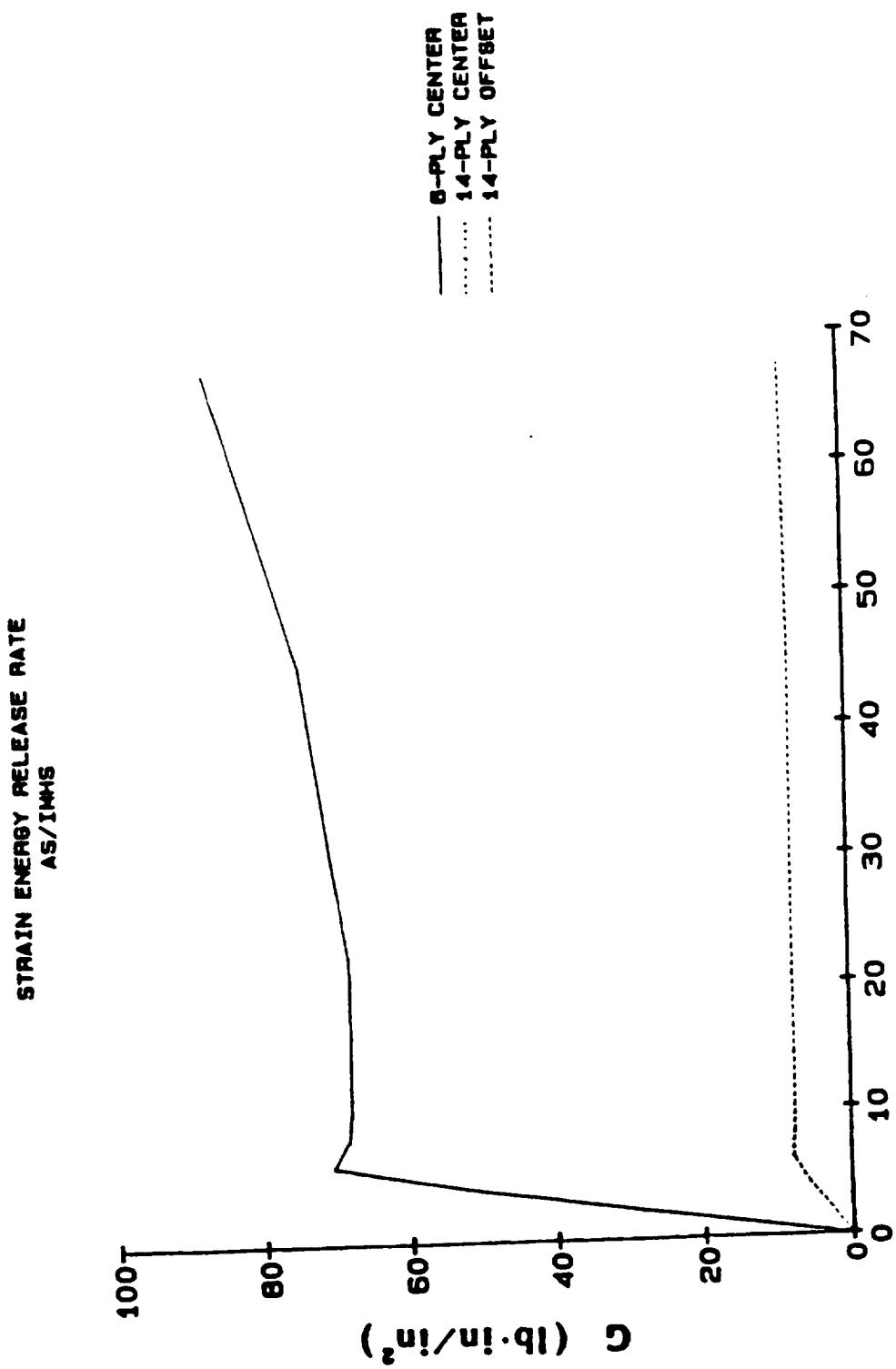
STRAIN ENERGY RELEASE RATE
AS/IM6
8-PLY CENTER
14-PLY CENTER
14-PLY OFFSET
G (lb·in/in²)
100
80
60
40
20
0
0
10
20
30
40
50
60
70
% AREA DELAMINATED

Figure 12

increases, a given delamination is less likely to propagate. Not only does the magnitude of the SERR decrease, but also the curve flattens out. Thus, the delamination crack growth process becomes more stable for a constant load, and for the delamination to propagate, the load would need to be increased. Note also in figure 12, that the SERR for the 14-ply center and 14-ply offset cases is the same. This means that the same amount of energy is needed to produce single or multiple delaminations in a given laminate.

The next series of figures, 13-15, serve to show how the strain energy release rate is affected by different materials. Comparing the AS graphite fiber composite systems in figure 13, the IMHS matrix has a higher SERR than that of the stiffer HMHS matrix composite. This means that the weaker composite, AS/IMHS, is more likely to delaminate than the AS/HMHS composite. Since the S-G/IMHS composite is less stiff than the AS/IMHS composite, it is expected to have a higher SERR. But as shown in figure 13, the S-G/IMHS composite has the lowest SERR of all the composite systems and is, therefore, the least likely to delaminate. This trend is also observed in the 14-ply center, Figure 14, and 14-ply offset cases, Figure 15.

Some results that are of particular interest are those dealing with the pocket delamination pattern. Recall that it was believed that this type of initial delamination is representative of experimental observations. The results in figures 16-18 support this view. Note the large jump in SERR. This large amount of strain energy released corresponds to the point where all of the individual pockets of delamination

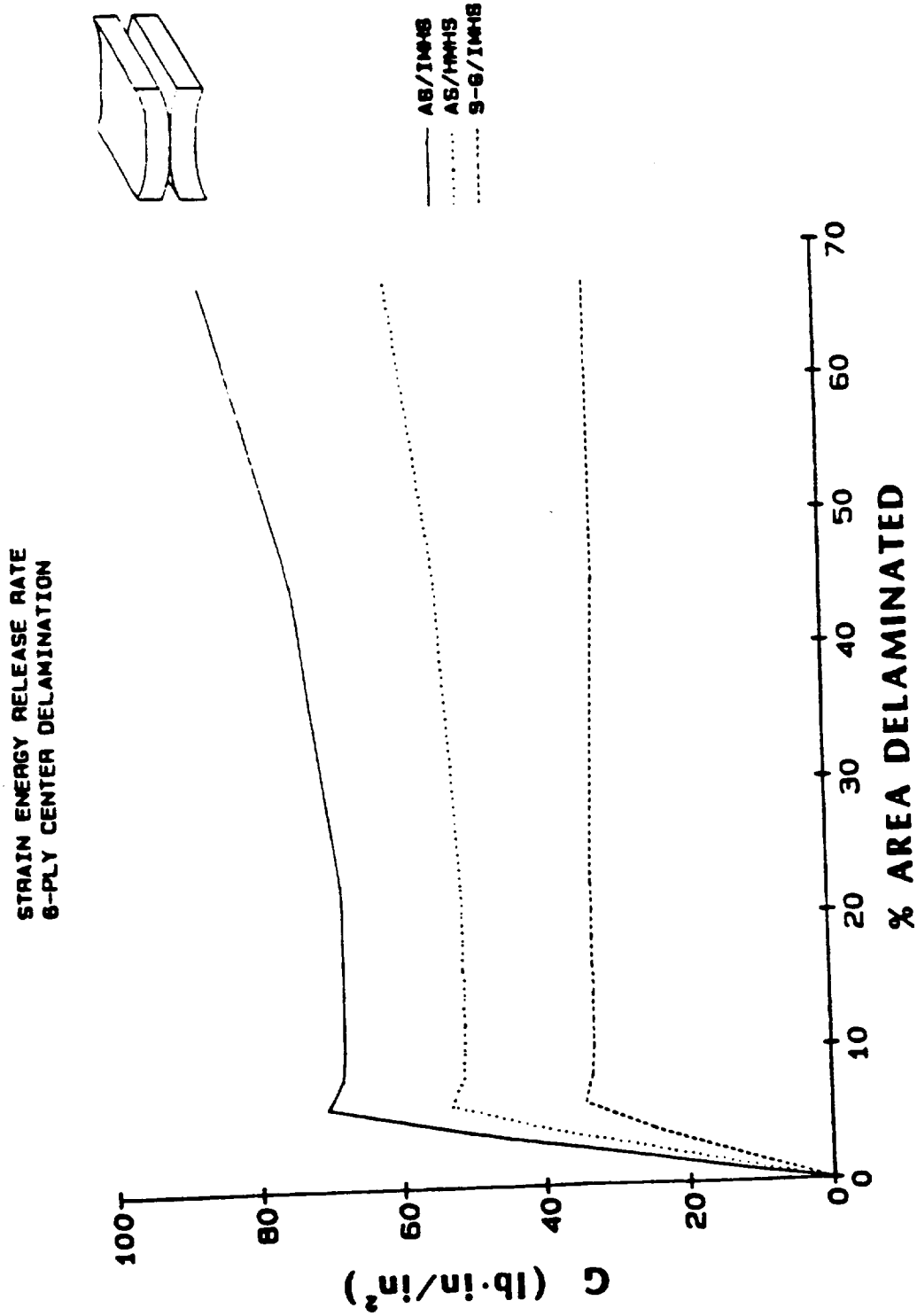
STRAIN ENERGY RELEASE RATE
6-PLY CENTER DELAMINATION
AS/IM6S
AS/HM1S
S-G/IM6S
G (lb·in/in²)
100
80
60
40
20
0
0
10
20
30
40
50
60
70
% AREA DELAMINATED

Figure 13

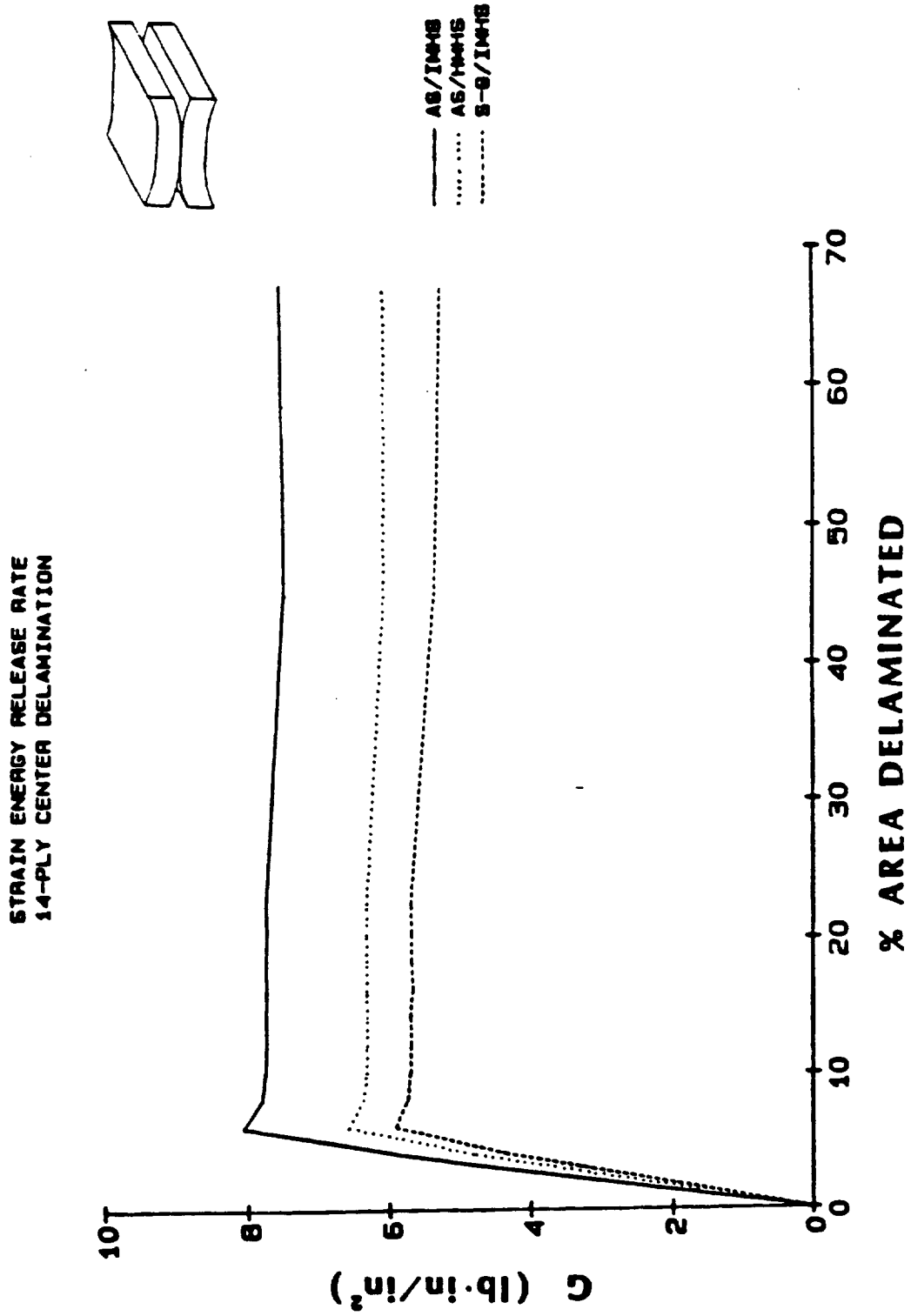
STRAIN ENERGY RELEASE RATE
14-PLY CENTER DELAMINATION
AS/IM7B
AS/HMHS
S-G/IM7B
G (lb·in/in²)
% AREA DELAMINATED
0
2
4
6
8
10
0
10
20
30
40
50
60
70

Figure 14

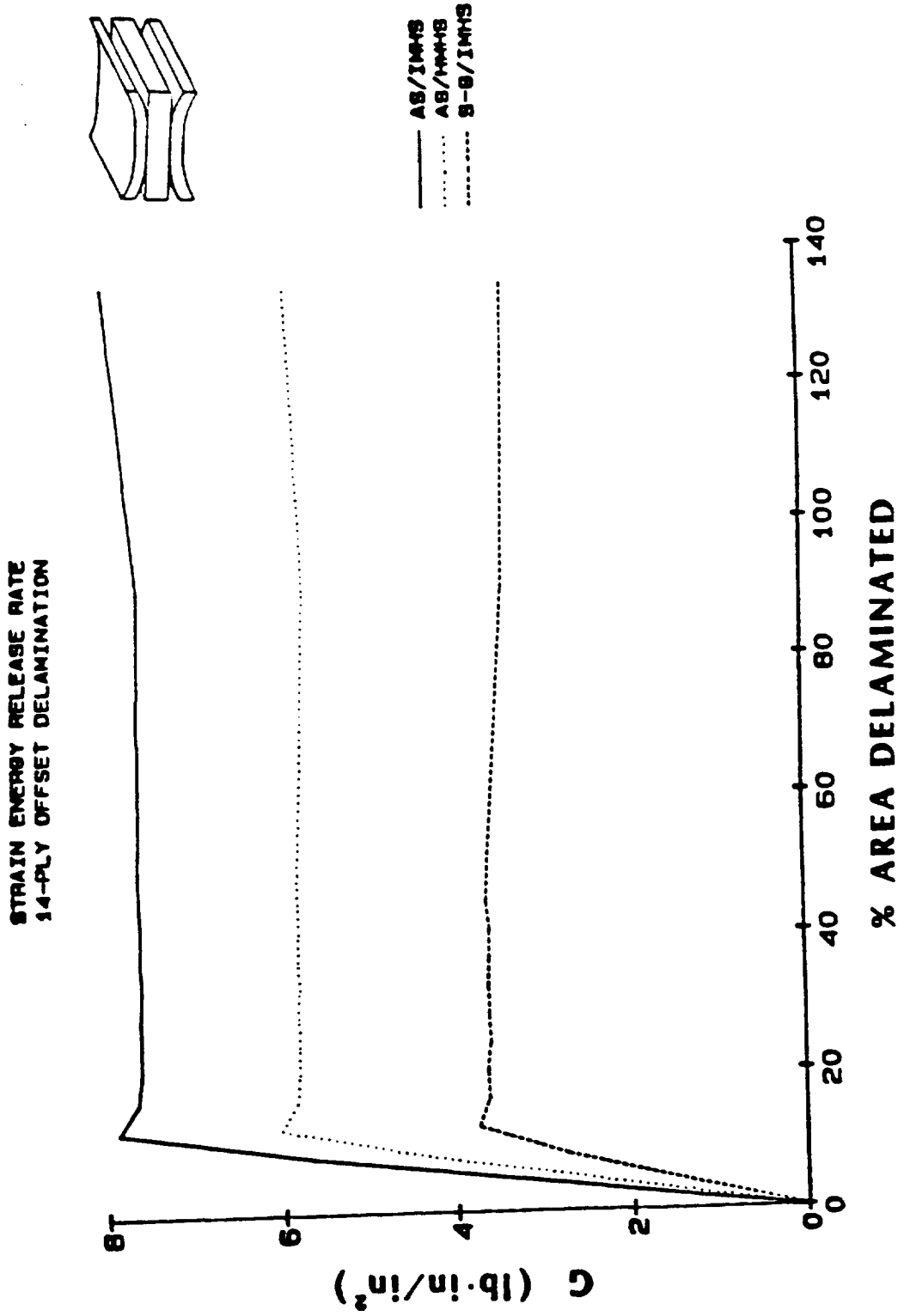
STRAIN ENERGY RELEASE RATE
14-PLY OFFSET DELAMINATION
AS/IM3
AS/MM3
S-G/IM3
G (lb·in/in²)
% AREA DELAMINATED
0
2
4
6
8
0
20
40
60
80
100
120
140

Figure 15

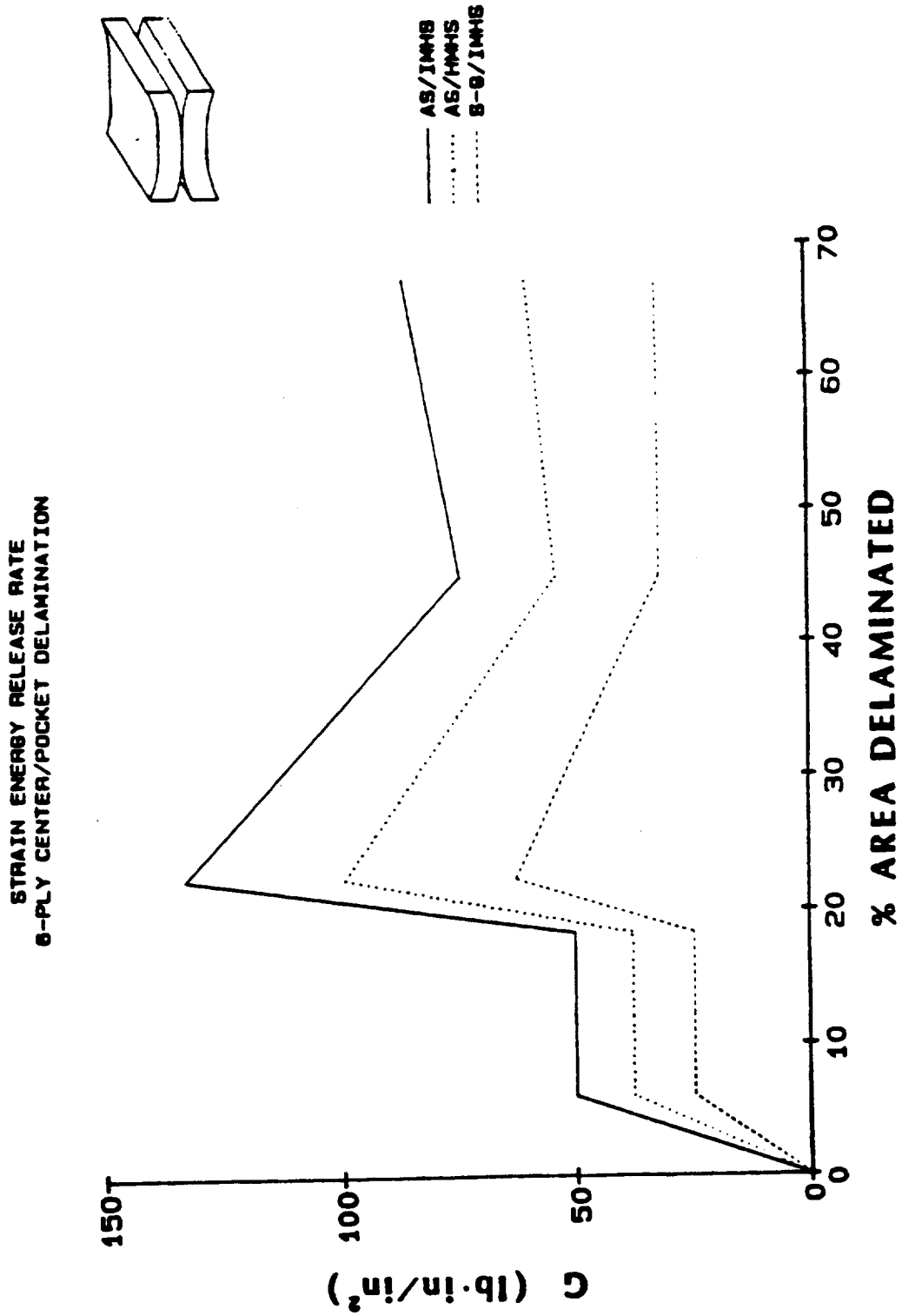
STRAIN ENERGY RELEASE RATE
8-PLY CENTER/POCKET DELAMINATION
AS/IM6
AS/HMS
S-G/IM6
G (lb·in/in²)
150
100
50
0
0
10
20
30
40
50
60
70
% AREA DELAMINATED

Figure 16

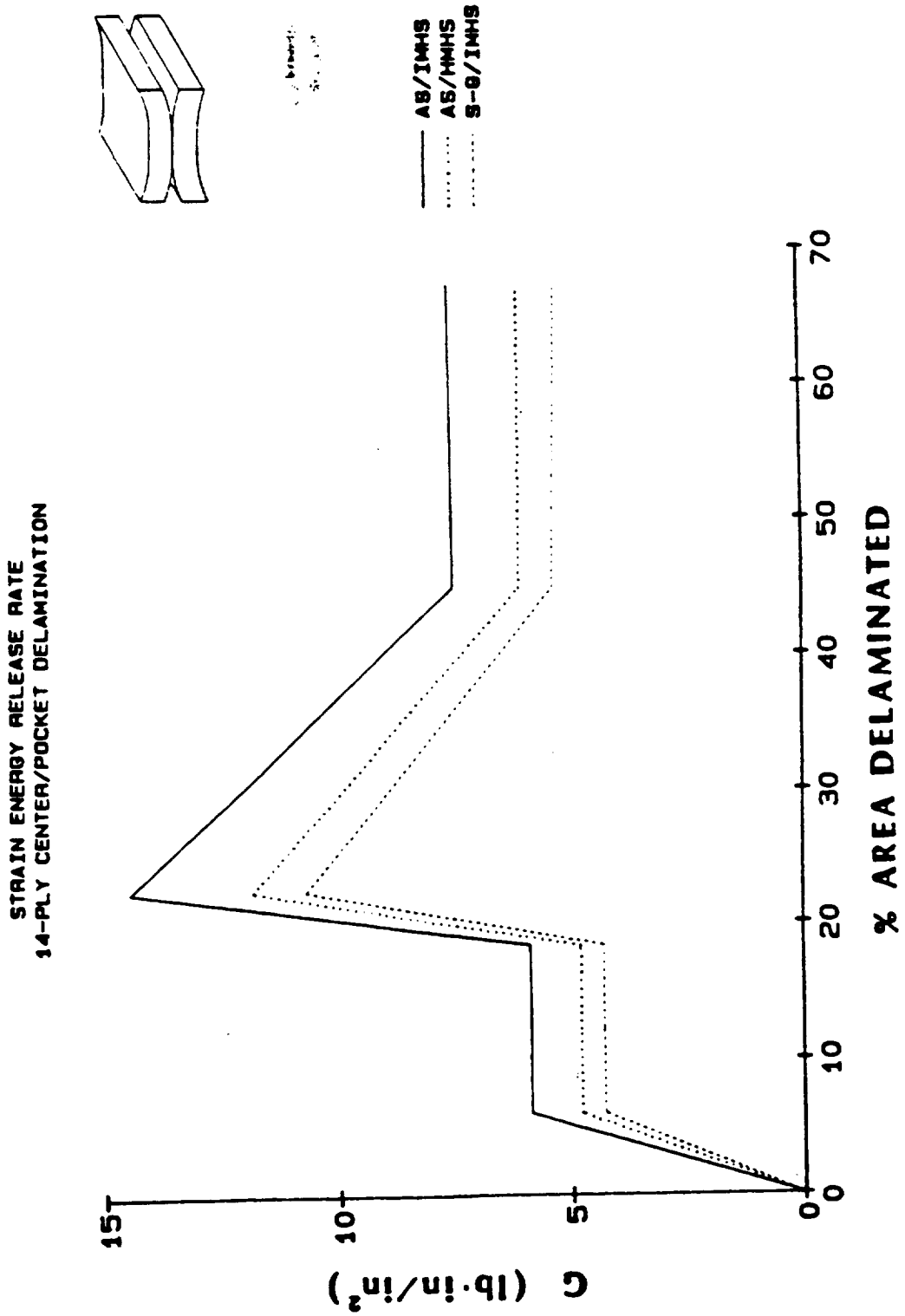
STRAIN ENERGY RELEASE RATE
14-PLY CENTER/POCKET DELAMINATION
AS/IMHS
AS/HMHS
S-G/IMHS
G (lb·in/in²)
15
10
5
0
0
10
20
30
40
50
60
70
% AREA DELAMINATED

Figure 17

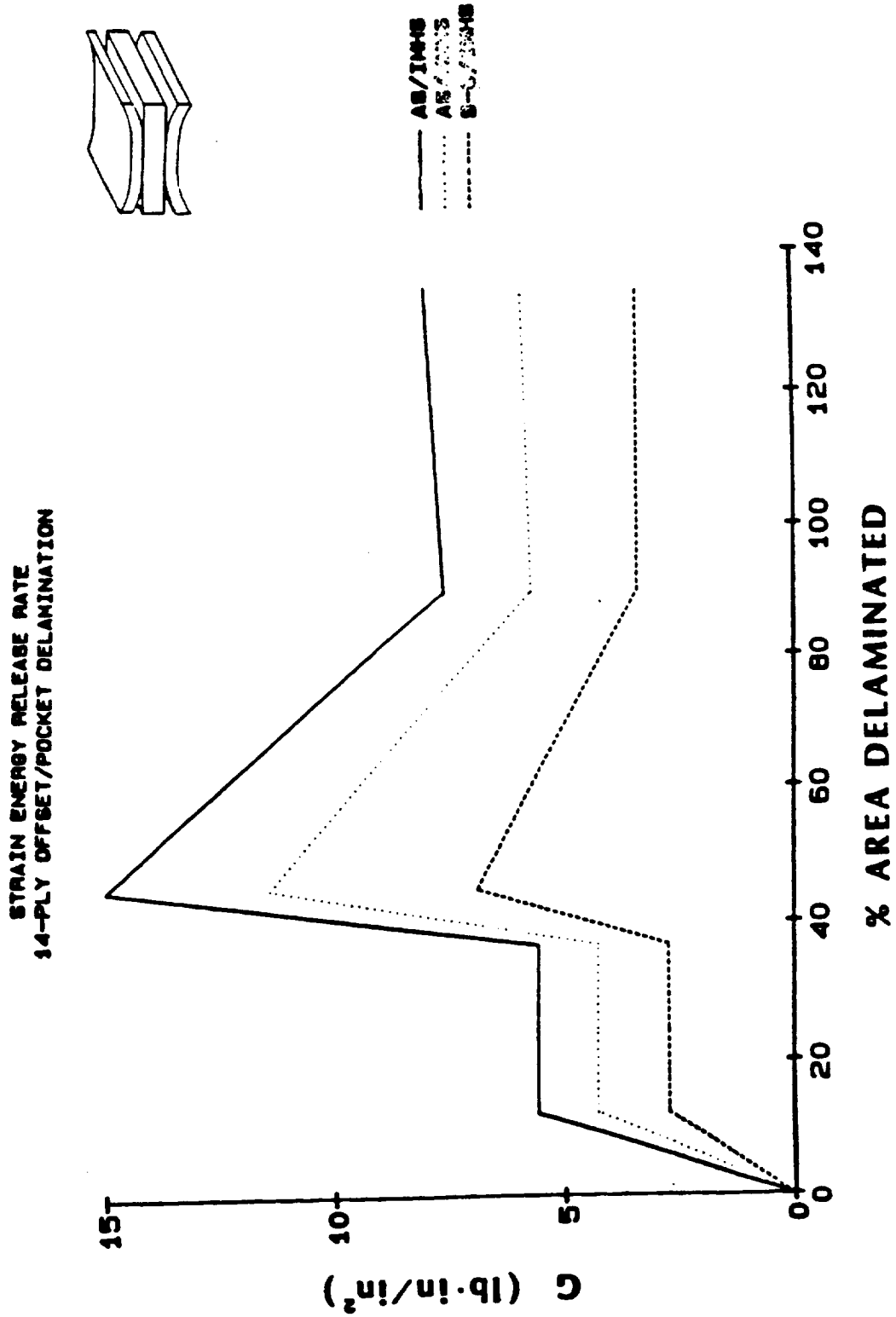
STRAIN ENERGY RELEASE RATE
14-PLY OFFSET/POCKET DELAMINATION
AS/IM6
G (lb·in/in²)
15
10
5
0
0
20
40
60
80
100
120
140
% AREA DELAMINATED

Figure 18

are combined into one uniform delamination along the edge. Because there is a larger amount of energy released, as compared to the uniform delamination pattern, it can be concluded that the pockets will initially appear and then coalesce into one uniform delamination along the edge.

In addition to free-edge delamination, a case of interior delamination is simulated. The effects evaluated in terms of SERR, show that as the delamination is increased, there is no corresponding release of strain energy, figure 19. Not until the delamination is allowed to extend totally through the width of the model, is there any measurable strain energy released. Thus, it can be concluded that any form of interior delamination that is present will not propagate under a tensile load.

3.4 Structural Response

One of the objectives of this study is to evaluate what effects delamination has on the structural response of a composite laminate. Figures 20-37 show in detail how delamination affects axial stiffness, buckling load and vibration frequency for the 6-ply center, 14-ply center, and 14-ply offset cases. The results obtained show a linear degradation for each of these structural responses as the delaminated area propagates. Also from the figures it can be noted that the amount of degradation does not become large until a significant amount, almost 80%, of delamination is present. In Table 3, the results from the previous figures are summarized in terms of the total percent reduction in axial stiffness, buckling load and first mode vibration frequency.

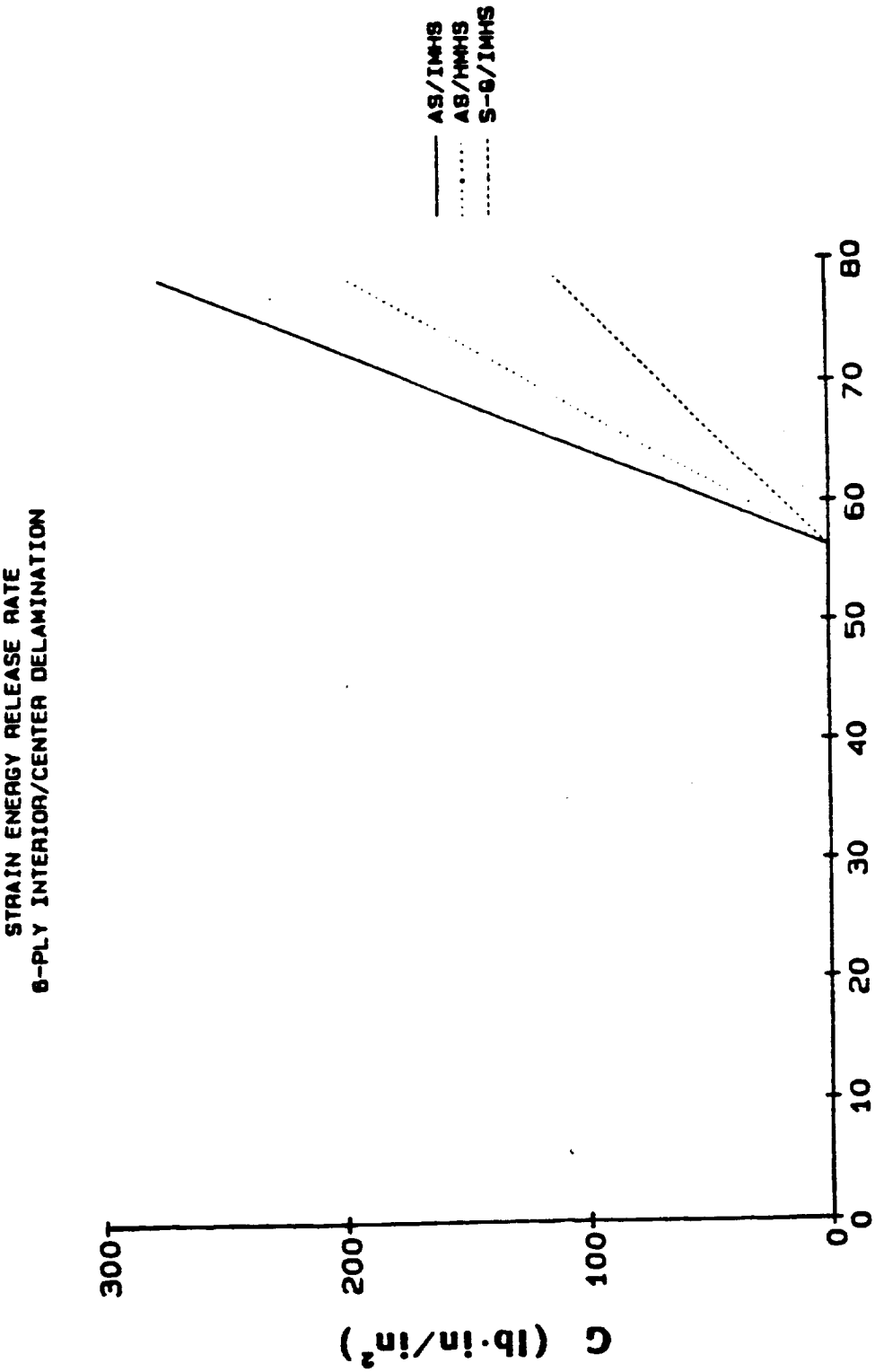
STRAIN ENERGY RELEASE RATE
8-PLY INTERIOR/CENTER DELAMINATION
AS/IM6S
AS/HM6S
S-6/IM6S
G (lb·in/in²)
300
200
100
0
0
10
20
30
40
50
60
70
80
% AREA DELAMINATED

Figure 19

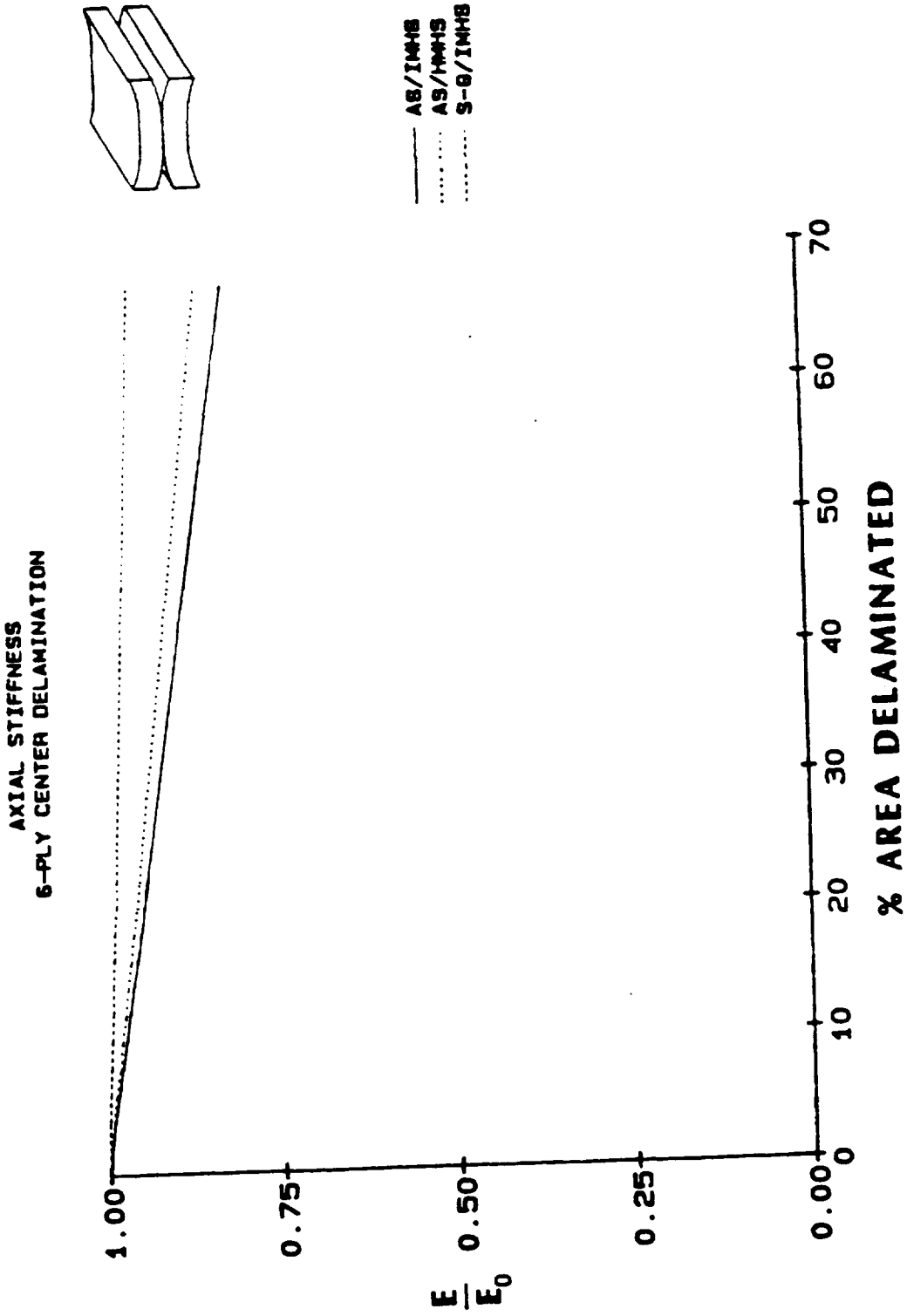
AXIAL STIFFNESS
6-PLY CENTER DELAMINATION
AS/IM7S
S-G/IM7S
1.00
0.75
0.50
0.25
0.00
E/E0
0
10
20
30
40
50
60
70
% AREA DELAMINATED

Figure 20

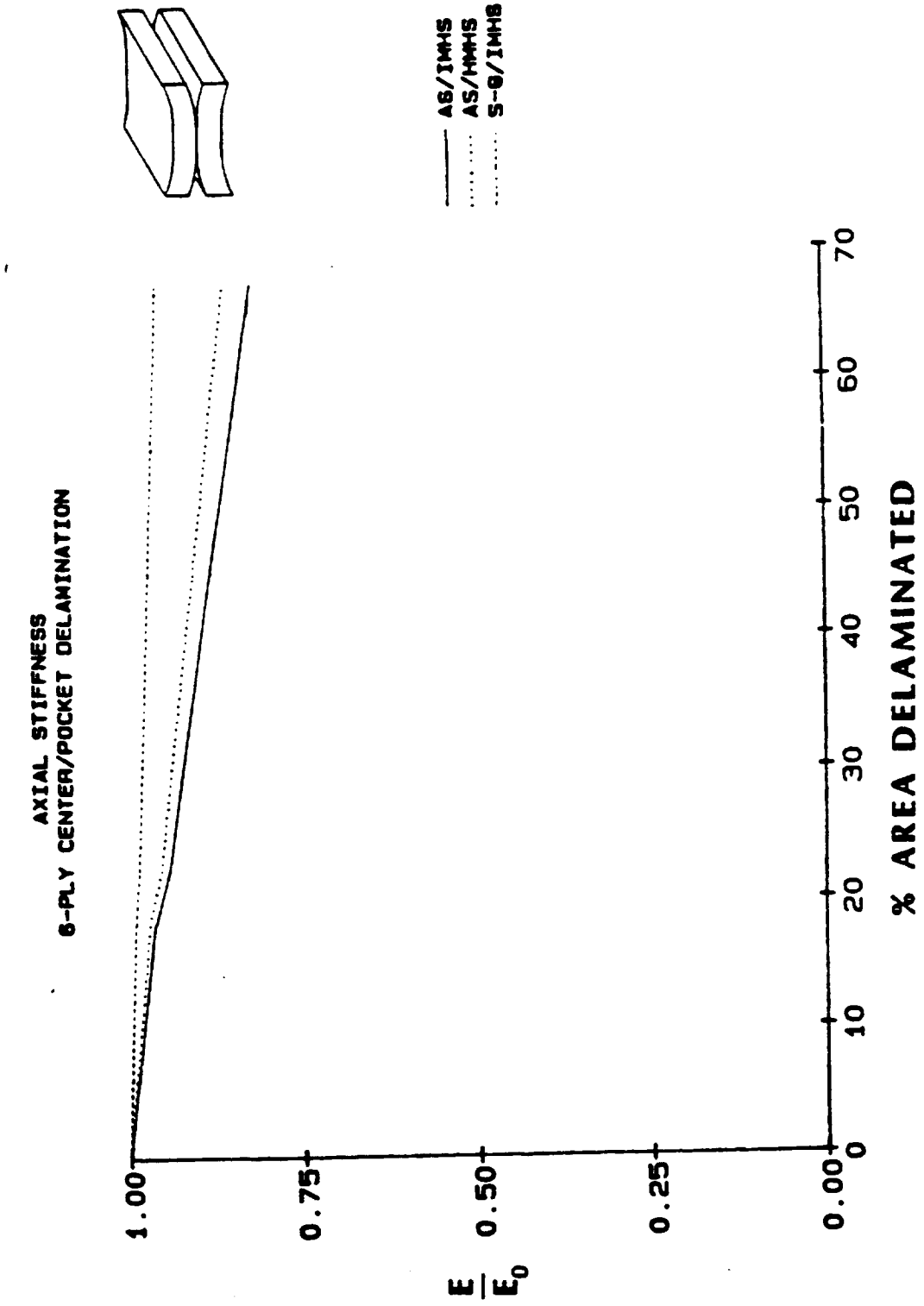
AXIAL STIFFNESS
6-PLY CENTER/POCKET DELAMINATION
AS/IMHS
AS/HMHS
S-G/IMHS
1.00
0.75
0.50
0.25
0.00
E/E0
0
10
20
30
40
50
60
70
% AREA DELAMINATED

Figure 21

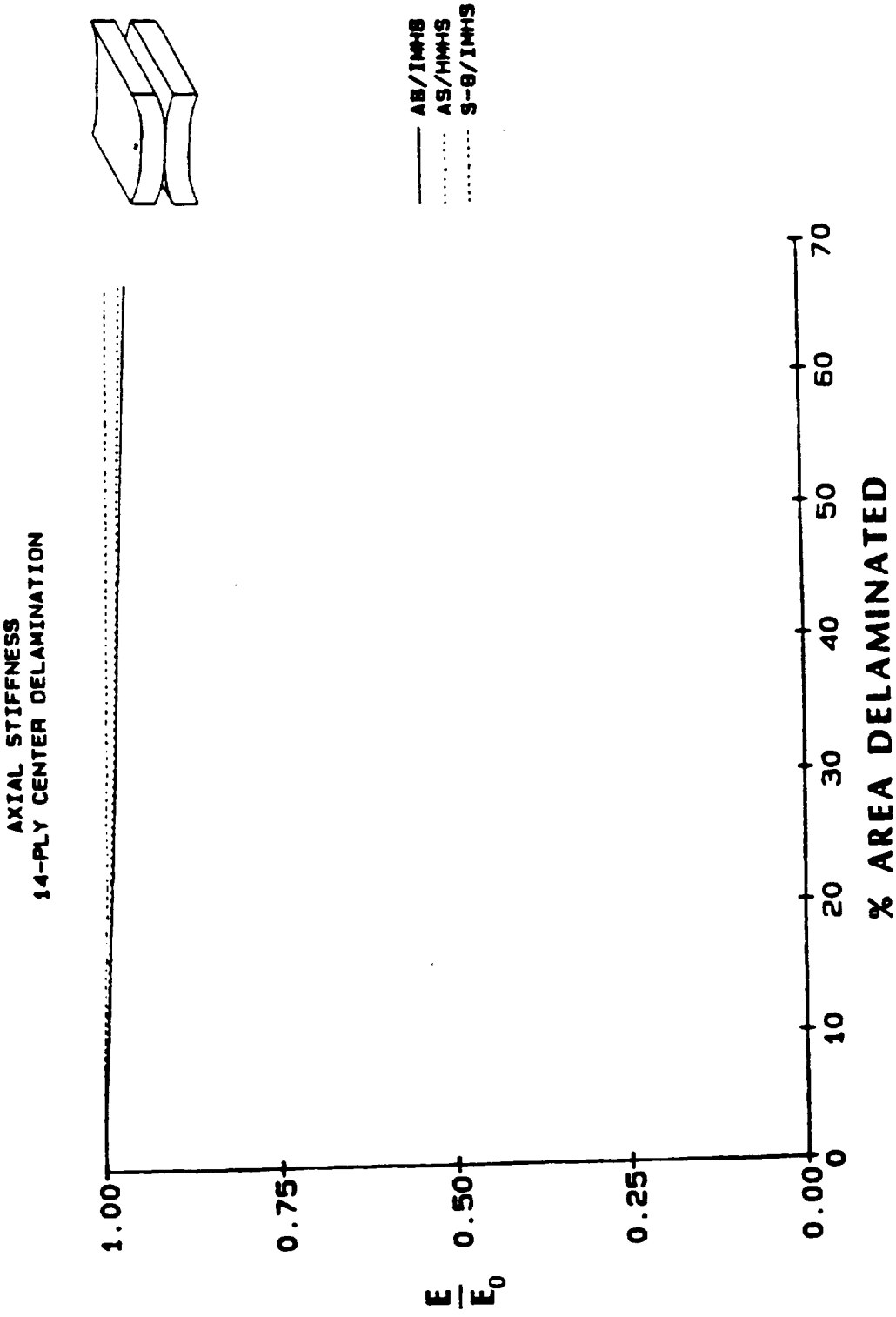
AXIAL STIFFNESS
14-PLY CENTER DELAMINATION
AS/HMHS
S-G/IMHS
1.00
0.75
0.50
0.25
0.00
E/E0
0
10
20
30
40
50
60
70
% AREA DELAMINATED

Figure 22

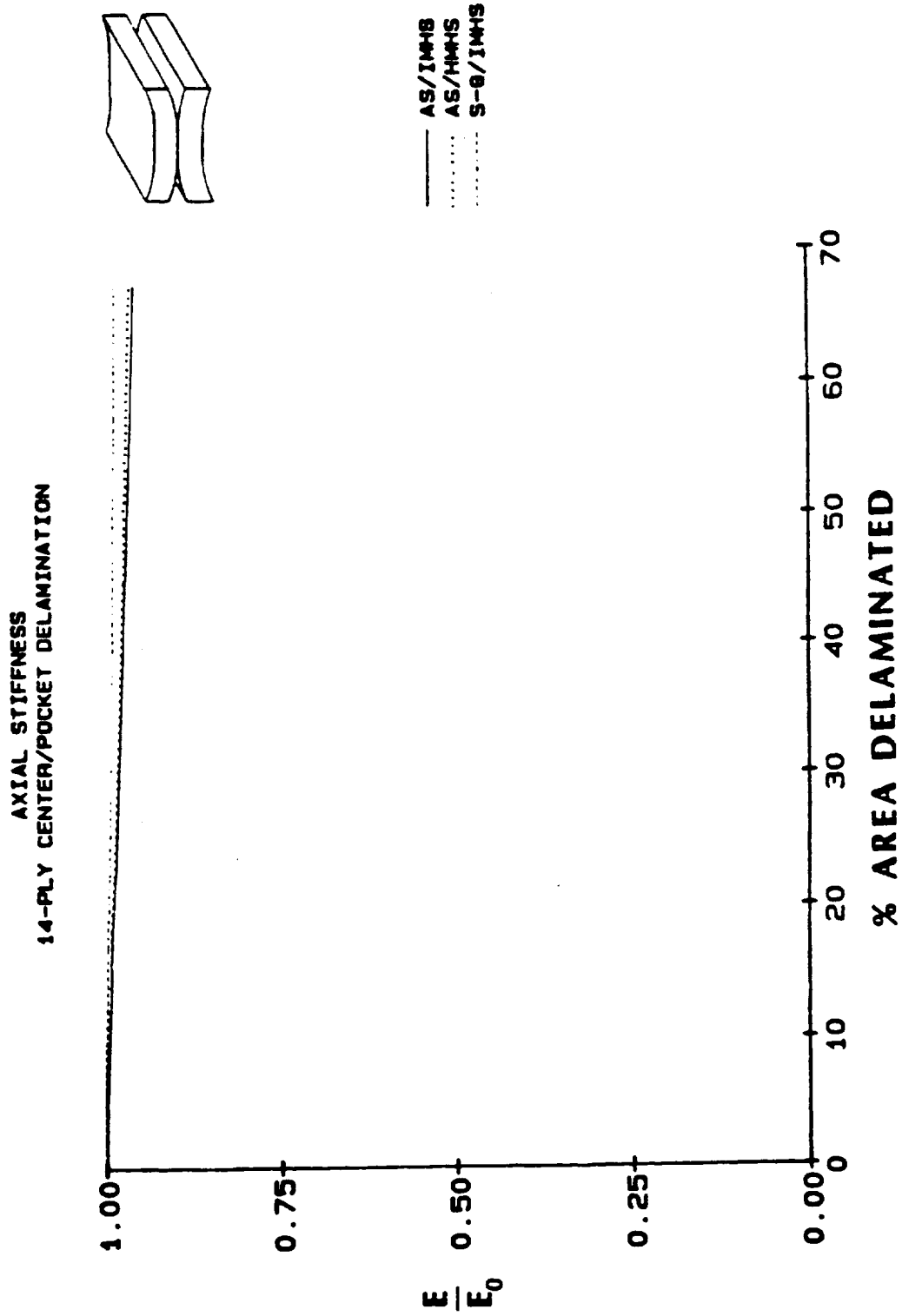
AXIAL STIFFNESS
14-PLY CENTER/POCKET DELAMINATION
AS/IM6
AS/HM6S
S-G/IM6S
1.00
0.75
0.50
0.25
0.00
E/E0
0
10
20
30
40
50
60
70
% AREA DELAMINATED

Figure 23

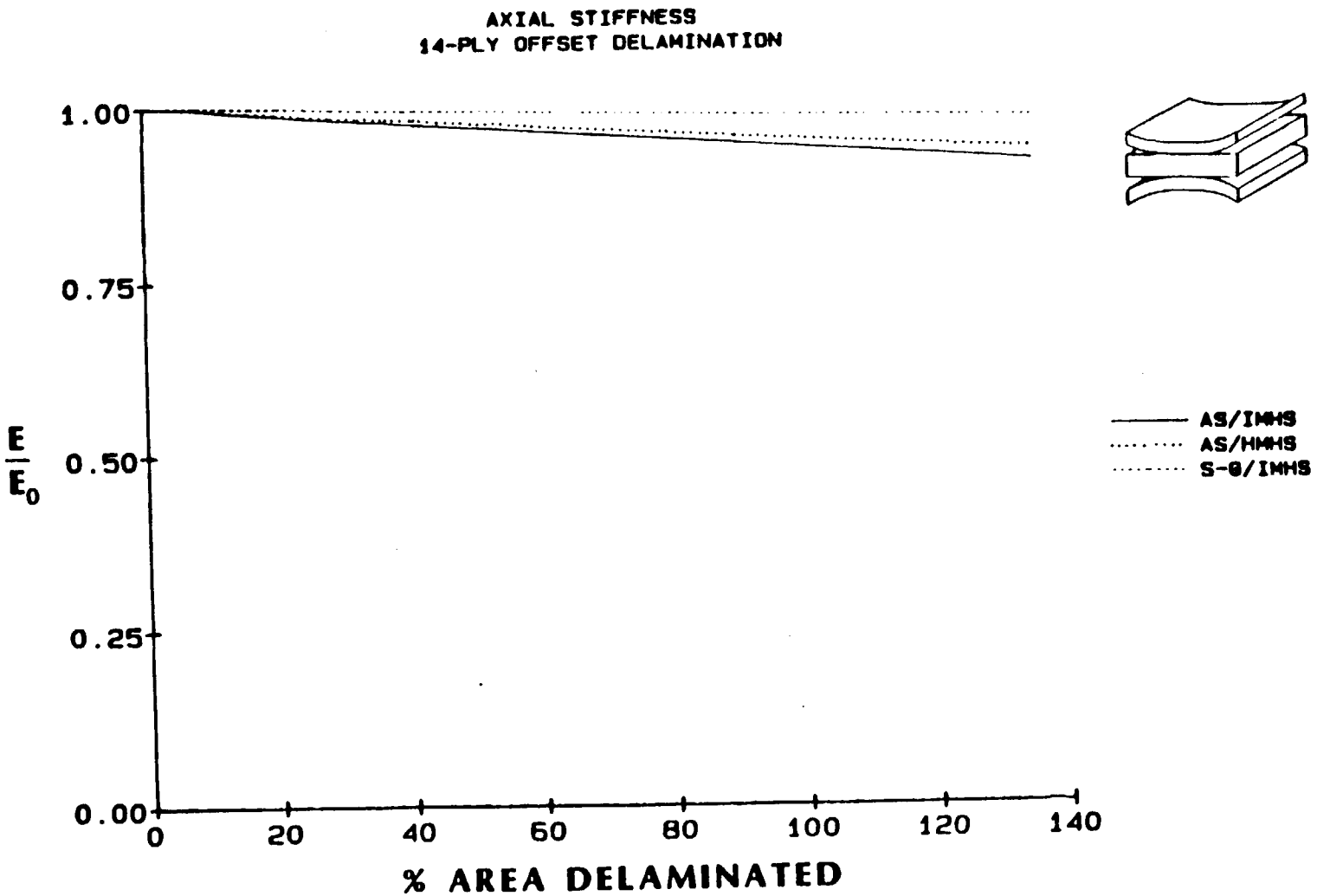
AXIAL STIFFNESS
14-PLY OFFSET DELAMINATION
1.00
0.75
0.50
0.25
0.00
E/E0
0
20
40
60
80
100
120
140
% AREA DELAMINATED
AS/IMHS
AS/HMHS
S-G/IMHS

Figure 24

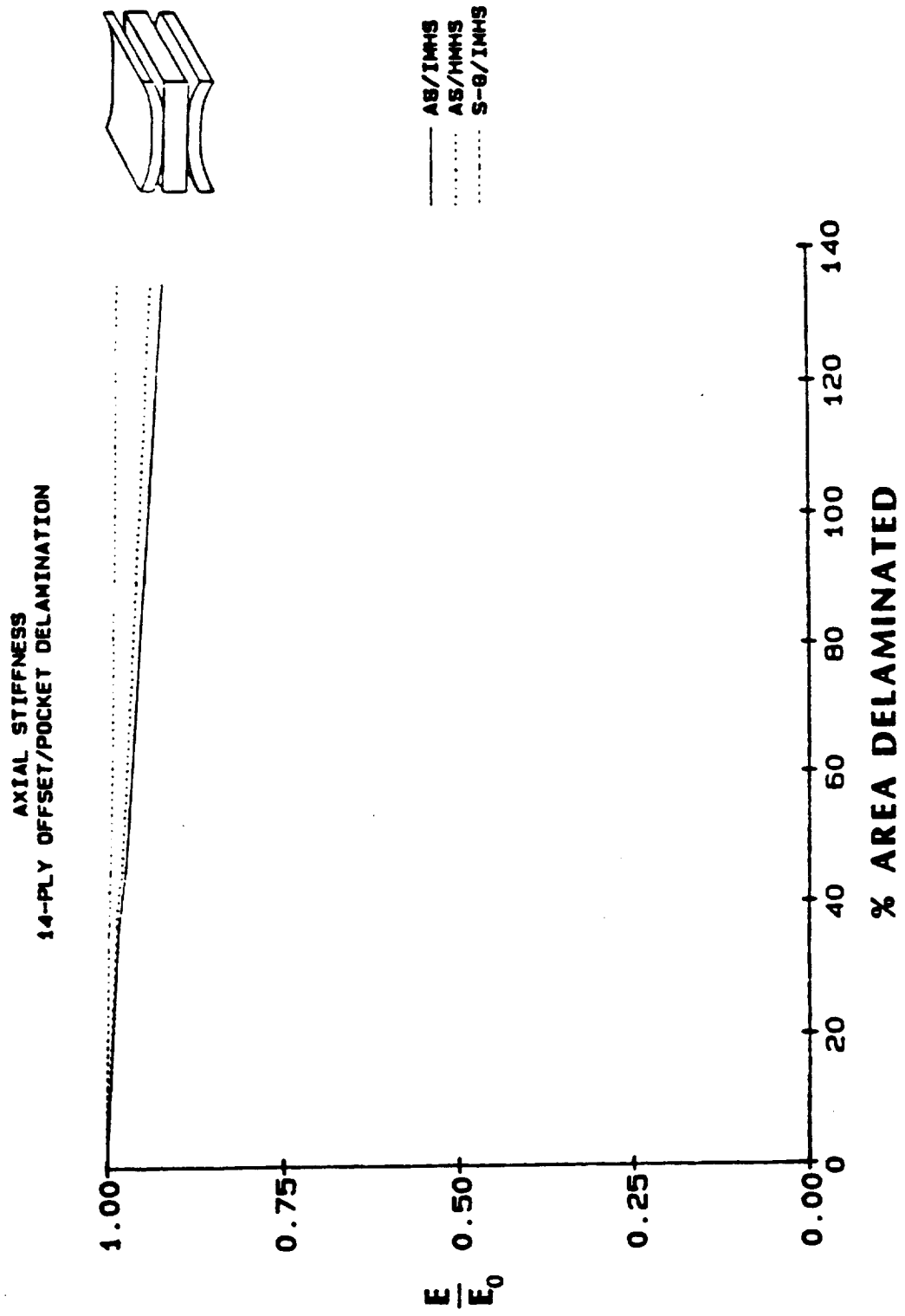
AXIAL STIFFNESS
14-PLY OFFSET/POCKET DELAMINATION
AS/IM6S
AS/HM6S
S-G/IM6S
1.00
0.75
0.50
0.25
0.00
E/E0
0
20
40
60
80
100
120
140
% AREA DELAMINATED

Figure 25

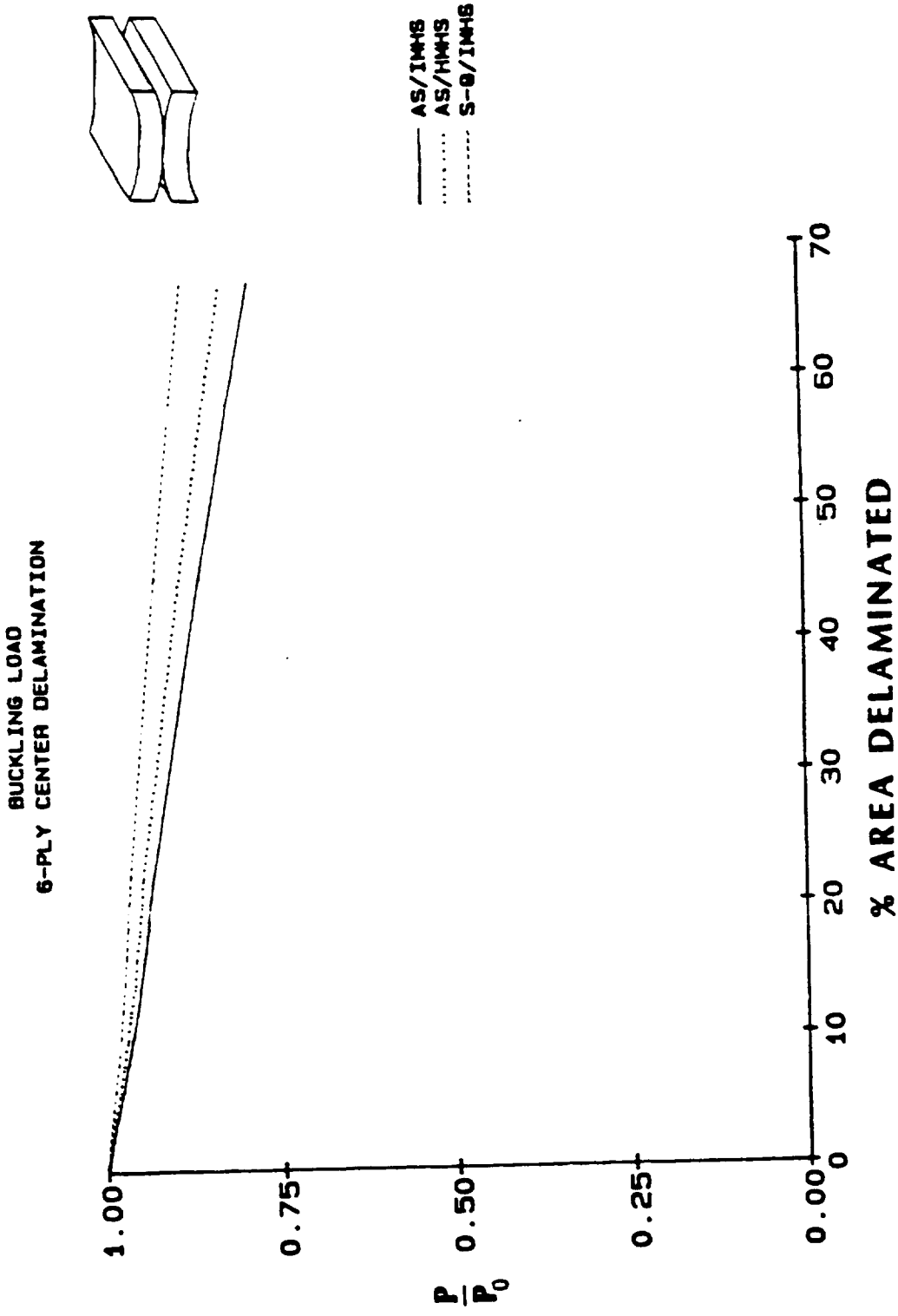
BUCKLING LOAD
6-PLY CENTER DELAMINATION
AS/IM6S
AS/HM6S
S-G/IM6S
1.00
0.75
0.50
0.25
0.00
P/P0
0
10
20
30
40
50
60
70
% AREA DELAMINATED

Figure 26

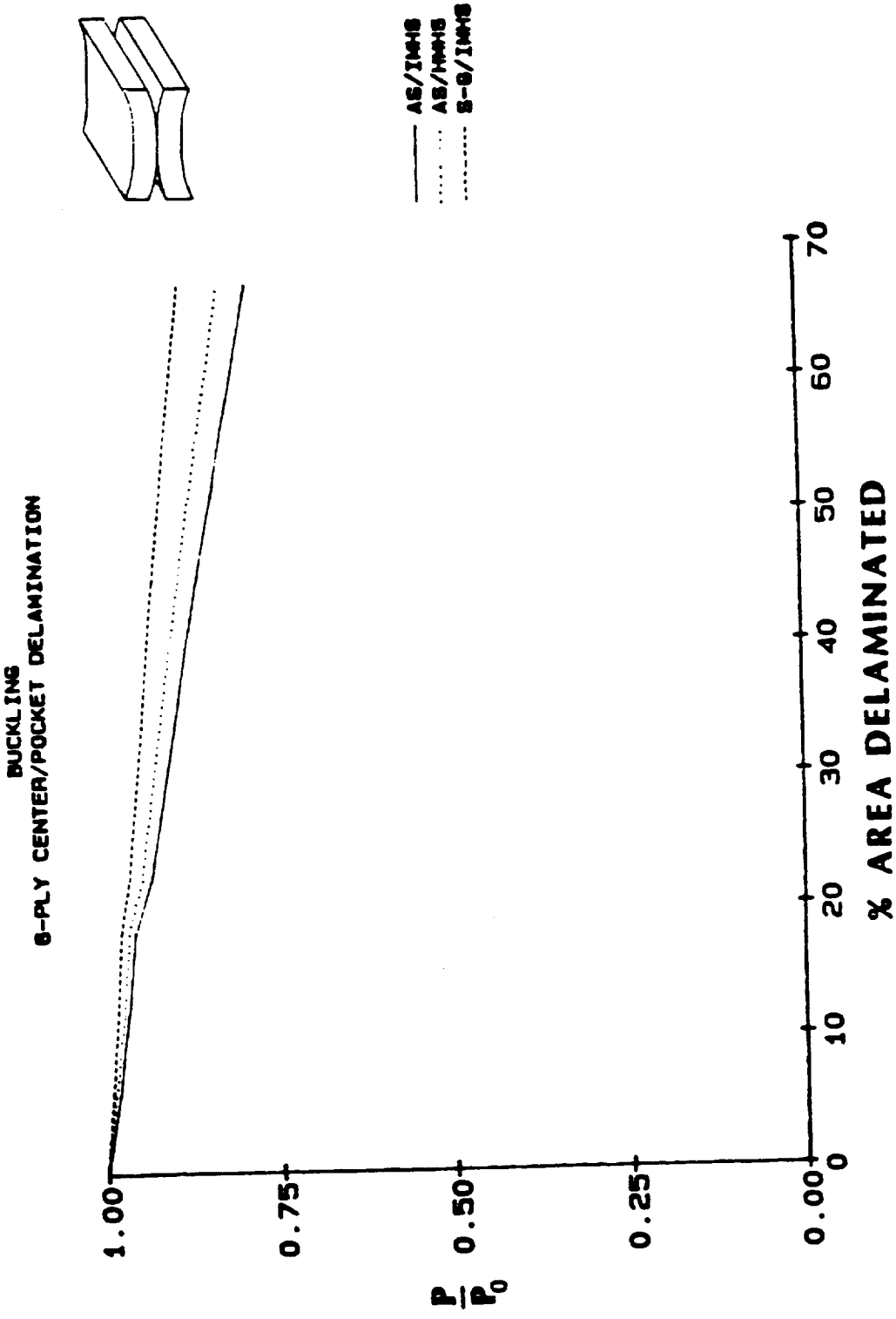
BUCKLING
8-PLY CENTER/POCKET DELAMINATION
AS/IM6
AS/HM6
S-G/IM6
P/P0
1.00
0.75
0.50
0.25
0.00
0
10
20
30
40
50
60
70
% AREA DELAMINATED

Figure 27

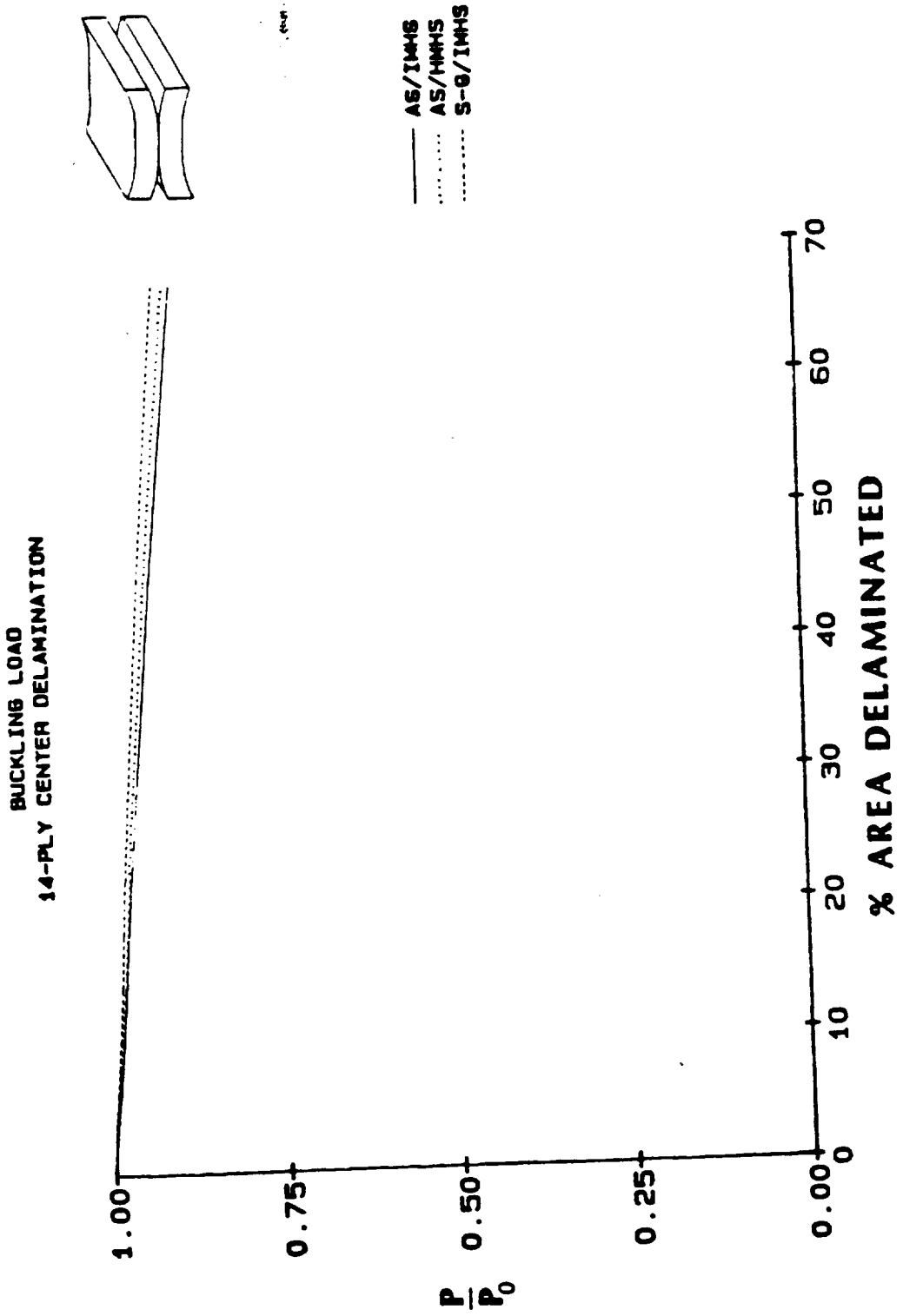
BUCKLING LOAD
14-PLY CENTER DELAMINATION
AS/IM6S
AS/HM6S
S-G/IM6S
1.00
0.75
0.50
0.25
0.00
P/P0
0
10
20
30
40
50
60
70
% AREA DELAMINATED

Figure 28

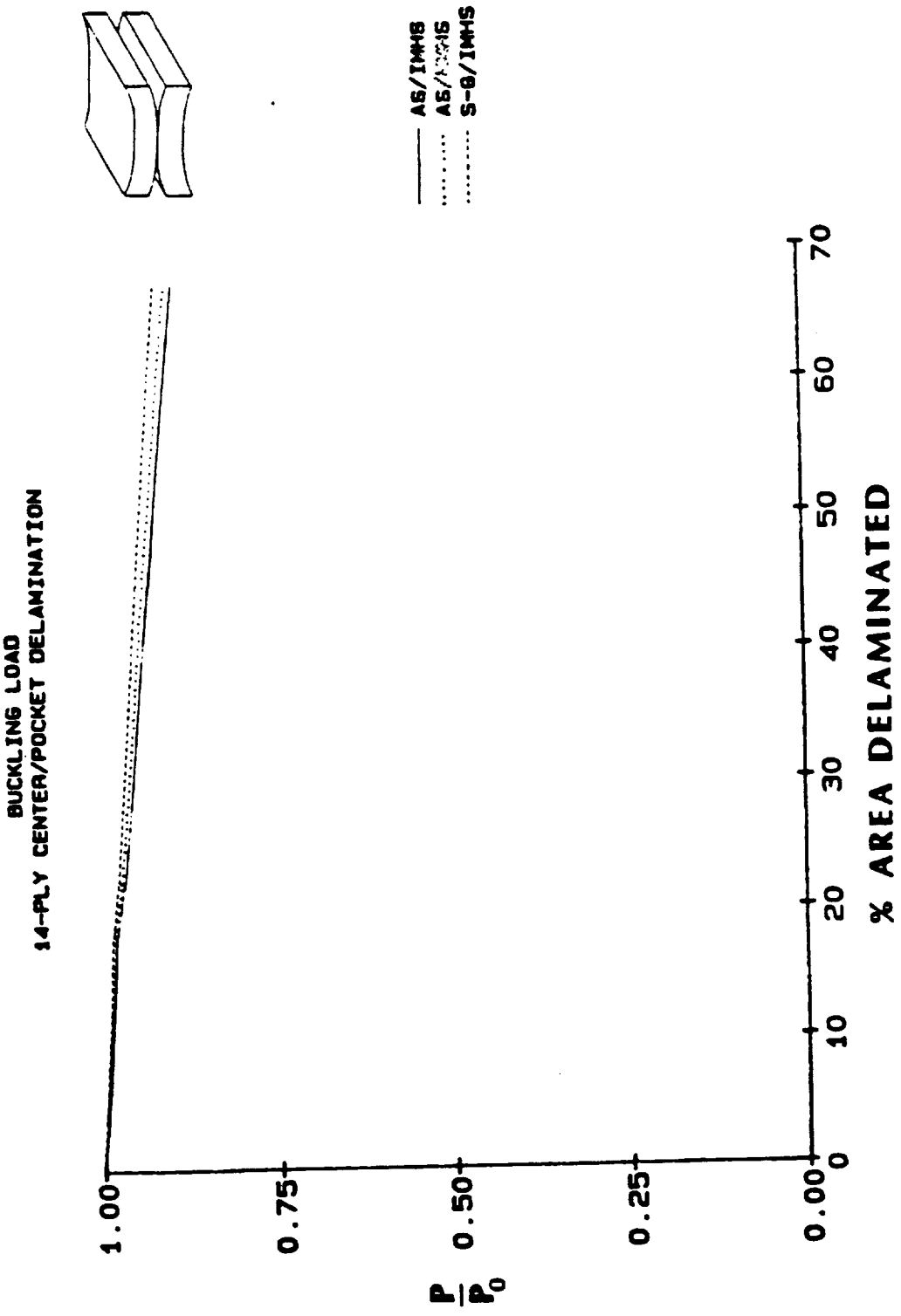
BUCKLING LOAD
14-PLY CENTER/POCKET DELAMINATION
AS/IM6S
AS/[illegible]S
S-6/IM6S
1.00
0.75
0.50
0.25
0.00
P/P0
0
10
20
30
40
50
60
70
% AREA DELAMINATED

Figure 29

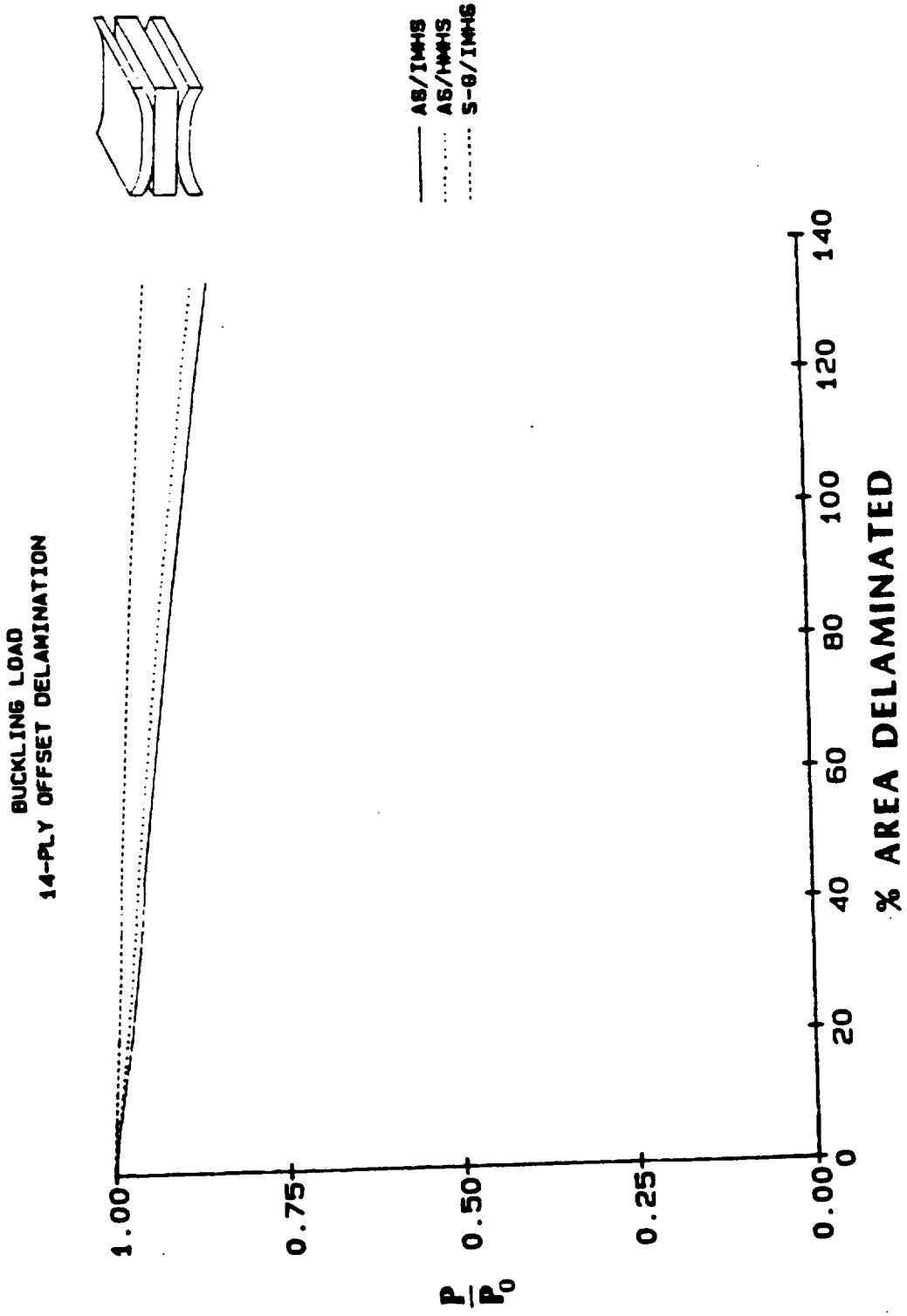
BUCKLING LOAD
14-PLY OFFSET DELAMINATION
AS/IM6S
AS/HMHS
S-G/IM6S
1.00
0.75
0.50
0.25
0.00
P/P0
0
20
40
60
80
100
120
140
% AREA DELAMINATED

Figure 30

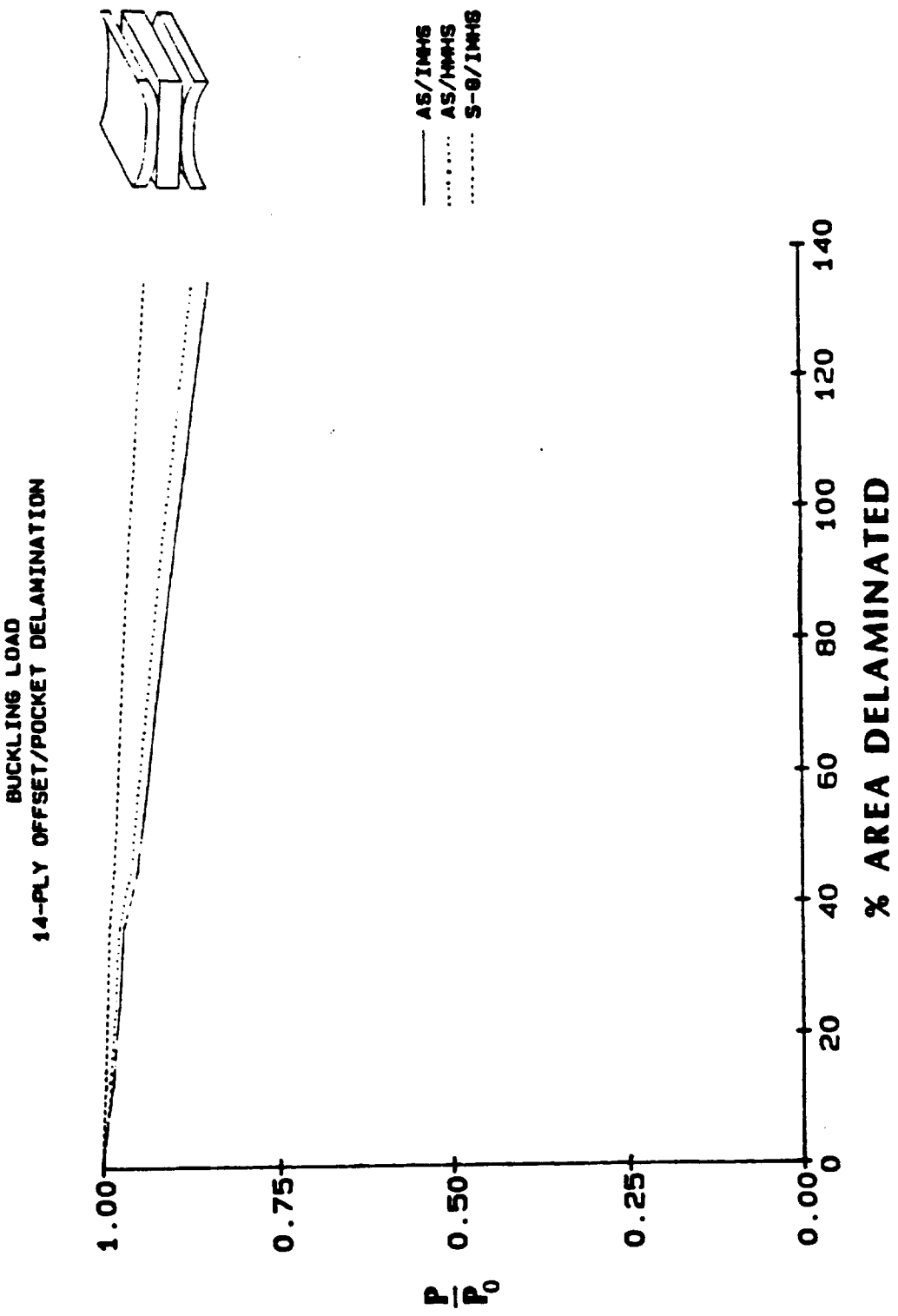
BUCKLING LOAD
14-PLY OFFSET/POCKET DELAMINATION
AS/IM6S
AS/HM6S
S-6/IM6S
1.00
0.75
0.50
0.25
0.00
P/P0
0
20
40
60
80
100
120
140
% AREA DELAMINATED

Figure 31

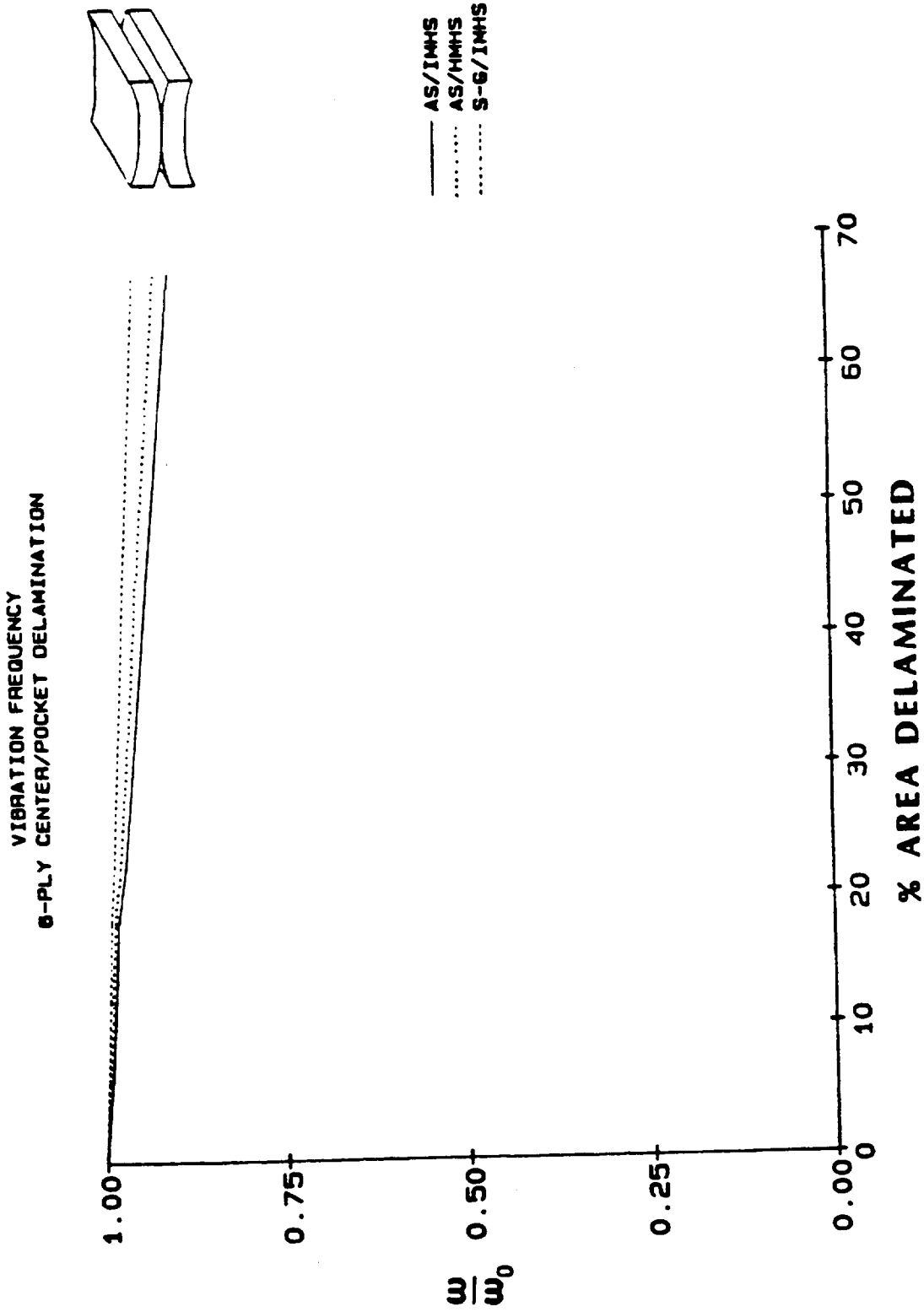
VIBRATION FREQUENCY
8-PLY CENTER/POCKET DELAMINATION
AS/IMHS
AS/HMHS
S-G/IMHS
1.00
0.75
0.50
0.25
0.00
ω/ω0
0
10
20
30
40
50
60
70
% AREA DELAMINATED

Figure 32

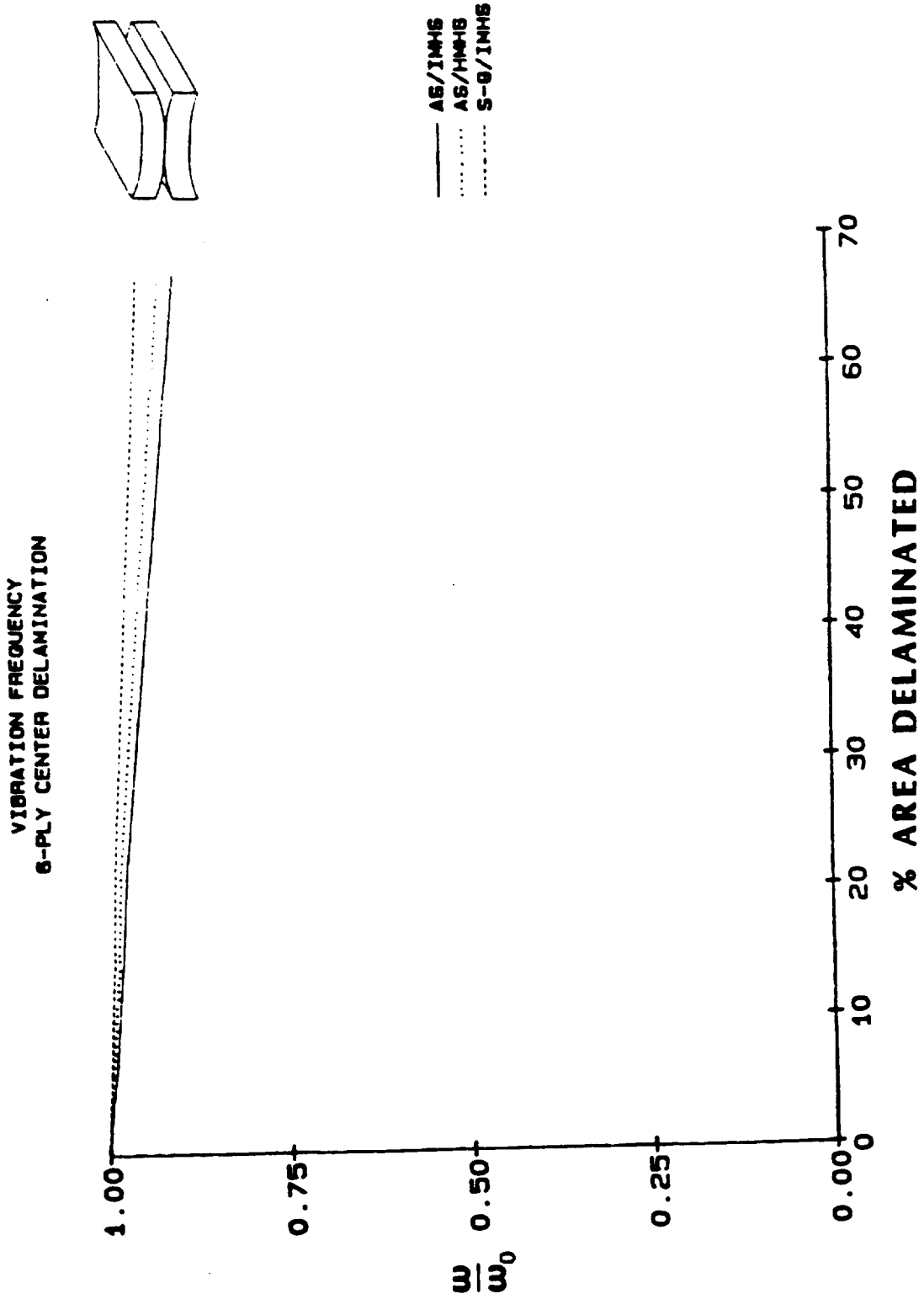
VIBRATION FREQUENCY
6-PLY CENTER DELAMINATION
AS/IM16
AS/HM18
S-6/IM16
1.00
0.75
0.50
0.25
0.00
ω/ω0
0
10
20
30
40
50
60
70
% AREA DELAMINATED

Figure 33

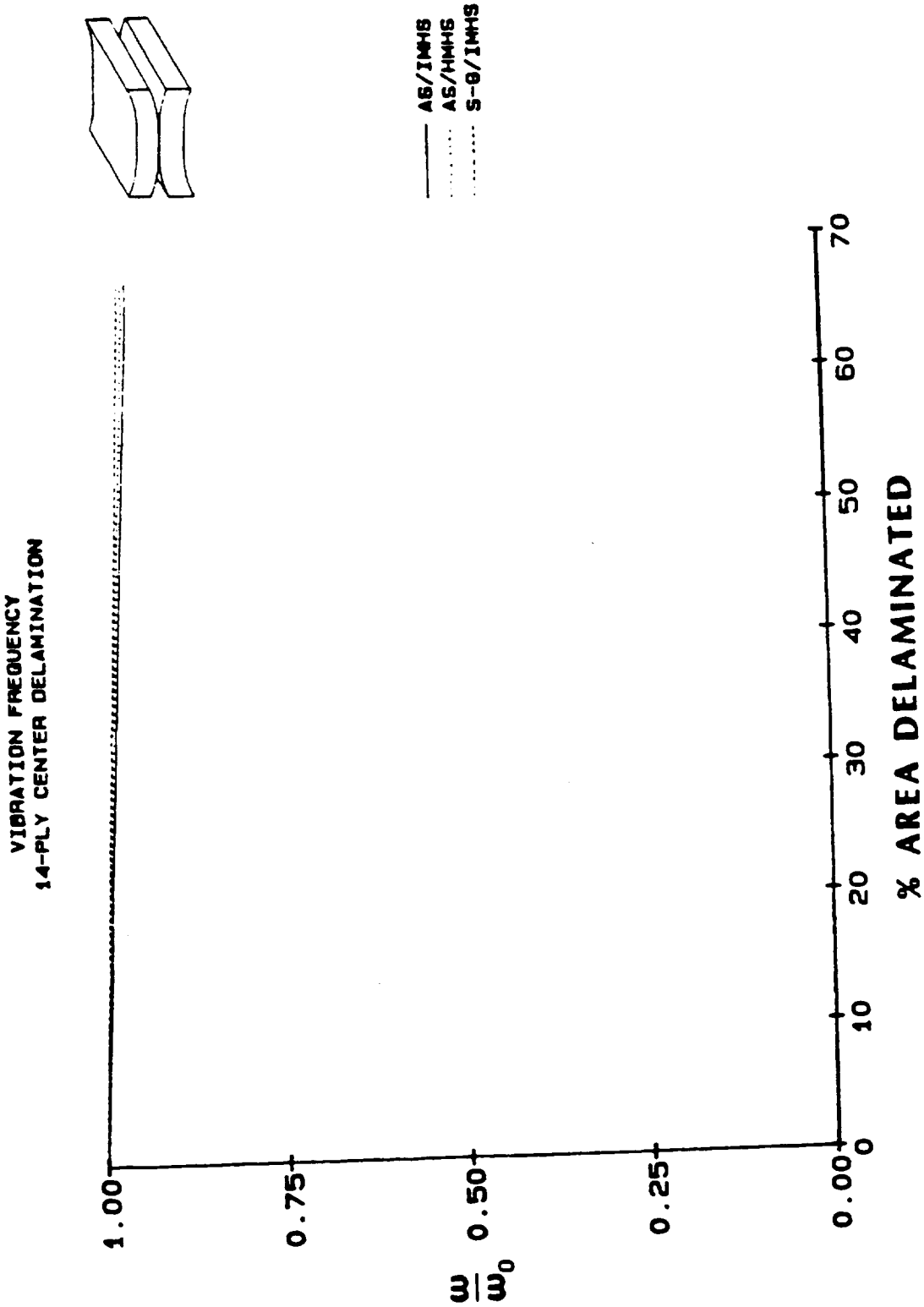
VIBRATION FREQUENCY
14-PLY CENTER DELAMINATION
AS/IM6S
AS/HM6S
S-6/IM6S
1.00
0.75
0.50
0.25
0.00
ω/ω0
0
10
20
30
40
50
60
70
% AREA DELAMINATED

Figure 34

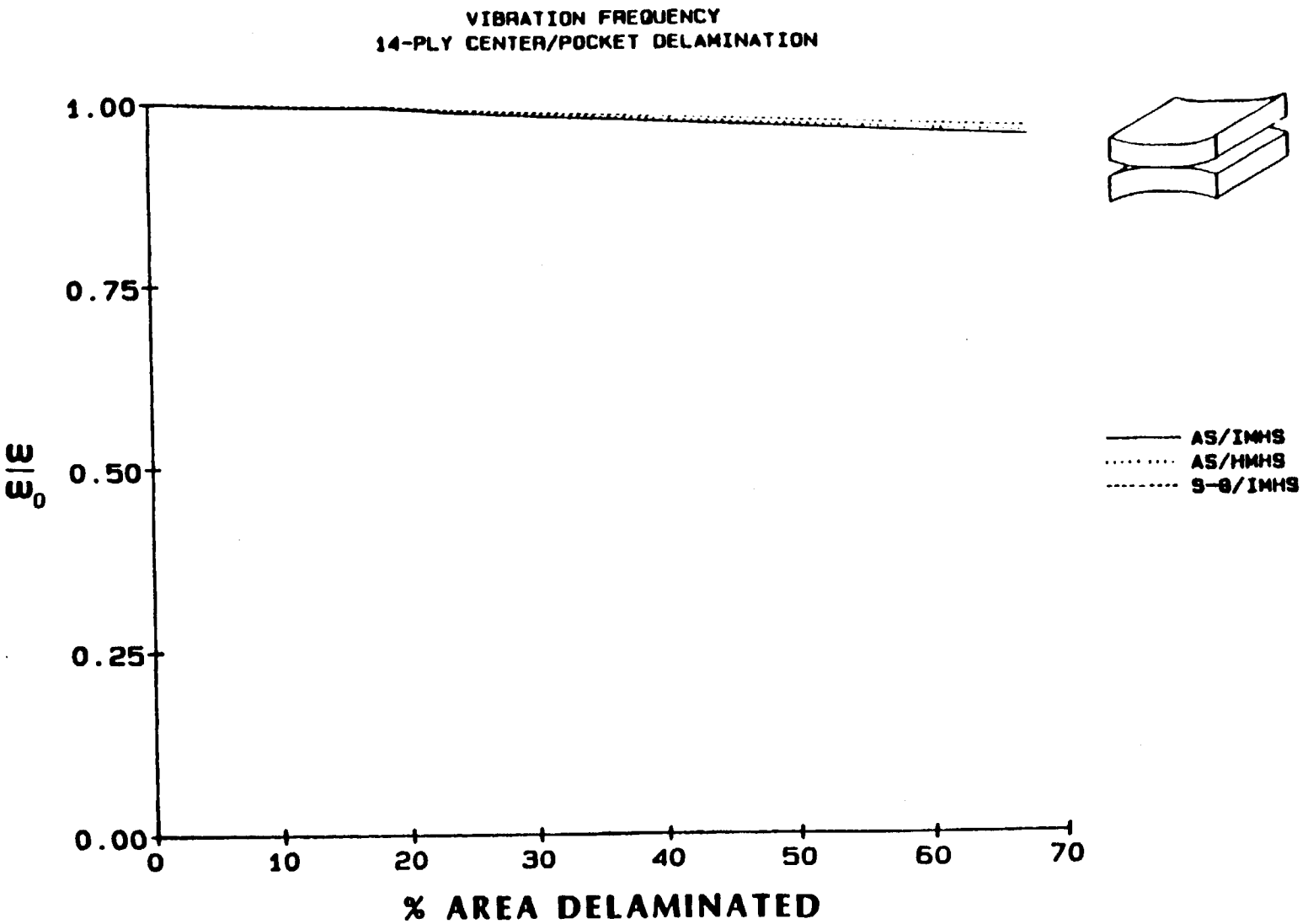
VIBRATION FREQUENCY
14-PLY CENTER/POCKET DELAMINATION
1.00
0.75
0.50
0.25
0.00
ω/ω0
0
10
20
30
40
50
60
70
% AREA DELAMINATED
AS/IMHS
AS/HMHS
S-G/IMHS

Figure 35

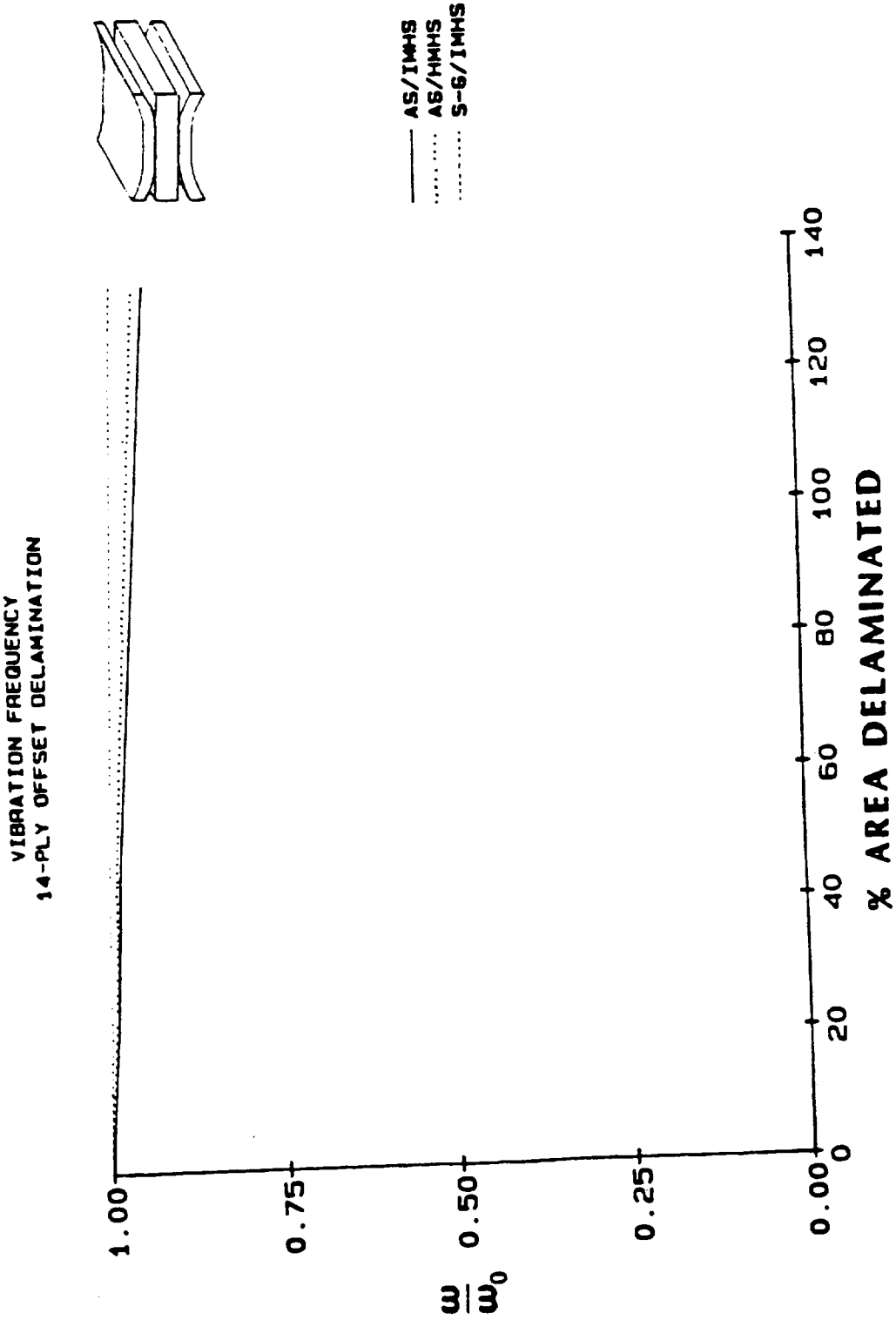
VIBRATION FREQUENCY
14-PLY OFFSET DELAMINATION
AS/IM6S
AS/HM6S
S-6/IM6S
1.00
0.75
0.50
0.25
0.00
ω/ω0
0
20
40
60
80
100
120
140
% AREA DELAMINATED

Figure 36

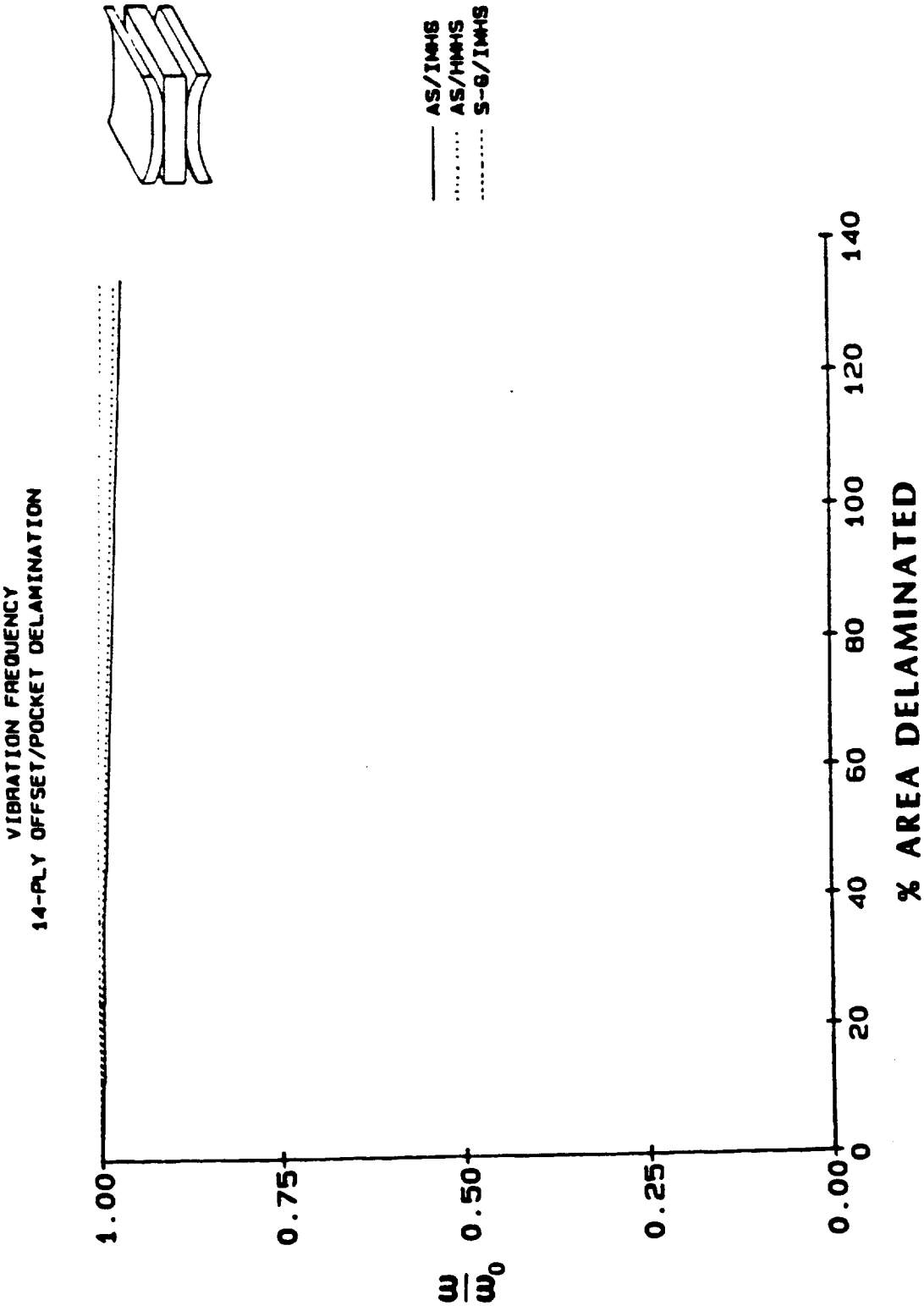
VIBRATION FREQUENCY
14-PLY OFFSET/POCKET DELAMINATION
AS/IMHS
AS/HMHS
S-G/IMHS
1.00
0.75
0.50
0.25
0.00
ω/ω0
0
20
40
60
80
100
120
140
% AREA DELAMINATED

Figure 37

Table 3

Summary of Structural Response
Percent Degradation

Case	Axial Stiffness	Buckling Load	Vibration Frequency
6-ply center			
AS/IMHS	18.3	21.6	10.3
AS/HMHS	14.4	17.7	8.4
S-G/IMHS	4.8	12.2	5.5
14-ply center			
AS/IMHS	4.5	11.2	5.0
AS/HMHS	3.8	10.1	4.5
S-G/IMHS	1.8	8.6	3.8
14-ply offset			
AS/IMHS	8.7	15.9	7.7
AS/HMHS	7.0	13.6	6.3
S-G/IMHS	2.3	6.8	3.1

area delaminated = 80%

Looking at the axial stiffness results, the 6-ply center case shows a larger decrease in stiffness as compared to the 14-ply center case. Intuitively, this is to be expected since as the laminate becomes thicker, i.e. stiffer, a single delamination should have less of an effect. On the other hand, the 14-ply offset case shows more reduction in stiffness as compared to the 14-ply center. This result is consistent since the amount of delamination damage is twice that of the center delamination case.

Since delamination causes no increase or decrease in the mass of the structure, it seems reasonable that the overall trend in vibration response should agree with the buckling load trend. Specifically, the changes in both buckling load and vibration frequency should basically reflect the changes in bending stiffness of the laminate. Again, referring to Table 3, the results for both buckling load and vibration frequency follow the same general trend as the one present in the changes of axial stiffness, except in the case of the S-G/IM-S composite system. Note that the 14-ply offset case shows less degradation in buckling load and vibration frequency response than that of the 14-ply center case, unlike the AS/IM-S and AS/IM-S systems. This result is interesting in that it does not follow the expected trend.

In order to provide an explanation for this behavior, the stiffness coefficients for the laminates used are studied. Tables 4-6 show the axial, bending and coupling coefficients that are used in the material property cards of the finite element models. These values are obtained directly from Integrated Composite Analyzer (ICAN) output. Once

Table 4

STIFFNESS COEFFICIENTS FOR

[±30/90] SUBLAMINATE

AXIAL STIFFNESS (lb/in^2)

AS/IMHS	.7919+7	.2432+7	-.1150+1	.7919+7	.6799+1	.2744+7
AS/HMHS	.8185+7	.2425+7	-.1314+1	.8185+7	.6641+1	.2880+7
S-G/IMHS	.4153+7	.1240+7	-.2621+0	.4153+7	.2286+1	.1450+7

BENDING STIFFNESS (lb/in^2)

AS/IMHS	.6426+7	.1961+7	.2518+7	.1036+8	.8854+6	.2272+7
AS/HMHS	.6691+7	.1971+7	.2475+7	.1059+8	.9003+6	.2425+7
S-G/IMHS	.3671+7	.1079+7	.8363+6	.4958+7	.2783+6	.1295+7

COUPLING STIFFNESS (lb/in^2)

AS/IMHS	-.1120+7	-.3534+6	-.6294+6	.1827+7	-.2213+6	-.3534+6
AS/HMHS	-.1120+7	-.3409+6	-.6188+6	.1803+7	-.2251+6	-.3409+6
S-G/IMHS	-.3618+6	-.1208+6	-.2091+6	.6035+6	-.6957+5	-.1208+6

Table 5

STIFFNESS COEFFICIENTS FOR

$[\pm 30/90/\pm 30/90_2]$ SUBLAMINATE

AXIAL STIFFNESS (lb/in^2)

AS/IMHS	.6959+7	.2129+7	0.68833	.9485+7	.9622+1	.2441+7
AS/HMHS	.7224+7	.2133+7	0.88222	.9730+7	.9376+1	.2587+7
S-G/IMHS	.3843+7	.1137+7	0.11019	.4671+7	.3215+1	.1353+7

BENDING STIFFNESS (lb/in^2)

AS/IMHS	.6254+7	.1907+7	.7927+6	.1064+8	.2788+6	.2218+7
AS/HMHS	.6519+7	.1918+7	.7792+6	.1087+8	.2835+6	.2373+7
S-G/IMHS	.3615+7	.1061+7	.2633+6	.5051+7	.8762+5	.1277+7

COUPLING STIFFNESS (lb/in^2)

AS/IMHS	-.8230+6	-.2596+6	-.2312+6	.1342+7	-.8131+5	-.2596+6
AS/HMHS	-.8232+6	-.2505+6	-.2273+6	.1324+7	-.8267+5	-.2505+6
S-G/IMHS	-.2658+6	-.8877+5	-.7681+5	.4433+6	-.2555+5	-.8877+5

Table 6

STIFFNESS COEFFICIENTS FOR

$[\pm 30/90_4/\pm 30]$ SUBLAMINATE

AXIAL STIFFNESS (lb/in^2)

AS/IMHS	.6239+7	.1902+7	.29297	.1066+8	.1104+2	.2214+7
AS/HMHS	.6504+7	.1914+7	.39063	.1089+8	.1074+2	.2368+7
S-G/IMHS	.3611+7	.1059+7	.00000	.5059+7	.3674+1	.1275+7

BENDING STIFFNESS (lb/in^2)

AS/IMHS	.1002+8	.3095+7	.1593+7	.4494+7	.5603+6	.3406+7
AS/HMHS	.1029+8	.3065+7	.1566+7	.4805+7	.5697+6	.3519+7
S-G/IMHS	.4832+7	.1467+7	.5292+6	.3022+7	.1761+6	.1683+7

COUPLING STIFFNESS (lb/in^2)

AS/IMHS	.000000	.45776	.30518	-.27657	.3815-1	.30518
AS/HMHS	.30518	.30518	.15259	-.31471	.3815-1	.30518
S-G/IMHS	.15259	.23842	.9537-2	.9537-1	.1907-1	.43869

the symmetric laminates begin to delaminate, the individual sublaminates are now nonsymmetric with coupling effects present. Therefore, the quantities of particular interest are the coupling stiffnesses.

Looking at the stiffness terms individually fails to give any explanation of the behavior of the S-G/IMHS composite system. Thus, an alternate set of stiffness coefficients are used. Those considered are reduced stiffnesses, that is, the axial and bending stiffness coefficients are calculated with the coupling effects included. In Table 7, the percent difference in the reduced stiffness of the delaminated plies as compared to the total intact laminate are given. Recall that buckling loads and vibration frequencies will be sensitive to changes in bending stiffness. Thus, the bending stiffness coefficients are of primary importance.

First, the bending stiffness quantities D_{11} and D_{33} both exhibit the same trend inthe 14-ply center and 14-ply offset cases. Specifically, for each case the S-G/IMHS laminate shows the smallest reduction in stiffness due to coupling effects, as compared to the AS/IMHS or AS/HMHS laminates. Also for the S-G/IMHS laminate, there is less reduction in stiffness in the 14-ply offset case than there is in the 14-ply center case. These two trends seem to indicate that the S-G/IMHS laminate is afffected less by the coupling effects present in the damaged laminate. This could possibly account for the fact that the S-G/IMHS laminate shows consistently less degradation in structural response, (refer to Table 3).

Table 7

Reduced Stiffness Coefficients
Percent Reduction
Due to Coupling Effects

Case	Axial Stiffness			Bending Stiffness		
	A_{11}	A_{22}	A_{33}	D_{11}	D_{22}	D_{33}
14-ply center						
AS/IMHS	60.0	63.5	58.3	93.5	83.2	92.9
AS/HMHS	59.2	62.4	56.9	93.2	83.1	92.4
S-G/IMHS	53.5	56.3	53.2	90.9	84.0	90.7
14-ply offset						
AS/IMHS	48.8	35.8	48.2	79.8	85.4	79.9
AS/HMHS	48.6	36.1	47.7	79.8	85.2	80.0
S-G/IMHS	46.3	38.1	46.1	80.3	83.6	80.4

3.5 Laminate Post-Buckling Behavior

The premise for investigating this series of cases is to see how the "popped-out" sublaminate behaves in a laminate subjected to a compressive uniaxial load. Intuitively, it is expected that as the load increases and the laminate begins to bend further, the separation distance between the delaminated sublaminate and the remainder of the laminate should increase. That is, in the delaminated area, the delaminated sublaminate should continue to buckle outward in a direction opposite of the overall laminate buckling.

Figure 38 shows a side view of the simply supported laminate as the load is increased. Note that the laminate bends such that the "popped-out" sublaminate is located on the compressive side of the laminate. This series of views shows that as the laminate continues to bend due to the increasing compressive load, the "pop-out" sublaminate actually begins to close up. This is due to the fact that since the "pop-out" is located on the compression side, the bending moment is forcing the sublaminate inward.

In the case of the clamped-clamped laminate, the laminate displaces in the direction of the "pop-out". Thus it is possible to investigate how the post-buckled behavior changes when the "pop-out" is on the tension side of the laminate. Figure 39 shows a selected set of side views of the clamped-clamped laminate as the compressive load is increased. Note how in this case, the delaminated sublaminate retains its "pop-out" shape throughout the load increase. An explanation could be that since the plies are on the tension side of the laminate, the

Simply Supported Laminate

P = 7.10 lb

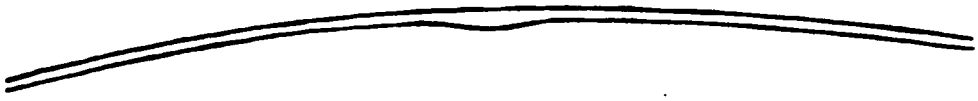

P = 10.65 lb

P = 14.21 lb

P = 28.40 lb

Figure 38

Clamped-Clamped Laminate

P = 7.10 lb

P = 14.21 lb

P = 42.6 lb

P = 71.0 lb

Figure 39

bending moment at the "pop-out" location is acting to push the "pop-out" outward. Thus, even in the last view in figure 39, the "pop-out" is still visible. A note should be made that the views in figures 38-39 are slightly magnified so that the small lateral displacements are observable.

Figures 40 and 41 are plots of the axial stresses located at various points in the two sublaminate layers. Figure 40 shows the axial stresses of the simply supported laminate. Of particular interest are the stresses at location C of the laminate. Note the point where the stresses at the top and bottom locations of the sublaminate change in sign. This point corresponds to the load at which the "pop-out" begins to bend in the opposite direction and close up. Figure 41 shows the axial stresses for the clamped-clamped laminate. Note in this case there is no change in sign of the stresses since the "pop-out" never begins to close up as in the previous case.

The next portion of the results deals with investigating how the strain energy release rate is affected by the position of the post-buckled laminate. Specifically, if the laminate is in a buckled state and has delamination damage, will the damage spread? In order to evaluate this, various laminate positions are taken from the previous post-buckling results. Here, the appropriate compressive load is held constant and the delamination area is increased as discussed in section 2.6. Figures 42-44 show selected side views of the laminate as the delamination area is increased. Again the views are magnified slightly to allow the displacements of the plies to be observed. Associated with

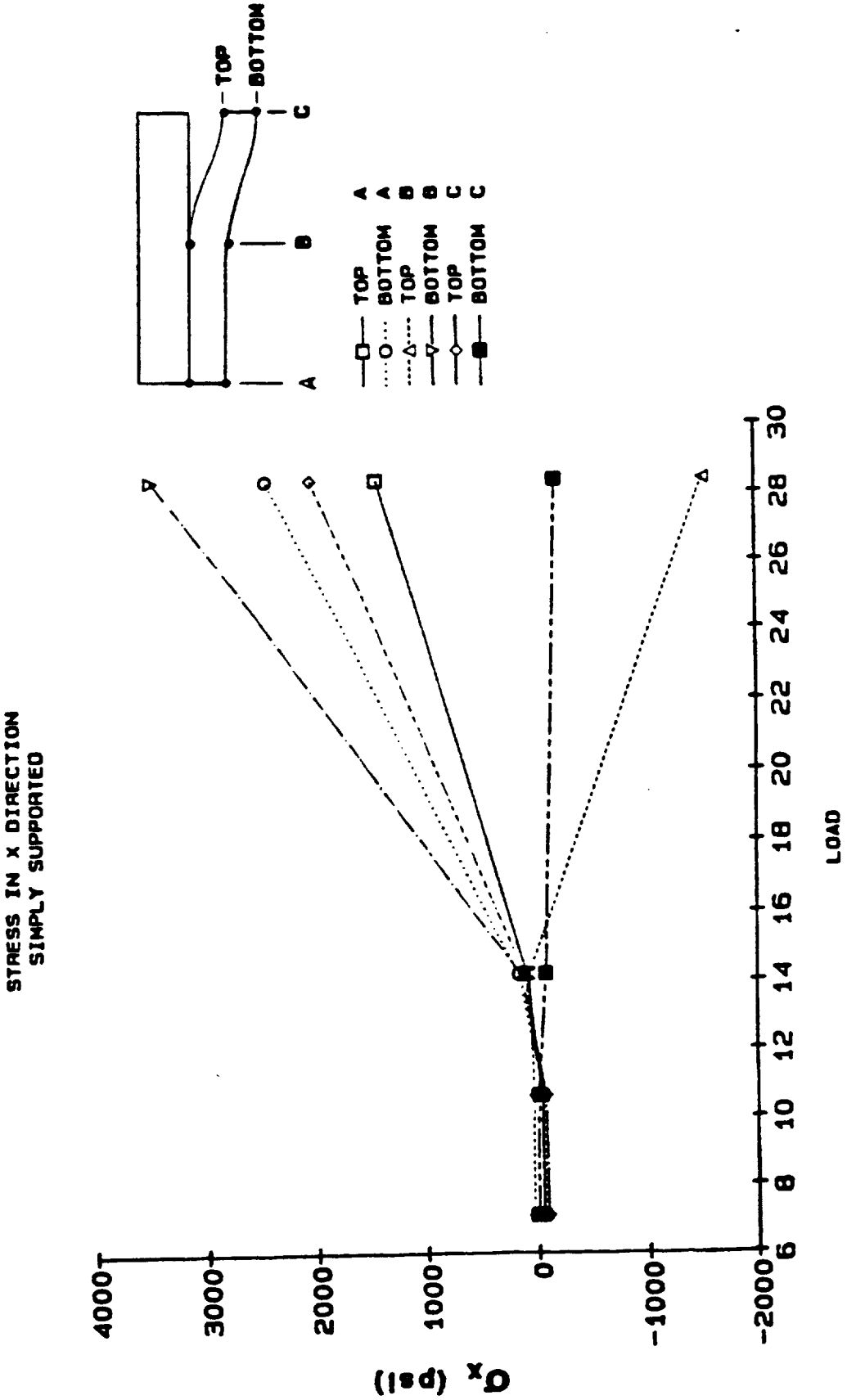
STRESS IN X DIRECTION
SIMPLY SUPPORTED
TOP
BOTTOM
A
B
C
TOP
BOTTOM
TOP
BOTTOM
TOP
BOTTOM
A
A
B
B
C
C
σ_x (psi)
4000
3000
2000
1000
0
-1000
-2000
6
8
10
12
14
16
18
20
22
24
26
28
30
LOAD

Figure 40

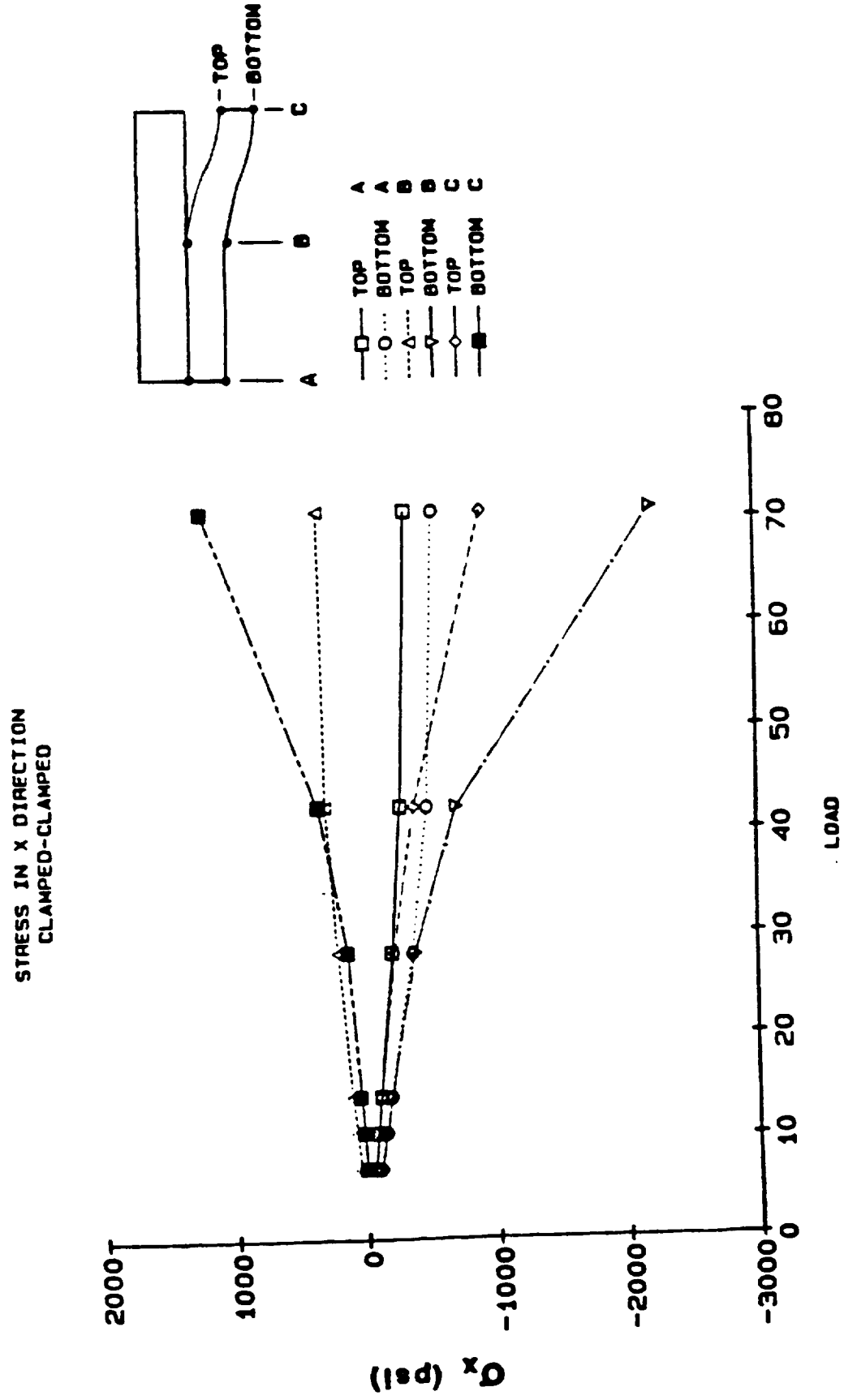
STRESS IN X DIRECTION
CLAMPED-CLAMPED
TOP
BOTTOM
A
B
C
TOP A
BOTTOM A
TOP B
BOTTOM B
TOP C
BOTTOM C
2000
1000
0
-1000
-2000
-3000
σ_x (psi)
0
10
20
30
40
50
60
70
80
LOAD

Figure 41

Simply Supported Laminate
Position 1

area delaminated = 14.3%

area delaminated = 28.6%

area delaminated = 50.0%

area delaminated = 64.3%

area delaminated = 78.6%

Figure 42

Simply Supported Laminate
Position 2

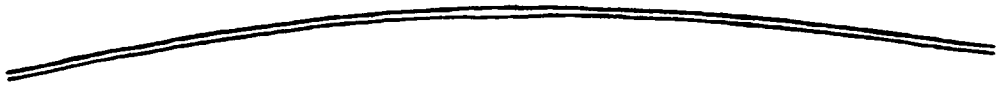

area delaminated = 14.3%

area delaminated = 28.6%

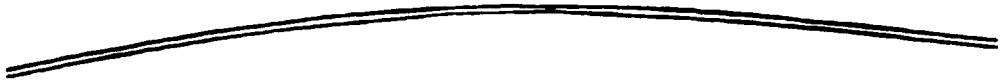

area delaminated = 50.0%

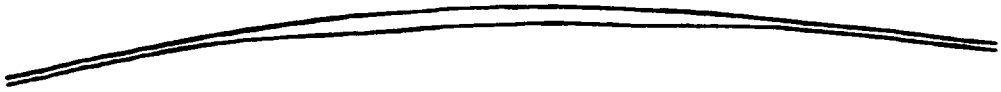

area delaminated = 64.3%

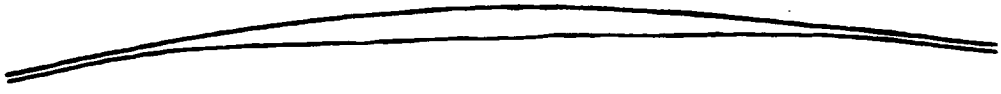

area delaminated = 78.6%

Figure 43

Simply Supported Laminate
Position 3

area delaminated = 14.3%

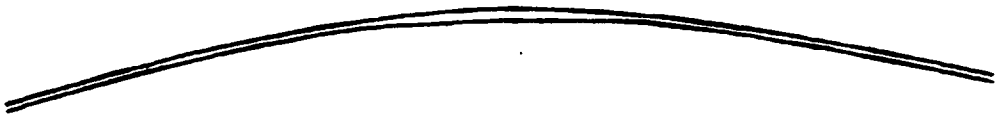

area delaminated = 28.6%

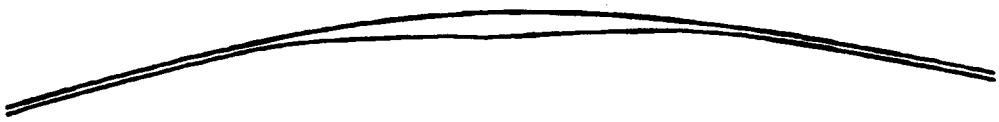

area delaminated = 50.0%

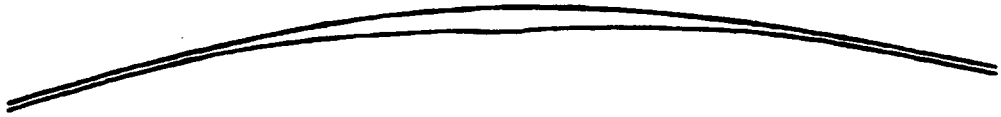

area delaminated = 64.3%

area delaminated = 78.6%

Figure 44

these figures are figures 45-47 which show the corresponding strain energy release rate, SERR, for the three post-buckled positions of the simply supported laminate. In general, it is observed that 1) the SERR is negligible and 2) there is an appreciable relative increase in SERR as the position changes. This relative increase is due to the fact that from position 1 to position 3, there is an increasing amount of initial curvature in the laminate making the laminate less stiff, thus producing larger end displacements. And since the SERR is a function of the end displacements of the laminate, this would account for its increase.

Also note that as the laminate moves from position 1 to position 3, the trend in each individual strain energy release rate curve changes. In position 1, the curve shows some instability in that it begins to slope upward as 80% delamination is approached, figure 45. But in positions 2 and 3, the SERR curves change and slope downward more as 80% delamination is approached, figures 46 and 47.

Figures 48-50 show the 3 positions of the clamped-clamped laminate under a constant, compressive load as the delamination area is allowed to propagate. Note that in the first two positions, figures 48 and 49, the delaminated sublaminate "pop-out" deforms further as the multi-point constraints are released. But in position 3, figure 50, the "pop-out" does not increase in size. Figures 51-53 are the corresponding strain energy release rates associated with positions 1 to 3. Again the SERR is negligible and the results are similar to the simply supported case. From positions 1 to 3, there is a relative increase in

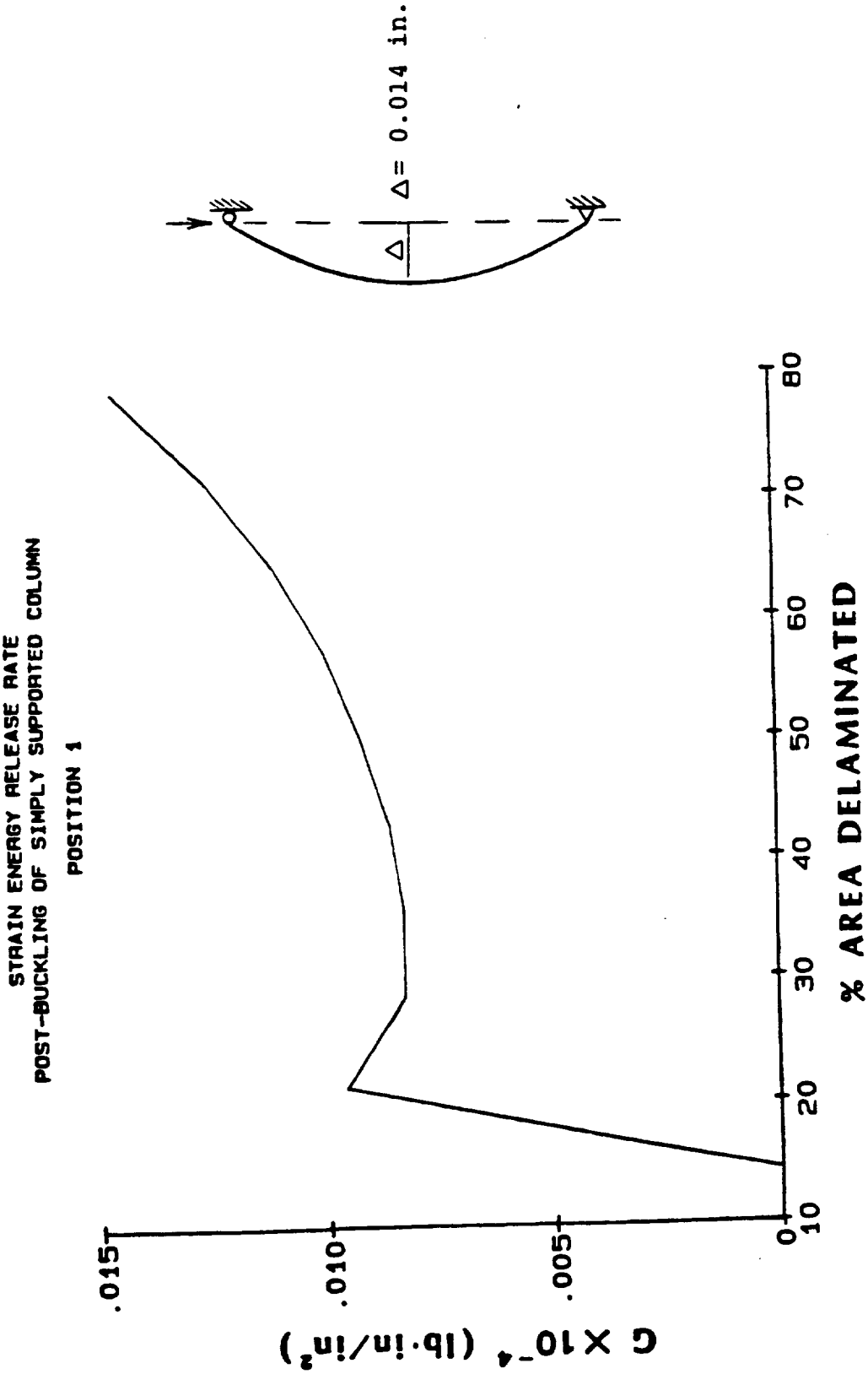
STRAIN ENERGY RELEASE RATE
POST-BUCKLING OF SIMPLY SUPPORTED COLUMN
POSITION 1
Δ= 0.014 in.
Δ
G X 10⁻⁴ (lb·in/in²)
.015
.010
.005
0
10
20
30
40
50
60
70
80
% AREA DELAMINATED

Figure 45

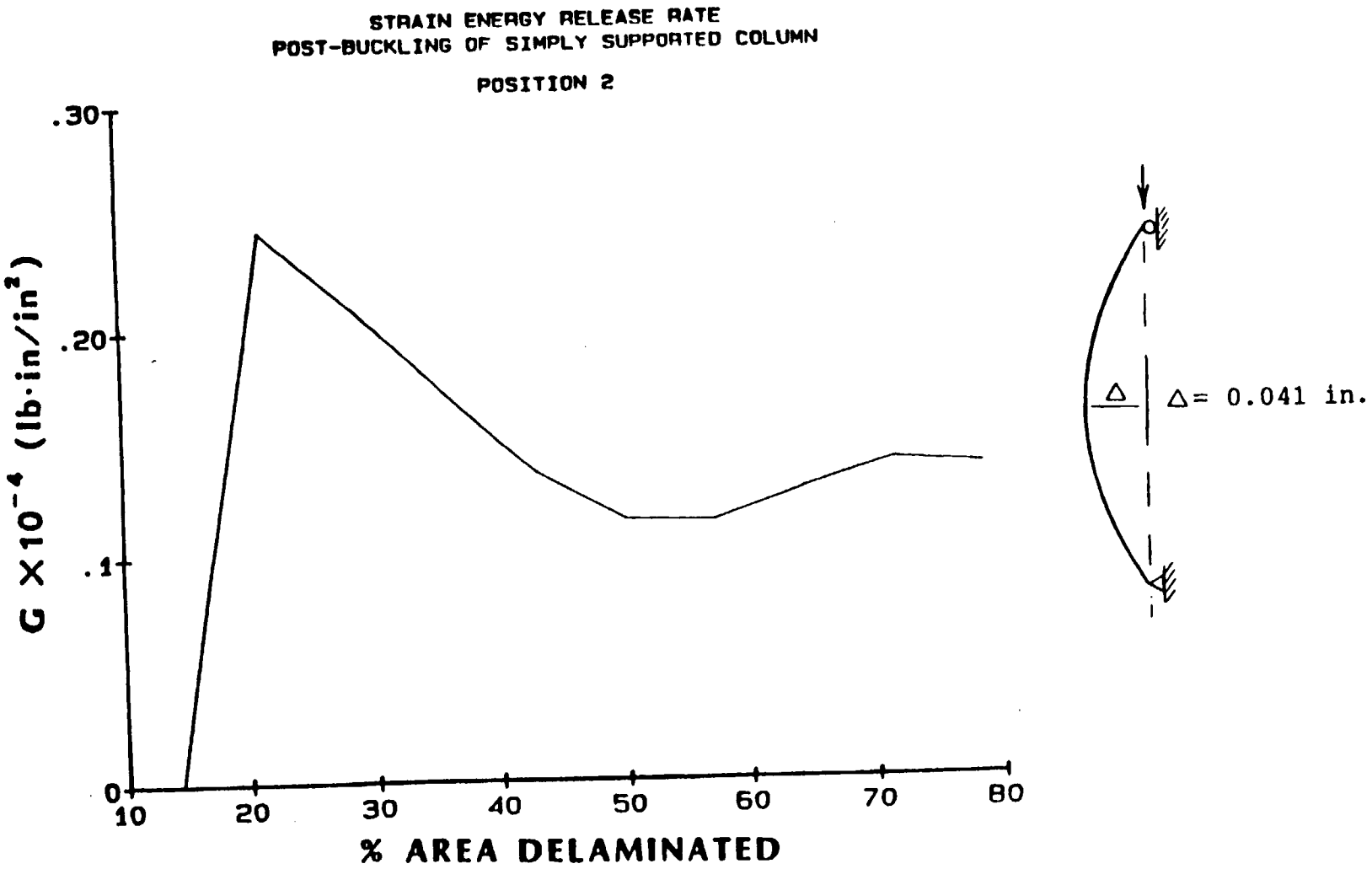
STRAIN ENERGY RELEASE RATE
POST-BUCKLING OF SIMPLY SUPPORTED COLUMN
POSITION 2
.30
.20
.1
0
G X10⁻⁴ (lb·in/in²)
10
20
30
40
50
60
70
80
% AREA DELAMINATED
Δ
Δ= 0.041 in.

Figure 46

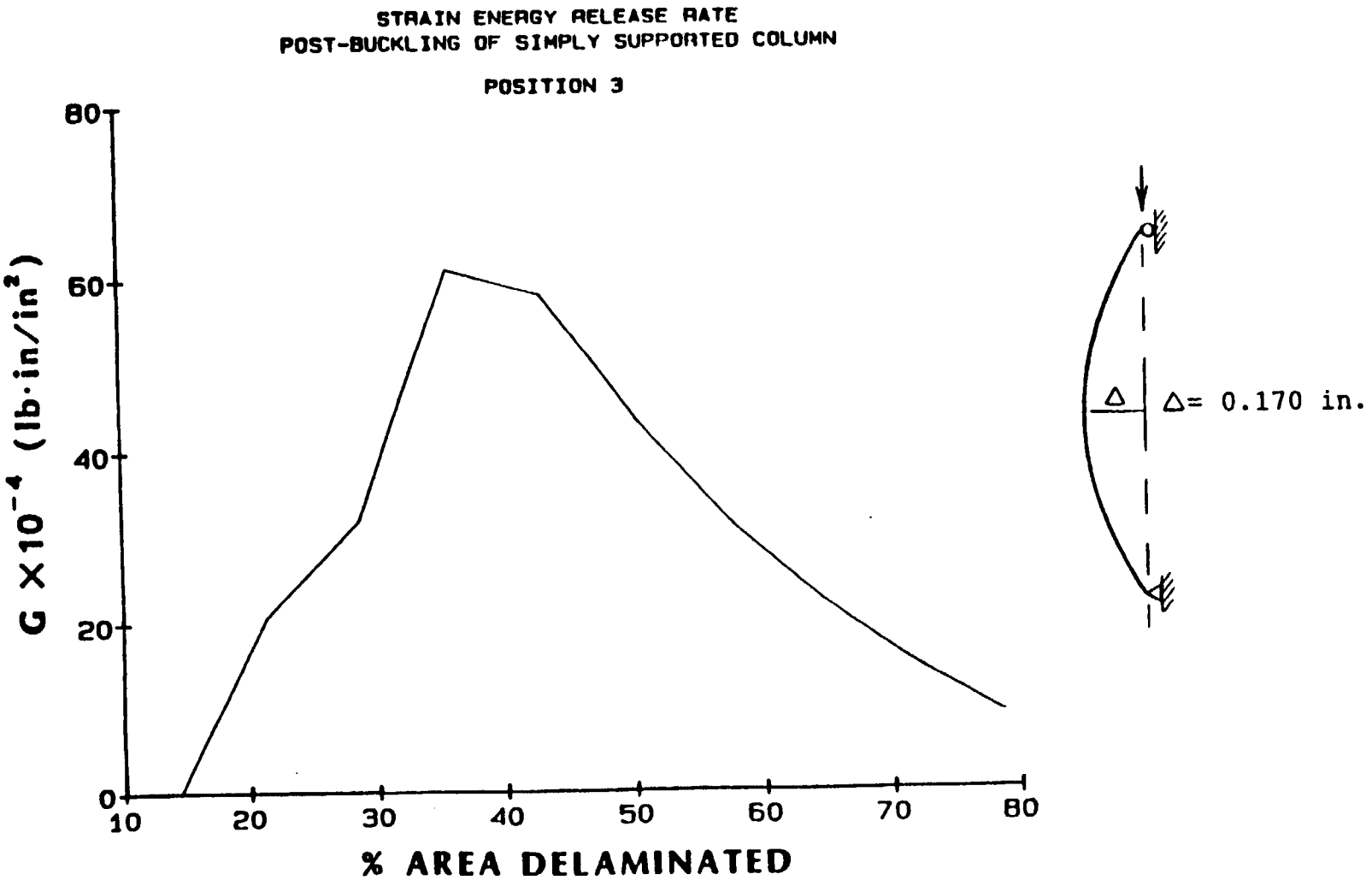
STRAIN ENERGY RELEASE RATE
POST-BUCKLING OF SIMPLY SUPPORTED COLUMN
POSITION 3
G X10⁻⁴ (lb·in/in²)
80
60
40
20
0
10
20
30
40
50
60
70
80
% AREA DELAMINATED
Δ
Δ= 0.170 in.

Figure 47

Clamped-Clamped Laminate
Position 1

area delaminated = 14.3%

area delaminated = 28.6%

area delaminated = 50.0%

area delaminated = 64.3%

area delaminated = 78.6%

Figure 48

Clamped-Clamped Laminate
Position 2

area delaminated = 14.3%

area delaminated = 28.6%

area delaminated = 50.0%

area delaminated = 64.3%

area delaminated = 78.6%

Figure 49

Clamped-Clamped Laminate
Position 3

area delaminated = 14.3%

area delaminated = 28.6%

area delaminated = 50.0%

area delaminated = 64.3%

area delaminated = 78.6%

Figure 50

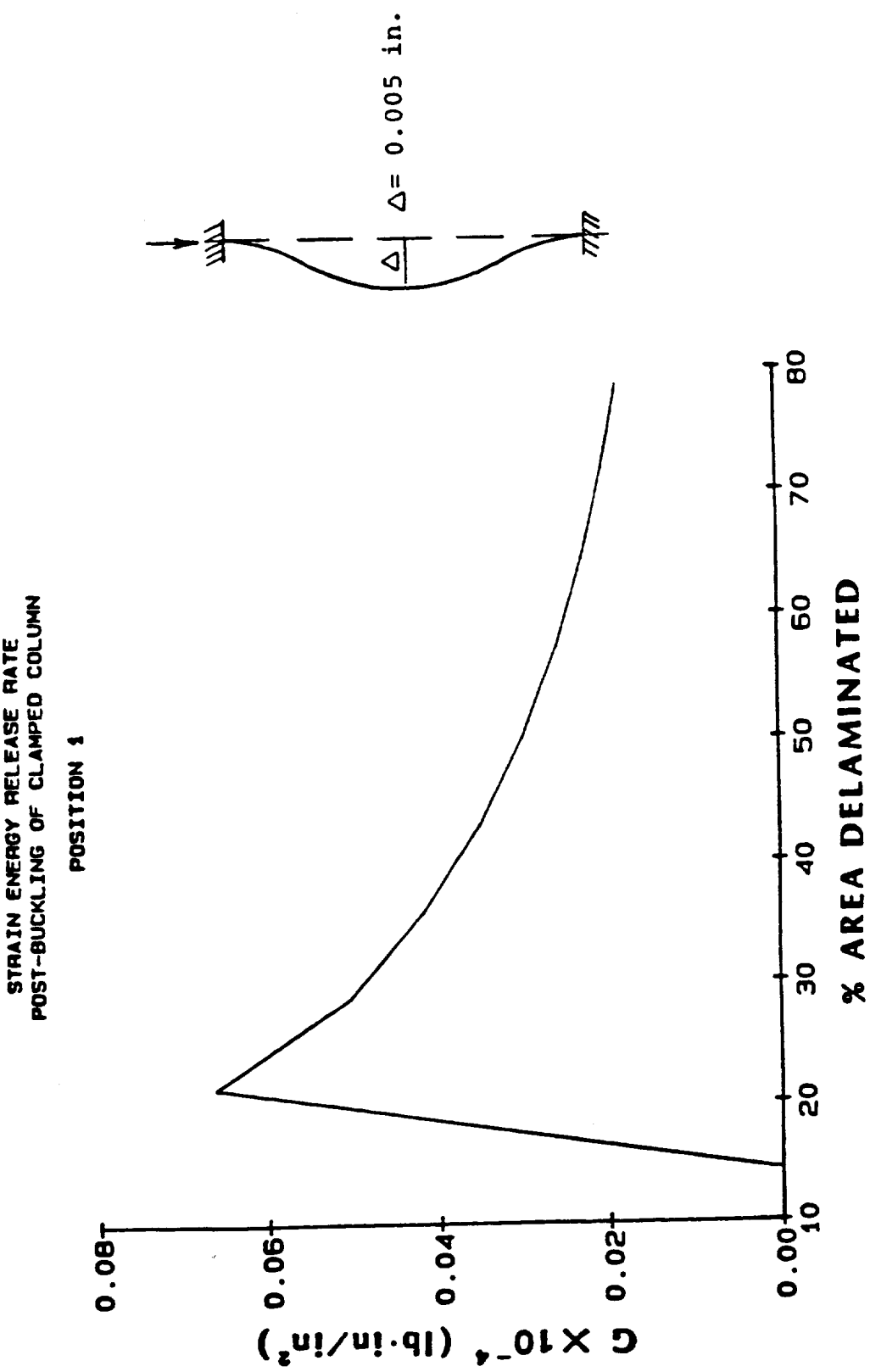
STRAIN ENERGY RELEASE RATE
POST-BUCKLING OF CLAMPED COLUMN
POSITION 1
Δ= 0.005 in.
Δ
G X 10⁻⁴ (lb·in/in²)
0.00
0.02
0.04
0.06
0.08
10
20
30
40
50
60
70
80
% AREA DELAMINATED

Figure 51

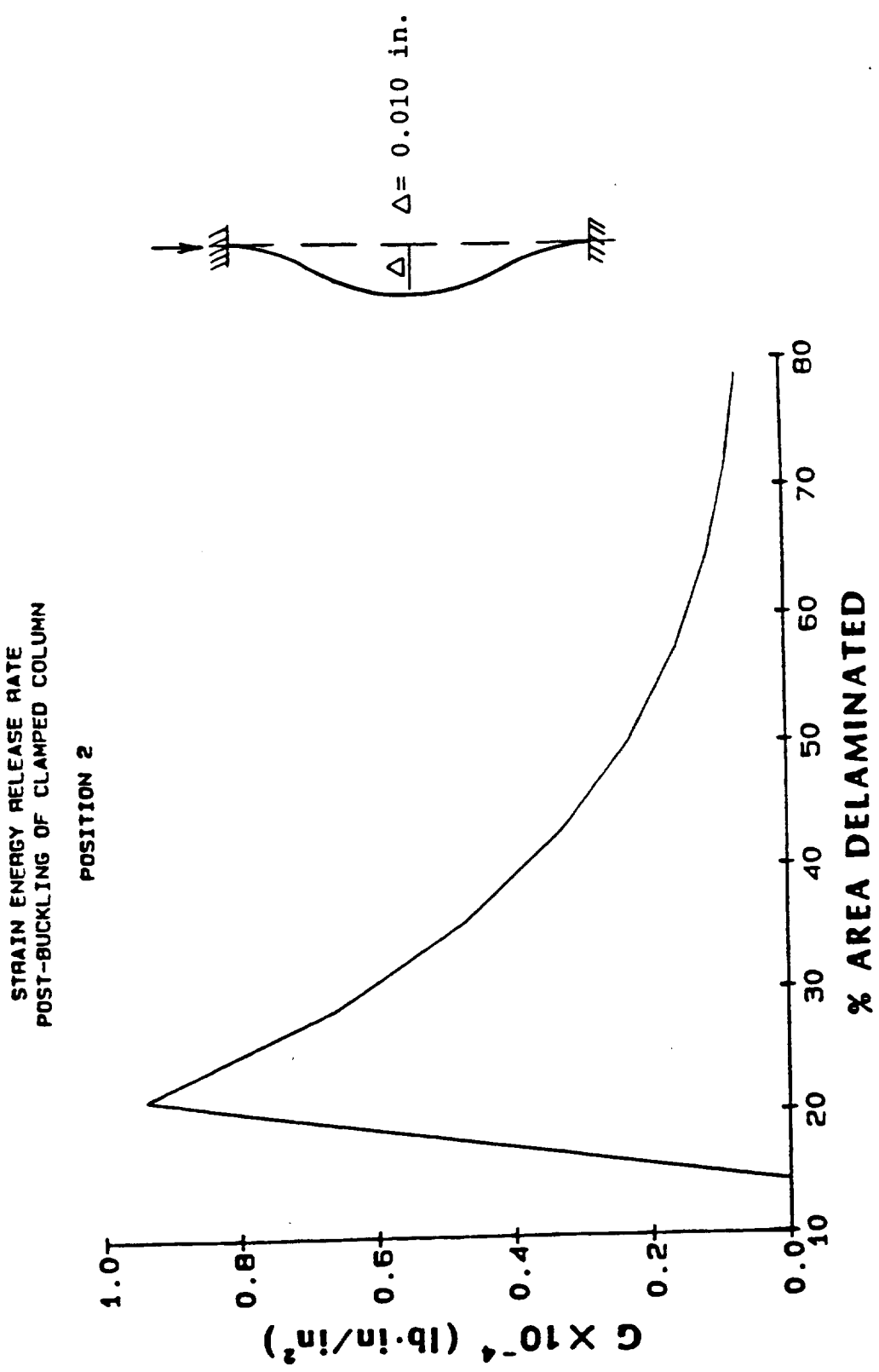
STRAIN ENERGY RELEASE RATE
POST-BUCKLING OF CLAMPED COLUMN
POSITION 2
Δ= 0.010 in.
Δ
G X 10⁻⁴ (lb·in/in²)
1.0
0.8
0.6
0.4
0.2
0.0
10
20
30
40
50
60
70
80
% AREA DELAMINATED

Figure 52

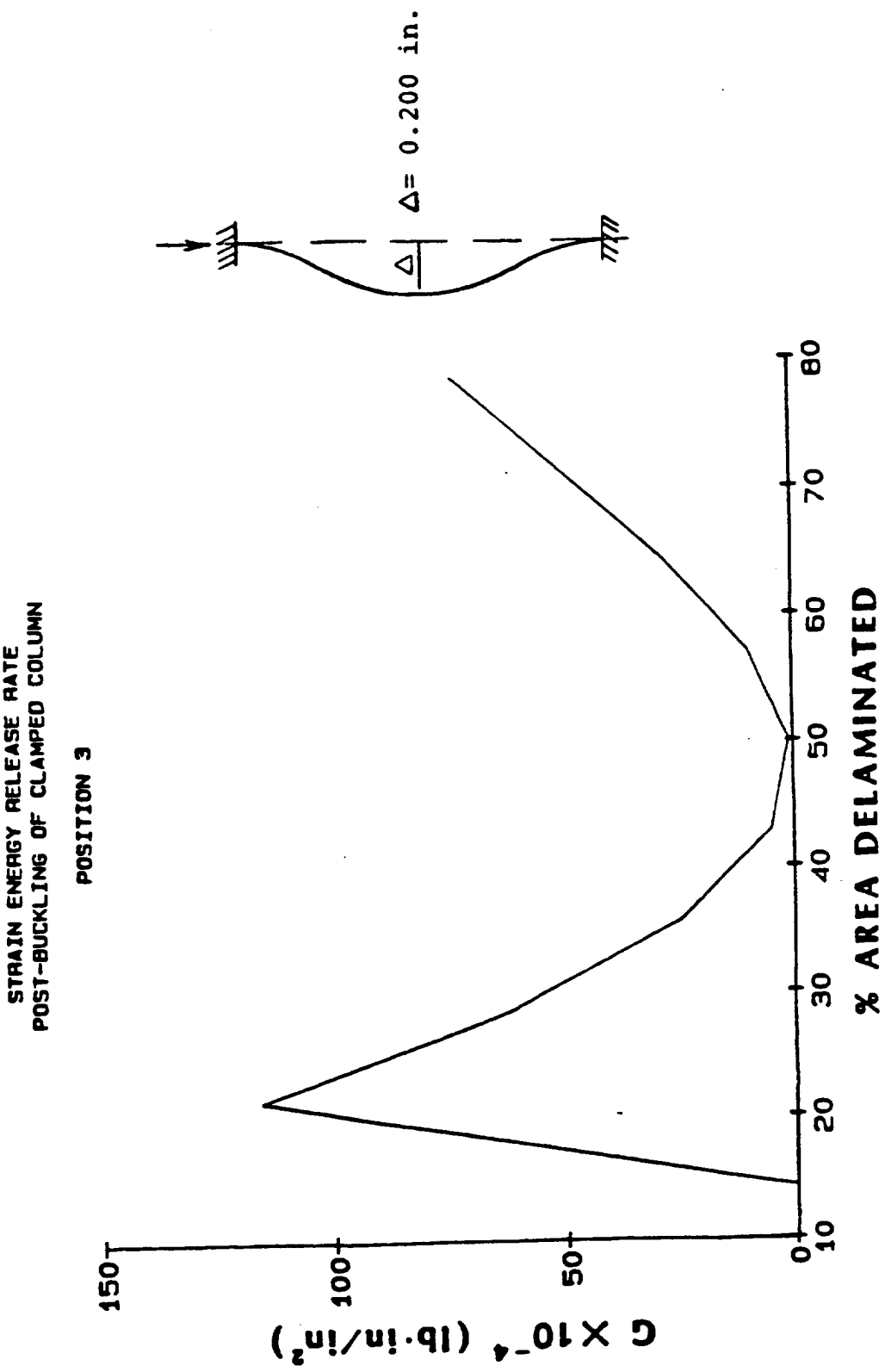
STRAIN ENERGY RELEASE RATE
POST-BUCKLING OF CLAMPED COLUMN
POSITION 3
Δ= 0.200 in.
Δ
G X 10⁻⁴ (lb·in/in²)
150
100
50
0
10
20
30
40
50
60
70
80
% AREA DELAMINATED

Figure 53

the overall SERR values due to the increasing end displacements as the laminate becomes less stiff. Figures 51 and 52 show the SERR curves for positions 1 and 2, respectively. Note how the strain energy released decreases at a more rapid rate as the position changes. By referring back to figures 48 and 49, as the amount of delamination increases, the lateral displacements of the laminate appear to decrease. This implies that the stiffness of the laminate is changing at a slower rate which again could be because the thicker sublaminate is contributing more to the overall laminate structural fracture toughness. This could account for the decrease in strain energy released.

Figure 52 shows the SERR curve for position 3 and it appears rather interesting. Note that at 50% delamination, practically no strain energy is released. Up to 50% delamination, the strain energy decreases because again it is believed that the thicker sublaminate begins to carry the majority of the compressive load. But at 50% delamination, the thicker sublaminate itself begins to bend more and the amount of energy released begins to increase. Therefore, the 50% delamination mark corresponds to the point where the thicker sublaminate becomes unstable and begins to buckle.

CHAPTER 4

SUMMARY

4.1 Overview

The objective of this study is, in part, to demonstrate the use of a computational method to characterize the effects of delamination damage on the structural response and fracture toughness of laminated composite structures. The effects on structural response are evaluated in terms of the changes in axial stiffness, critical buckling loads, and vibration frequencies. In a manner which is consistent with a fracture mechanics approach, the structural fracture toughness of the laminates is evaluated in terms of strain energy release rate, SERR. The above parameters are chosen because they are considered important factors in the design of a structural component.

To study these effects, a series of computationally simulated experiments are performed on various laminates. The laminates are represented by a group of finite element models which are then analyzed using MSC/NASTRAN. A unique feature of the finite element models and the approach used in this study is the use of bending-extensional coupling effects and multi-point constraints to simulate the delamination process.

Various delamination types are studied. Specifically, uniform and pocket free-edge delamination and interior delamination are considered for the structural fracture toughness studies. A through-the-width delamination is considered in the post-buckling analysis.

4.2 Summary of Results

In general, the fracture toughness results indicate that the growth of a uniform free-edge delamination in the laminates studied here, is a stable process. That is, for a given laminate, under a constant tensile load, the delamination crack will not propagate. The results also indicate that as the laminate thickness increases, the delamination crack becomes even more stable. The results indicate that the free-edge pocket delamination process is highly unstable. Specifically, a large amount of energy is released when the small, localized pockets of delamination are allowed to coalesce into one uniform delamination along the free-edge. This result indicates that the edge delamination is likely to initially occur as pockets, coalesce into one delamination, and then propagate inward.

The results for the case of an interior delamination shows no strain energy released until the delamination is allowed to extend through the free-edge. Thus, it can be concluded that an interior delamination, of any size and away from the free-edge, will not propagate under a tensile load.

In terms of material effects on fracture toughness, the AS-graphite laminates have the highest strain energy release rates, while the S-G/IMHS laminates have the lowest strain energy release rates.

This result is somewhat surprising in that it says the stiffer laminates have more energy available for delamination than do the less stiff S-G/IMHS laminates.

As mentioned, another means of characterizing the effects of delamination damage is by evaluating the changes in structural response of the laminates. The results for the most part agree with intuition. For example, for a centrally located delamination, the 6-ply laminate shows more degradation in response than does the 14-ply laminate. Thus, as the laminate thickness increases for a given amount of delamination damage, the effects on structural response decrease. The 14-ply laminate is also analyzed with multiple delaminations through the thickness and compared to the 14-ply laminate with a single delamination. As expected, the amount of structural degradation increases as the number of delaminations through-the-thickness increases.

In comparing the changes in structural response between laminates of different materials, the trend in degradation is similar to the previous trend observed in the fracture toughness results. The stiffer AS/HMHS laminates show less degradation than the less stiff AS/IMHS laminates, thus showing the influence of matrix strength. The weaker S-G/IMHS laminates show less degradation than either of the stiffer AS-graphite laminates. In addition to this, it is observed that for the same laminate thickness but with multiple delaminations, the S-G/IMHS laminates show even less response degradation. Whereas the AS-graphite laminates, as expected, show an increase in response degradation. This result is believed to be dependent on the amount of bending-extensional coupling present in the damaged laminate.

The last case studied is the post-buckling behavior of a laminate with a near surface delamination. The delaminated plies are assumed to have already undergone localized buckling and take the form of a "pop-out" on the laminate. Here, a model of a laminate with an initial "pop-out" is subjected to an increasing compressive load and the "pop-out" behavior is observed. Both simply supported and clamped-clamped boundary conditions are used to evaluate what effects the boundary conditions have on the post-buckled behavior.

For the simply supported case, the "pop-out" is located on the laminate's compression side and closes up and does not continue to buckle outward as the load is increased. In the clamped-clamped case, the "pop-out" is on the laminate's tension side and retains the initial "pop-out" shape under the increasing compressive load.

The strain energy release rate is calculated for various portions of the post-buckled laminate by allowing the initial "pop-out" delamination to spread. In general, the results show that the trends in the individual strain energy release rate curves change as the post-buckled position of the laminate changes. This shows that the strain energy release rate, i.e. fracture toughness, is affected by the position of the laminate.

4.3 Conclusions

Upon examining the results of this study, it can be concluded that delamination damage, if it does indeed occur, does not have significant effects on laminate behavior. The structural fracture toughness results show that delaminations occurring in the laminates studied are

stable and will not propagate under a constant load. In terms of the effects on structural response, it should be noted that large amounts of degradation, 15% - 20%, do not occur until a significant amount of delamination, 70% - 80%, is present. In most situations, a realistic amount of delamination is around 20% and at this amount the degradation effects are minimal in all cases considered here. From a structural analysis standpoint, the results show that very large amounts of delamination damage must be present before it needs to be of concern in the structural integrity of the component or structure.

4.4 Recommendations

The cases considered in this study are chosen so as to give insight into the effects of delamination on structural response, and obtain results which can be used as guidelines for design and analysis purposes. Thus, situations which could possibly be encountered by the structure during its in-service life need to be considered. Some additional cases will be presented below.

One case would be to see how the propagation of a delamination affects the transient response of the structure. A load of short time duration could be applied to simulate an impact on the laminate. This type of analysis could be used in determining how a structure, with delamination damage, would respond when subjected to some form of an impact load.

A similar problem would be a cyclic load, both tensile and compressive, applied to the structure. In this case, the time dependence or fatigue of the material properties could be taken into account in

the analysis. As the material properties and delamination size change as a function of time, how does the corresponding strain energy release rate, i.e. fracture toughness, of the laminate change? Also, how does the structural response change with time and delamination size? The cyclic compressive load could also be applied to the through-the-width delamination case to see if the initial "pop-out" spreads more readily with time by observing any changes in strain energy release rate.

Finally, in this study, only the damage mode of delamination is modeled and its effects studied. A next step would be the addition of transply cracking. As has been discussed, transply cracking and delamination usually occurs in combination. Either transply cracks form initially and lead to delamination, or, in some cases, delamination forms first and then leads to transply cracks. A methodology similar to that presented here could be used to model the cracks. By using further mesh refinements to incorporate double nodes along the length of the laminate, appropriate multi-point constraints, and specific node release sequences, computational simulation of transply cracking could be included. Actual crack locations could be determined by probabalistic methods, an area in which some work has been done already.

REFERENCES

1. Pipes, R.B., and Pagano, N.J., "Interlaminar Stresses in Composite Laminates Under Uniform Axial Extension", Journal of Composite Materials, 4(4), 1970, p. 538.

2. Pipes, R.B., and Pagano, N.J., "Interlaminar Stresses in Composite Laminates-An Approximate Elasticity Solution", Journal of Applied Mechanics, 41 E(3), 1974, p. 668.

3. Murthy, P.L.N. and Chamis, C.C., "A Study of Interply Layer Effects on the Free-Edge Stress Field of Angleplied Laminates, NASA TM 86924.

4. Murthy, P.L.N. and Chamis, C.C., "Free-Edge Delamination: Laminate Width and Loading Condition Effects," NASA TM 100238.

5. Wang, A.S.D., and Crossman, F.W., "Initiation and Growth of Transverse Cracks and Edge Delamination in Composite Laminates", Journal of Composite Materials Supplement, Vol.14, 1980, p. 71.

6. O'Brien, T.K., "Characterization of Delamination Onset and Growth in a Composite Laminate", Damage in Composite Materials, ASTM STP 775, K.L. Reifsnider, Ed., American Society for Testing and Materials, 1982, pp. 140-167.

7. O,Brien, T.K., 'Mixed-Mode Strain-Energy-Release Rate Effects on Edge Delamination of Composites", Effects of Defects in Composite Materials, ASTM STP 836, American Society of Testing and Materials, 1984, pp. 125-142.

8. Wang, A.S.D., Slomiana, M., Bucinell, R.B., "Delamination Crack Growth in Composite Laminates", Delamination and Debonding of Materials, ASTM STP 876, W.S. Johnson, Ed., American Society of Testing and Materials, Philadelphia, 1985, pp. 135-167.

9. O'Brien, T.K., "Analysis of Local Delaminations and Their Influence on Composite Laminate Behavior", Delamination and Debonding of Materials, ASTM STP 876, W.S. Johnson, Ed., American Society for Testing and Materials, Philadelphia, 1985, pp. 282-297.

10. Reddy, A.D., Rehfield, L.W., and Hagg, R.S., "Influence of Prescribed Delaminations on Stiffness-Controlled Behavior of Composite Laminates, Effects of Defects in Composite Materials, ASTM STP 836, American Society for Testing and Materials, 1984, pp. 71-83.

11. Murthy, P.L.N. and Chamis, C.C., "Composite Interlaminar Fracture Toughness: 3-D Finite Element Modeling for Mixed Mode I, II, and III Fracture, NASA TM 88872.

12. Grady, J.E., Chamis, C.C., and Aiello, R.A., "Dynamic Delamination Buckling in Composite Laminates Under Impact Loading: Computational Simulation, NASA TM 100192.

13. Murthy, P.L.N., and Chamis, C.C.: Integrated Composite Analyzer (ICAN): Users and Programmers Manual, NASA TP-2515, 1986.

14. Hoskin, B.C., and Baker, A.A., Composite Materials for Aircraft Structures, American Institute of Aeronautics and Astronautics, Inc., New York, 1986.

REPORT DOCUMENTATION PAGE

Form Approved
OMB No. 0704-0188

1. AGENCY USE ONLY (*Leave blank*)	2. REPORT DATE	3. REPORT TYPE AND DATES COVERED
	March 1994	Final Contractor Report

4. TITLE AND SUBTITLE

Computational Simulation of Composite Structures With and Without Damage

5. FUNDING NUMBERS

WU-505-63-5B
G-NAG3-50

6. AUTHOR(S)

Thomas F. Wilt

7. PERFORMING ORGANIZATION NAME(S) AND ADDRESS(ES)

The University of Akron
Akron, Ohio 44325

8. PERFORMING ORGANIZATION REPORT NUMBER

E-8240

9. SPONSORING/MONITORING AGENCY NAME(S) AND ADDRESS(ES)

National Aeronautics and Space Administration
Lewis Research Center
Cleveland, Ohio 44135-3191

10. SPONSORING/MONITORING AGENCY REPORT NUMBER

NASA CR-194433

11. SUPPLEMENTARY NOTES

This report was submitted as a dissertation in partial fulfillment of the requirements for the degree Master of Science in Civil Engineering to the University of Akron, Akron, Ohio. Project Manager, Christos C. Chamis, Structures Division, organization code 5200, NASA Lewis Research Center (216) 433-3252.

12a. DISTRIBUTION/AVAILABILITY STATEMENT

Unclassified - Unlimited
Subject Category 24

12b. DISTRIBUTION CODE

13. ABSTRACT ***(Maximum 200 words)***

A methodology is described which uses finite element analysis of various laminates to computationally simulate the effects of delamination damage initiation and growth on the structural behavior of laminated composite structures. The delamination area is expanded according to a set pattern. As the delamination area increases, how the structural response of the laminate changes with respect to buckling and strain energy release rate are investigated. Rules are presented for laminates of different configurations, materials and thickness. These results demonstrate that computational simulation methods can provide alternate methods to investigate the complex delamination damage mechanisms found in composite structures.

14. SUBJECT TERMS

Glass fibers; Graphite fibers; Epoxy matrices; Delamination; Edge; Center; Pocket; Buckling; Strain-energy; Release rate

15. NUMBER OF PAGES

16. PRICE CODE

17. SECURITY CLASSIFICATION OF REPORT	18. SECURITY CLASSIFICATION OF THIS PAGE	19. SECURITY CLASSIFICATION OF ABSTRACT	20. LIMITATION OF ABSTRACT
Unclassified	Unclassified	Unclassified	